THE UNIVERSITY *of* EDINBURGH

Analysis of the interaction between DVAP, the orthologue of human VAPB, and *Drosophila* Sac1

Manuela Marescotti

Thesis presented for the Degree of Doctor of Philosophy

University of Edinburgh University

2013

Declaration

I declare that this thesis was composed by myself and the work described is my own except where it is explicitly stated in the text, and the work reported has not been submitted for any other degree or professional qualification except when specified.

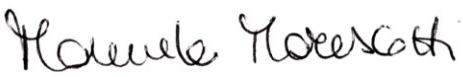

Manuela Marescotti

May, 2013

Abstract

Amyotrophic Lateral Sclerosis (ALS) is a motor neuron disease characterizeby devastating symptoms, such as muscle weakness, paralysis, and death within 5 years of disease onset. Mutations in *human (VAMP)-associated protein B* (*hVAPB*) gene cause ALS8. Interestingly, the *Drosophila* VAPB (DVAP) is required at the *Drosophila* larval neuromuscular junction (NMJ), to control bouton morphology. In Pennetta's lab *Drosophila* Sac1, a phosphoinositide-4-phosphate (PI4P) phosphatase, was identified during a genome-wide yeast two-hybrid screen, as a DVAP binding partner. VAP plays a role in regulating PI4P turnover in yeast and phosphoinositides are implicated in some neurodegenerative processes. In this PhD thesis, Sac1-DVAP interaction is used as the starting point to identify the mechanism that is altered when DVAP function is impaired. Thus, the possibility that the cellular pathways regulated by PI4P are affected in VAPB-mediated neurodegeneration was explored. First, the Sac1-DVAP association was confirmed *in vitro* by coimmunoprecipitation. Subsequently, we found that these two proteins colocalize *in vivo* at the ER membranes. Then, immunohistochemical analysis of *Drosophila* larval NMJ revealed that Sac1 and DVAP are involved in similar pathways. They both have a function in microtubule stabilization in the presynaptic boutons and axonal vesicle transport at the presynaptic compartment. They also seem to contribute to the spectrin-actin cytoskeleton stabilization at the postsynaptic compartment of the NMJ. Lastly, we reported that reduced levels of Sac1 phosphatase cause progressive neurodegeneration. Moreover, Sac1 is trapped into cytosolic aggregates induced by the expression of the ALS8-mutant allele of DVAP, and it does not localize to its original place in the cell. All together these results suggest that in ALS8 hVAPB seems to have a dominant negative effect on Sac1. Sac1 mislocalization could inhibit the dephosphorylation of PI4P. This PhD work further confirms Sac1-DVAP interaction and it suggests a mechanism underlying ALS8 pathogenesis, supporting the idea that altered metabolism of phosphoinositides can cause neurodegeneration.

“Dicette o’ pappice ‘nfacce a noce…. ‘Damme o’ tiempo ca te spertoso!’ ”

“The caterpillar said to the walnut…’Just give me time and I will bore into you!’ “

Neapolitan proverb

Acknowledgements

I am indebted to Dr Virender Sahota and Prof David Finnegan for providing valuable comments on my thesis during my thesis writing.

My sincere thanks go to Prof Andrew Hall for his support during the last year of my PhD.

Of course I would like to thank my Mum and Dad and my sister Valentina who have been through everything on the end of a phone line in Naples. Thank you for all your time, patience and support, and for being there for a chat when I needed it.

I am also grateful to Emanuele because he was always there to support and to encourage me with kindness and love. He made me realize that a PhD and a career are meaningless without your soul mate.

I would like to thank in particular my friend Raquel that has been with me almost every day of my PhD and that knows more than other people the effort made to go till the end of this trip; Diana, my only flat mate, besides my family, indeed, she has been a second family for me; Mara, the most close friend from Edinburgh.

Finally, I would like also to thank all the friends that made these PhD years unforgettable.

This thesis is dedicated to my grandparents. Nonna Anna, nonna Maria, and nonno Mario have followed all the moments of my PhD from heaven, and nonno Lello that joined them few days before my PhD viva. They have always been with me.

Table of contents

Table of Figures

List of Tables

Abbreviations

aa	Amino acid
Ab	Antibody
AD	Activation Domain
ALS	Amyotrophic Lateral Sclerosis
ANG	Angiogenin
bp	Base pair
brp	bruchpilot
BSA	Bovine Serum Albumin
CC	Coiled-coil
CERT	Ceramide Transport protein
Chr	Chromosome
cm	centimeters
CNS	Central Nervous System
Co-IP	Co-immunoprecipitation
COS-7	**C**V-1 in **O**rigin, and carrying the **S**V40 genetic material-7
CS	Canton S
CSP	Cysteine String Protein
CTRL	Control
Cy3	Cyanine 3
C9orf72	Chromosome 9 open reading frame 72
DB	Binding domain
dH_2O	Deionized H_2O
DIAP1	*Drosophila* inhibitor of Apoptosis 1
DLG	Discs Large
DMEM	Dulbecco's Modified Eagle Medium
DSHB	Developmental Studies Hybridoma Bank
DTT	Dithiothreitol

ECL	Enhanced Chemi-luminescence
EDTA	Ethylenediaminetetraacetic Acid
elav	Embryonic lethal, abnormal vision
ER	Endoplasmic Reticulum
FALS	Familial Amyotrophic Lateral Sclerosis
FBS	Fetal Bovine Serum
FFAT	Diphenylalanine in acidic tract
FIG4	Factor-Induced Gene
FITC	Fluorescein isothiocyanate
FTD	Fronto-temporal Dementia
FUS	Fused in sarcome
FWD	Fourwheel drive
g	grams
GFP	Green Fluorescent Protein
GM130	Golgi matrix protein-130
h	hours
HD	Huntington's Disease
HRP	Horseradish Peroxidase
IPTG	Isopropyl-β-D-1thiogalactopyranoside
JNK	Jun N-terminal kinase
kb	Kilobase
kDa	kilodalton
KU	kilounits
L	Liter
Lam	Lamin
LB	Lysogeny Broth
MCS	Multiple Cloning Site
mM	Millimolar
MNDs	Motor Neuron Diseases
MSP	Major Sperm Protein
MTs	Microtubules

MW	Molecular weight
NGS	Normal Goat Serum
NMJ	Neuromuscular junction
O/N	Overnight
OD_{600}	Optical Density 600 nm
OPT	Optineurin
OP1p	Overproduction of Inositol
ORP	OSBP related proteins
OSBP	Oxysterol binding protein
PBS	Phosphate Buffered Saline
PBT	PBS-0.1% triton
PD	Parkinson's Disease
PH	Pleckstrin Homology
PI4P	Phosphoinositide-4-monophosphate
PIPs	Phosphoinositide phosphates
PM	Plasma Membrane
PMSF	Phenylmethanesulfonyl Fluoride
PNS	Peripheral Nervous System
PSD	Post-synaptic density
RNAi	RNA interference
RT	Room Temperature
SALS	Sporadic Amyotrophic Lateral Sclerosis
SCA	Spino-cerebellar Ataxia
SDS	Sodium dodecyl-sulphate
SDS-PAGE	SDS- PolyAcrylamide Eel Electrophoresis
SEM	Scanning Electron Microscopy
SETX	Senataxin
SigmaR1	Sigma non-aploid receptor 1
SOB	Super Optimal Broth
SOC	Super Optimal Catabolite repression
SOD1	Super oxide dismutase 1

SPG11	Spatacsin
SR	Serine-repeat
SSR	Subsynaptic reticulum
START	Steroidogenic acute regulatory protein (STAR)-related protein
STT4	Stauroporine and temperature sensitive-4
TBST	Tris-buffered solution-0.1% Tween
TDP43	Tar-DNA-binding protein 43
TE	Tris EDTA
TM	Trans-Membrane
UAS	Upstream Activator Sequence
UBQL2	Ubiquilin 2
VCP	Valosin Containing Protein
VDRC	Vienna *Drosophila* RNAi Center
w.t.	Wild-type
β-ME	β-mercaptoethanol
µl	microlitre
µm	micrometer
25-HCO	25-Hydroxycholesterol

INTRODUCTION

Chapter 1: Introduction

The main focus of this PhD thesis is to understand how mutations in the *VAPB* gene can lead to neurodegeneration in a subgroup of Amyotrophic Lateral Sclerosis (ALS), using *Drosophila melanogaster* as an experimental model. Firstly, this chapter will briefly introduce the reader to motor neuron diseases, and then, describe the main features of ALS. Secondly, the use of fruit flies in studying neurodegenerative diseases will be illustrated. The main characteristics of VAP proteins will be examined. Thirdly, the ALS subtype caused by mutations in the *human VAPB* gene will be examined. Lastly, some of the known interacting partners of VAP proteins, in particular those involved in lipid metabolism and homeostasis, will be discussed, in order to understand whether VAPB is involved in controlling a particular class of lipids with regulatory functions, such as the Phoshoinositide phosphates (PIPs).

1.1 Neurodegenerative diseases

Neurodegenerative diseases are devastating disorders characterized mainly by progressive death of particular neuron subtypes. This group of disease includes, among others, Alzheimer's disease (AD), Parkinson's disease (PD), Huntington's disease (HD) and ALS. Neurons of the cerebral cortex and of the hippocampus are degenerated in the AD [Zarow et al., 2005]. Loss of pigmented dopaminergic neurons in the pars compacta of the substantia nigra was observed in PD cases [Atasoy et al., 2004]. Degeneration of neurons in the cerebral cortex and in the striatum was reported to be associated to HD cases [Rosas et al., 2008]. Lastly, motor neurons are degenerated in ALS [Ferraiuolo et al., 2007]. The reason for this neuronal selectivity is still an ill-defined aspect of these diseases [Bonini and Fortini, 2003; Bruijn et al., 1998].

Much effort has been invested in research aimed at identifying the molecular

causes of these diseases and a number of intracellular mechanisms/processes are altered in neurodegenerative diseases [Bossy-Wetzel et al., 2004]. Mitochondrial dysfunction, increased oxidative stress, altered vesicle transport, altered endocytosis, autophagy, disruption of the proteosome system and the unfolded protein response, synaptic activity, and apoptosis are only some of the intracellular problems that have been reported in neurodegenerative diseases, so far [Bossy-Wetzel et al., 2004]. Nevertheless, the exact molecular mechanisms underlying the pathogenesis of these diseases are still poorly understood [Bossy-Wetzel et al., 2004].

1.2 Amyotrophic Lateral Sclerosis

ALS belongs to the group of motor neuron diseases (MNDs) that are neurodegenerative disorders in which motor neurons are selectively affected [Ferraiuolo et al., 2007]. This disease is the most common and best-characterized MND, and is also known as Lou Gehrig's disease after the baseball player who died because of this fatal disorder.

A main feature of ALS is the progressive loss of both upper and lower motor neurons. Selective dysfunction and consequent death of these neuronal cells in the brain and spinal cord leads to denervation of skeletal muscles [Leigh and Garofolo, 1995]. As motor neurons directly (lower motor neurons) or indirectly (upper motor neurons) control muscle contraction, spasticity, hyper-reflexia, paralysis, general weakness, and atrophy of voluntary muscles occurs in ALS sufferers [Mulder, D.W., 1986; Talbot, K., 2002]. Respiratory failure due to denervation of the diaphragm and respiratory muscles usually culminates in death of the ALS patient [Mulder 1986; Talbot et al 2002]. Nevertheless, there is increasing evidence showing that in ALS, neurodegeneration does not affect only motor neurons, but also neurons in different areas of the brain, such as the anterior and prefrontal temporal lobe [Zago et al., 2011]. In fact, clinical symptoms characteristic of lesions in the anterior and prefrontal temporal lobe,

as the ones of Fronto-temporal Dementia (FTD) have also been observed in some cases of ALS [Zago et al., 2011].

ALS is the most common motor neuron disease with an incidence of 5:100,000 individuals. The cases of sporadic ALS (SALS) are more frequent (90%) compared to 10% of familial (FALS) l form cases [Kunst et al., 2004]. The mean age of onset is between 45-60 years and the average survival is approximately five years from the first onset of symptoms [Mulder, D.W., 1986; Talbot, K., 2002]. Nevertheless, cases of juvenile ALS are characterized by age of onset of <25 years [Al-Saif et al., 2011].

Such devastating manifestations of ALS are accompanied by the formation of cytosolic inclusions of mutant proteins in the cell body and axons of motor neurons [Ince et al., 1998; Piao et al., 2003]. These aggregates can be detected in post-mortem brains from ALS patients [Kato et al., 1997]. In addition, protein aggregation has also been demonstrated to be present in ALS animal models in association with fundamental features of the disease, such as locomotion defects [Watanabe et al., 2001; Chai et al., 2008; Wang et al., 2009]. It is still unclear what role the protein inclusions play in the disease: whether they are a cause or consequence of neurodegeneration or, in addition, whether they have a protective effect on the motor neurons [Brown Jr., 1998; Couillard-Despres et al., 1998]. The protective role of these cytosolic aggregates may be the trapping of harmful proteins.

ALS is genetically diverse, with at least 18 loci that have been found to be mutated in FALS cases (Table 1). The functional analysis of the proteins encoded by the ALS-causing genes and their interacting partners has helped in determining some of the cellular pathways that are altered in this MND [Ferraiuolo et al., 2007]. The genes that are altered in ALS patients encode proteins implicated in several molecular pathways including endosomal trafficking (Alsin in ALS2), oxidative stress (SOD1 in ALS1), protein

degradation pathways (Ubiquilin-2 in ALS15), and RNA processing (TDP-43 in ALS10). These proteins are not always associated with loss-of-function mutations in ALS pathogenesis. In fact, there is evidence that ALS cases are associated with SOD1 gain-of-function mutations [Siddique et al., 1997; Stathopulos et al., 2003]. So far, 18 loci have been found linked to FALS: among them 15 loci (ALS1-15) are associated with typical ALS, whereas two loci (ALS16 and *C9ORF72*-mediated) are associated with FTD, in fact they are also named ALS-FTD1 (ALS16) and ALS-FTD2 (ALS-*C9ORF72*-mediated). The fact that mutations in a locus can be associated to ALS and FTD clinical symptoms suggest that different neurodegenerative diseases are characterized by the alterations of the same molecular processes. The presence of common molecular pathways makes the study of a neurodegenerative disease more fruitful, perhaps, as the study of a disease may illuminate the pathogenesis of another disease and designing therapies may become easier as well. Now 16 ALS causative genes have been identified in these loci so far, they are listed in Table 1. However, the genetic cause of the majority of the ALS cases is still unknown. The identification of new ALS causative genes by molecular analysis of ALS patients can spot the protein that is altered in the disease. However, this approach is important, but not sufficient to pin-point the molecular pathway that is altered into the disease. In fact, the identification of the interacting partners of the protein mutated, and following genetic validation and functional analysis of the interaction can clarify the molecular pathways in which the protein is involved in normal conditions. Understanding how a particular cellular process works in normal conditions can help in elucidating why alteration of that pathway leads to such dramatic manifestations as in the case of ALS. In my PhD work, the interaction between VAPB, a protein found mutated in a particular type of ALS, and Sac1, is the starting point to identify the mechanism that is altered when VAPB function is impaired.

Genes and Loci associated with ALS pathogenesis:

Disease	Locus	Gene	Reference
ALS1	21q22.21	*Superoxide dismutase 1* (*SOD1*)	Rosen, 1993
ALS2	2q33	*Alsin* (*ALS2*)	Yong et al., 2001
ALS3	18q21	?	
ALS4	9q34	*Senataxin* (*SETX*)	Chen et al., 2004
ALS5	15q15.1-q21.1	*Spatacsin (SPG11)*	Orlacchio et al., 2010
ALS6	16p12	*Fused in sarcoma* (*FUS*)	Kwiatkowski et al., 2009 Vance et al., 2009
ALS7	20ptel	?	Sapp et al., 2003
ALS8	20q13.33	*VAMP-associated protein B* (*VAPB*)	Nishimura et al., 2004
ALS9	14q11	*Angiogenin* (*ANG*)	Greenway et al., 2006
ALS10	1p36	*Tar-DNA-binding protein* (*TDP-43*)	Sreedharan et al., 2008
ALS11	6q21	*Poliphosphoinositide phosphatase* (*FIG4/Sac3*)	Chow et al., 2009
ALS12	10p15	*Optineurin* (*OPTN*)	Maruyama et al., 2010
ALS13	12q24	*Ataxin-2*	Ross et al., 2011
ALS14	9p13	*Valosin-containing protein* (*VCP*)	Johnson et al., 2010
ALS15	Xp11	*Ubiquilin-2* (*UBQLN2*)	Deng et al., 2011
ALS-FTD1 (ALS16)	9p13	*σNon-opioid receptor1* (*SigmaR1*)	Al-Saif et al.2011 Luty et al., 2010
ALS-FTD2	9q21-22	*Chromosome-9-open reading-frame-72 (C9ORF72)*	Hosler et al., 2009
ALS18	17p13.2	*Profilin 1 (PFN1)*	Wu et al., 2012

Table 1. Genes and loci implicated in ALS pathogenesis

1.3 *Drosophila* as a model organism to study neurodegeneration

Drosophila has become a useful animal model with which to uncover and characterize molecular pathways that are perturbed in human diseases [Marsh and Thompson, 2006]. The findings emerging from research carried out in fruit flies can help in determining new therapeutic targets [Marsh and Thompson, 2006]. Several reasons highlight why *Drosophila* is exploited as an experimental system in which to study human pathological processes. First of all, the majority (75%) of the human disease-related genes have a homologue in fruit flies. In addition, the majority of these genes are involved in neurological and neurodegenerative impairments suggesting that many cellular pathways in the nervous system were conserved through evolution [Robin et al., 2000; Fortini et al., 2000; Reiter et al., 2001].

Moreover, *Drosophila* also has the advantages of having a rapid generation time, of being easy to rise in the lab, and importantly, of being very prolific, and the genetics become easier when the animal has a large progeny [Cauchi, and van den Heuvel, 2006]. Furthermore, several genetic tools have been developed which allow researchers to control the spatiotemporal expression of target genes in various *Drosophila* tissues. I will introduce the basic genetic tools that I used during my thesis work.

1.3.1 The UAS/Gal4 system

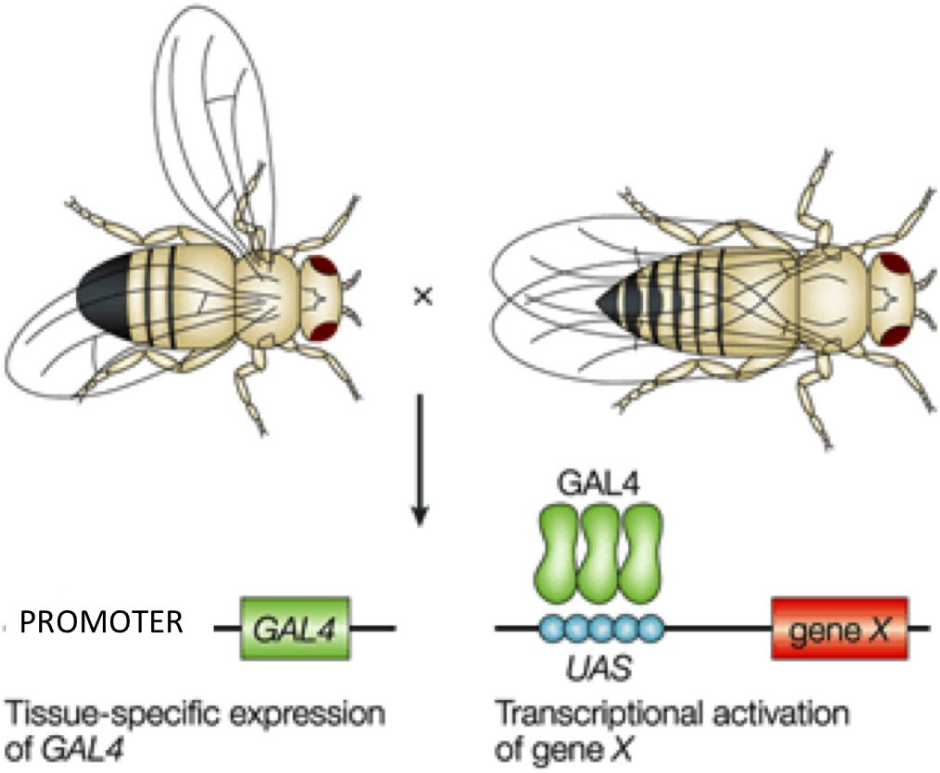

Figure 1. The UAS-GAL4 system. Figure adapted from St.Johnston 2002.

A useful tool that has been employed to precisely regulate gene expression is the binary UAS/Gal4 system (Fig. 1) [Brand and Perrimon, 1993]. Here two transgenic fly strains are crossed to each other. One comprises a tissue- and/or time-specific promoter (driver) upstream of the gene encoding the yeast Gal4 transcription factor. The second *Drosophila* strain has a GAL4-responsive Upstream Activator Sequence (UAS), located upstream the target gene. The cross between these two *Drosophila* strains will generate flies that direct the expression of the protein encoded by the target gene in the desired tissue and at the desired developmental stage, under the control of the GAL4 driven enhancers [Brand and Perrimon, 1993; Brand and Darmand, 1995].

1.3.2 The *Drosophila* larval Neuromuscular Junction

A number of processes such as structural and functional synaptic plasticity, neurotransmitter release, and synapse physiology and ion channel function involve molecules that are highly conserved between *Drosophila* and humans [Fortini et al., 2000]. Thus, *Drosophila* is a suitable animal model for the study of these pathways. In particular, the *Drosophila* larval Neuromuscular Junction (NMJ) is a genetic model system that has played and still plays an important role in the study of cellular pathways regarding the neuroscience field [Ruiz-Canada and Budnik, 2006]. The reason why this genetic model system is useful is that the synapses at the NMJ can respond to a number of changes [Griffith and Budnik, 2006]. In addition, the easy accessibility, the simplicity, the easy manipulation by several genetic tools make the *Drosophila* larval NMJ a powerful system [Ruiz-Canada and Budnik, 2006]. The synapse is also where some of the earlier symptoms of motor neuron diseases are thought to occur [De Vos et al., 2008; Saxena and Caroni, 2007; Plowey and Chu, 2011]. This makes the NMJ quite a useful experimental model in the study of neurodegenerative diseases.

The larval body wall muscle is made up of abdominal segments and each abdominal segment is made up of two hemisegments. Each hemisegment comprises 30 skeletal muscles. The organization of these skeletal muscles is the same in each hemisegment. [Ruiz-Canada and Budnik, 2006]. This reiterated and highly stereotyped organization is useful in the sense that makes possible a careful and detailed phenotypic analysis.

1.3.3 The adult *Drosophila* eye

Several cellular pathways have been genetically dissected by using the adult *Drosophila* eye, including cell death pathways, the different steps of the cell

cycle, and growth factor signaling mediated by tyrosine kinase receptor [Agapite and Steller, 1997; Tanenbaum et al., 2000; Wolff et al., 2007]. Interestingly, the cellular pathways involved in eye development, often affect the photoreceptors, which is a specialized type of neuron that converts light into neuronal activity [Warrick et al., 1998]. Many neurodegenerative conditions are caused by deleterious mutations that often cause massive neuronal death, which can be lethal for the animal. However, by directing the expression of a mutant gene specifically in the eye, lethality can often be avoided, as only the photoreceptor neurons will be impaired. These neurons are not required for fertility or viability, thereby allowing neurodegeneration studies to be conducted over time in living flies.

The photoreceptors are packed in groups of eight, and each group is called an ommatidium [Jackson et al., 1998]. The adult *Drosophila* eye comprises 800 ommatidia, which are regularly arranged. Any impairment in cellular pathways implicated in either differentiation or cell-fate determination can be easily observed in the eye [St. Johnston 2002]. The extent of any disruption is directly related to the number of ommatidia that are damaged. Disruption can result in a 'rough-eye phenotype', which can be easily scored using a dissecting microscope on living flies. This straightforward method is typically used in screens aimed at identifying genetic interactors of a target gene by overexpressing either wild type or mutated proteins specifically in the eye [St. Johnston 2002].

1.4 VAPB- induced Amyotrophic Lateral Sclerosis (ALS type 8)

ALS type 8 is a subtype of ALS that is associated with mutations in human *VAPB* (*hVAPB*) gene [Nishimura et al., 2004]. ALS8 sufferers present lower motor neuron lesions that are sometimes associated with postural tremor and bulbar palsy as clinical features [Nishimura et al., 2004]. All ALS8 cases are associated with an onset of the disease symptoms between the third and fifth

decade of life [Nishimura et al., 2004; Chen et al., 2010; van Blitterswijk et al., 2012]. ALS type 8 patients also present the major hallmarks of Amyotrophic Lateral Sclerosis including cytoplasmic protein aggregates in motor neurons, motor neuron death and impaired movements [Ferraiuolo et al., 2011]. Cytosolic inclusions containing the disease protein, are characteristic of many neurodegenerative diseases, such as ALS, AD, HD and PD [Ross and Poirier, 2005].

Interestingly, problems in lipid metabolism were reported to be associated with ALS8 cases. In fact, high levels of triglycerides and cholesterol were observed in ALS8 patients [Marques et al., 2006]. In addition, altered energy metabolism was found to be a characteristic not only of ALS8, but also a feature of ALS in general. In particular, ALS patients present high lipid levels and increased energy expenditure was observed in ALS patients [Dupuis et al., 2008]. SOD1 and TDP-43 transgenic murine models of ALS also presented hypermetabolism, as ALS patients, but low levels of lipid in the blood [Dupuis et al., 2011]. Indeed a diet high in lipid content leads to increased survival in SOD1 mouse model [Dupuis et al., 2004]; and hyperlipidemia is a protective factor in ALS patients [Dupuis et al., 2008].

1.5 Vesicle-associated-membrane-protein(VAMP)/synaptobrevin associated proteins (VAPs)

VAP proteins (VAPs) are type II integral membrane proteins, thus, they pass only once through the membrane and the C-terminal region of the protein faces the ER lumen [Lev et al., 2008]. A high throughput yeast two-hybrid screen performed to uncover interacting proteins of VAMP/synaptobrevin in *Aplysia californica* identified a VAP family member (aVAP-33). The role of this VAP protein was linked to neurotransmitter release, as anti-VAP antisera inhibited neurotransmitter release in cultured neuronal cells binding and blocking

aVAP-33 [Skehel et al 1995].

Structurally, VAP proteins share a common overall domain organization across several species [Lev et al., 2008]. The main domains in VAPs are the following: the amino-terminal major sperm protein (MSP) domain, a coiled-coil domain (CCD), and a carboxyl terminal transmembrane domain (TMD) (Fig. 2) [Skehel et al 2000]. The N-terminal MSP 100-aa domain faces the cytoplasm and it shares 45% similarity and 25% identity to the nematode MSP proteins (MSPs) [Nishimura et al 2004]. MSPs are proteins abundantly expressed in the amoeboid sperm cells of nematodes where they drive the movement of sperm [Roberts and Stewart, 1995]. The forward movement of these cells is obtained by cyclical polymerization and depolymerization of non-polar filaments formed by MSPs [Tarr and Scott, 2005]. In *C. elegans*, oocyte meiotic maturation and ovarian muscle contractions are stimulated by MSPs through the antagonization of the ephrin/Eph receptor signaling [Miller et al., 2003].

hVAPA (27.3 kDa and 242 aa) is encoded by a gene on chromosome (chr.) 18 and represents the first human VAP protein to be characterized [Weir et al 1998]. hVAPA shares 68% identity with hVAPB (27 kDa and 243 aa) encoded by the *hVAPB* gene on chromosome 20. hVAPB has a splice isoform known as hVAPC (11 kDa and 98 aa) that lacks the putative TMD and CCD. In the same study hVAPB was defined as the actual human homologue of aVAP-33 after the analysis of the binding properties of hVAPA, hVAPB and hVAPC proteins [Nishimura et al., 1999]. aVAP-33 homologues have also been identified in other species such as *C. elegans*, *Drosophila*, mice, rats, and plants [Skehel et al., 1995; Kagiwada et al., 1998; Nishimura et al., 1999; Skehel et al., 2000; Pennetta et al., 2002] suggesting that VAP proteins are evolutionarily conserved. The evolutionary conservation of these proteins suggests that they play a fundamental role in cells. Mammalian VAPA and VAPB are expressed in all tissues [Nishimura et al., 1999], similar to the expression data observed in

Aplysia californica [Skehel et al 1995].

The MSP domain contains a conserved stretch of 16 amino acids, named 'VAP consensus sequence' (Fig. 2A). This consensus sequence is located at position 41-59 of the human protein and it is present in the MSP domains of all the VAPs, but not in the MSP proteins [Lev et al., 2008]. The 'VAP consensus sequence' is directly implicated in the interaction with the di-phenylalanine in acidic tract (FFAT) motif, together with CCD and TMD of VAPs that expose hydrophobic patches that seal the binding between VAPs and FFAT motif-containing proteins [Kim et al., 2010]. The FFAT binding motif will be discussed more extensively later in this section.

Intriguingly, the two ALS8 mutations identified in hVAPB protein are located in the 'VAP consensus sequence' [Nishimura et al., 2004] and the crystal structure of the VAP-FFAT motif interaction has been resolved, identifying T46 as one of the crucial residues of VAP proteins for binding the FFAT motif [Kaiser et al., 2005].

In *Drosophila*, *C. elegans*, and mammals, the MSP domain of VAPs has been proposed to be cleaved and secreted from the cell to function in extracellular signaling through the interaction with membrane receptors such as Ephrin (Eph) receptor [Tsuda et al., 2008], SAX3-Robo receptor, and CLR1/Lar receptor [Han et al., 2012]. In particular, the last two receptors are involved in regulating the mitochondrial arrangement on I-bands, besides the regulation of other cellular functions, in muscles in *C. elegans*. Interestingly, an ALS8 mutant allele of VAPB inhibits the MSP domain secretion, suggesting that this pathogenic mutation has a cell non-autonomous effect, because the motor neuron cells expressing the mutant allele of VAPB cause other cells, such as the muscle cell, to exhibit a mutant phenotype [Tsuda et al., 2008].

The central 44-aa CCD (Fig. 2A) has been found in all t-SNARE protein family

members, in fact it is also known as ‘t-SNARE domain’ [Weimbs et al., 1997], and also in vesicular transport proteins [Nishimura et al., 1999]. This CCD has been described as a motif that mediates protein-protein interactions as well as having a role in homo-dimerization [Weimbs et al 1997; Soussan et al 1999].

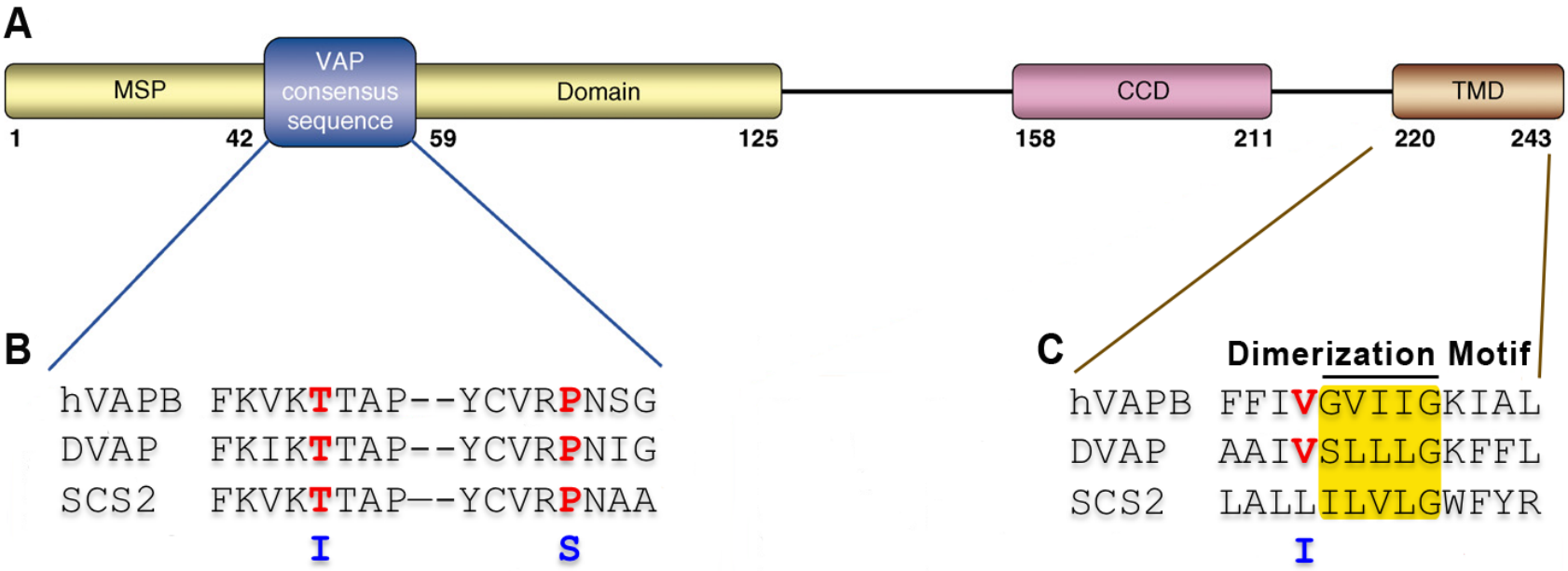

Figure 2. Schematic view of the domain organization of VAPs. (A) Three domains in are conserved through all the VAPs: the N-terminal MSP domain (1-125aa), the CCD (158-211 aa) and the C-terminal TMD (220-243 aa). (**B**) The MSP domain of VAPs has a 16-aa VAP consensus sequence (42-59 aa). The 16-aa motif present in its sequence highly conserved amino acids. Two out of three ALS8 mutations affect two amino acids included in this motif (T46 and P56). (**C**) TMD is highly conserved through different species and the recently identified ALS8 mutation affects an amino acids included in this domain (V234). The TMD contains a Dimerization Motif. The sequence that creates the dimerization motif is made of "small-aaXXXsmall-aa". Thus, it is often represented by either "GxxxG" or "SxxxG" aa sequences [Schneider et al., 2004]. GxxxG sequence is present in hVAPB, whereas SxxxG is placed into the TMD of the *Drosophila* protein. Interestingly, the dimerization motif is not completely conserved in the yeast homologue of hVAPB. This Figure adapted from Lev et al., 2008.

Finally, there is a C-terminal TMD acting as a membrane anchor [Nishimura et al., 2004]. Two glycines separated by three amino acids (GxxxG) form a dimerization motif [Kim et al., 2011]. The GxxxG motif localizes to the TMD of VAPB in mammals [Russ et al., 2000]. The TMD domain of hVAPB contributes to VAPB dimerization and oligomerization [Kim et al., 2011]. The VAPs are predominantly localized to the endoplasmic reticulum (ER) membranes, but can also be detected in the perinuclear region of the cell and at the plasma membrane [Kagiwada and Hashimoto, 2007].

VAPs have been implicated in microtubule dynamics in *Drosophila* and in mammals. The *Drosophila* orthologue of hVAPB (DVAP) is abundantly present in the *Drosophila* larval NMJ. Microtubule dynamics in the presynaptic compartment is required to control the bouton budding. The presynaptic morphology is highly perturbed in loss-of-function flies for DVAP showing fewer but bigger boutons. Conversely, more but smaller boutons are observed in larval NMJs from strains overexpressing DVAP. This protein seems to facilitate the formation of microtubule (MT) loops inside new forming boutons mediating the interaction between MTs and the plasma membrane [Pennetta et al., 2002]. In addition, VAPB together with the interacting partner Nir3 control microtubule dynamics in mammalian cells [Lev et al., 2008]. When these two proteins are overexpressed in mammalian cells two phenotypes are observed: perturbation of ER membrane morphology and accumulation of thick microtubule bundles around the ER. This evidence suggests that VAPB forms a complex with MTs and Nir3 [Amarilio et al., 2005].

1.5.1 VAP proteins are plasma-membrane-lipid sensors

Changes in the lipid composition of the plasma membrane can be ‘sensed’ by VAP proteins directly or indirectly through the interaction with other proteins [Loewen et al., 2004]. VAP proteins could ‘sense’ levels of specific PIPs by

directly binding them. In fact, a phosphoinositide (PI) binding domain has been identified in the MSP domain of Scs2p in yeast. In particular it overlaps with the 'VAP consensus sequence' that is directly implicated in the interaction with the FFAT motif. This domain interacts with phosphoinositide-4,5-bisphosphate ($P(4,5)P_2$) and with phosphoinositide-4-phosphate (PI4P) *in vitro*. The partial overlapping between the 'VAP consensus domain' and PIP binding domain suggest that PIP levels regulate the interaction between VAP proteins and the FFAT domain [Kagiwada and Hashimoto, 2007]. Interestingly, a DVAP interacting protein Sac1 regulates the PI4P turnover [Mayinger et al., 1995].

VAP proteins can also 'sense' lipid molecules through other proteins that bind lipid molecules [Loewen et al., 2004]. For instance in yeast Opi1p is an interacting partner of Scs2p and binds the phosphatidic acid (PA). Low levels of PA lead to the translocation of Op1p from the ER to the nucleus. PA is required for the synthesis of PIPs. The dissociation of Opi1p from Scs2p at the ER is a consequence of the production of PIPs that leads to decreased levels of PA. Thus, inositol synthesis is inhibited by Opi1p that dissociates from Scs2p, and translocates to the nucleus where it inhibits the transcription of *INO1* gene [Loewen et al., 2004].

VAP proteins localize to the ER that is the major site of synthesis of lipids. In addition, they interact with proteins that sense lipids, proteins that bind lipids and proteins that are involved in the metabolism of lipid molecules [Lev et al., 2008]. This suggests that VAPs can also play a role in lipid transport. The involvement of VAPs in lipid transport is demonstrated by their interaction with the cytosolic Ceramide Transfer Protein (CERT). This protein is required to transport ceramide from the ER to the Golgi complex [Hanada et al., 2003]. This lipid transfer protein localizes to the ER through its interaction with VAP, and localizes to the Golgi complex through the interaction with PI4P. The importance of VAPs in the function of CERT is proved by the fact that mutations in the FFAT motif of CERT inhibit its interaction with VAPs,

negatively affecting the transport of Ceramide between ER and Golgi [Kawano et al., 2006].

1.5.2 VAP proteins and the Unfolded Protein Response

VAP proteins are implicated in the Unfolded Protein Response (UPR) in yeast. In fact, *Scs2p* null mutant strains of *C. elegans* are sensitive to UPR following the ER stress induced by tunicamycin [Kagiwada et al., 1998]. Tunicamycin induces ER stress through the inhibition of N-linked glycosylation [Samali et al., 2010]. Nevertheless, overexpression of Scs2p in a null-background for hac1 protein suppresses the inositol auxotrophy phenotype [Nikawa et al., 1995]. Hac1 is a transcription factor that binds the UPR-elements that are present in the promoters of UPR-target genes. This transcription factor is activated by IRE1 in response to the accumulation of unfolded proteins in the ER lumen. IRE1 is an ER transmembrane protein that has also an endoribonuclease activity [Kagiwada et al., 1998]. This protein moves to the nucleus when it senses the accumulation of unfolded proteins in the ER. Ire1 in the nucleus activates Hac1 transcription factor.

1.5.3 ALS8-causative mutations in hVAPB

VAP proteins are implicated in a number of cellular functions and the majority of the pathways in which VAP function is implicated involve lipid molecules. A better understanding of all these pathways in which VAP proteins are implicated and how they are connected to each other can help in understanding the role of VAPs in ALS8 pathogenesis.

To date, three disease-causing mutations have been identified in the human *VAPB* (*hVAPB*) gene: the first mutation to be reported causes the change of a proline residue at position 56 to a serine (P56S) [Nishimura et al., 2004]; the

second mutation is a threonine-to-isoleucine substitution at position 46 (T46I) [Chen et al., 2010]; the third mutation is a valine-to-isoleucine substitution at position 234 (V234I) [van Blitterswijk et al., 2012]. The first two mutations affect two conserved amino acids placed in the 'VAP consensus sequence' in the MSP domain of hVAPB (Fig. 2B), whereas the third mutation affects a conserved amino acid of the TMD of hVAPB (Fig. 2C). However, a valine at the position 234 of hVAPB is not found in *Aplysia* and *S. cerevisiae* (Fig. 2C). Thus, this amino acid is less conserved than the threonine-46 and proline-56. Nevertheless, the V234I substitution was reported to be in association with repeat expansion in *C9orf72* gene. The presence of hexanucleotide repeat (GGGGCC) expansion in the intron of *C9orf72* gene has been found to be the major cause of ALS-FTD, so far [De-Jesus-Hernandez et al., 2011; Renton et al., 2011]. In addition, this repeat expansion has been reported also in FALS and FTD sufferers [van Blitterswijk et al., 2012]. The functional consequences of the mutations in hVAPB protein have not been investigated yet, because, to date, mutations in hVAPB are still considered a rare genetic cause of ALS8.

ALS8 *Drosophila* models for T46I and P56S mutations have been generated. The P56S and T46I in hVAPB correspond to residues P58S and T48I in DVAP, respectively. These diseased flies present the major hallmarks of the disease [Chai et al., 2008; Chen et al., 2010]. DVAP immunoreactive aggregates were observed in the brains and nerves of third instar larvae expressing DVAP-P58S pan-neuronally, and also in brains of third instar larvae expressing DVAP-T48I in the nervous system by immunohistochemical analysis [Chai et al., 2008; Chen et al., 2010]. In addition, DVAP immunoreactive aggregates were also observed in skeletal muscles of *Drosophila* larvae expressing DVAP-T48I mutant allele [Chen et al., 2010]. This last evidence has proved that the function of muscles is not only affected as a consequence of denervation, but also because the muscle is a direct site of the effects of mutant allele of DVAP expression. Moreover, neurodegeneration was observed in the *Drosophila* adult eye of flies expressing DVAP-T48I selectively in the visual system [Chen et al.,

2010]. Impaired movements and paralysis are some of the most common and earliest symptoms in ALS patients, and are also present in ALS experimental models [Mulder, 1982; Talbot, 2002; Hart et al., 2006]. In the fly model of ALS8, third instar larvae bearing DVAP-P58S showed a decreased frequency of peristaltic contractions, thus presenting locomotion defects when compared to control animals [Chai et al., 2008]. Rhythmic contractions of the body wall musculature are responsible for forward locomotion in *Drosophila* larvae. The central pattern generator (CPG) network in the nervous system gives rhythmic burst to the motor neurons causing rhythmic contraction waves [Caldwell et al., 2003].

Interestingly, hVAPB was found not only associated to ALS8, but also to Fronto-Temporal-Dementia-with-Parkinsonism-linked-to-chr.17 (FTDP-17). In fact, a murine model for FTDP-17 presents high levels of VAPB. In addition, neurodegeneration in a FTD *Drosophila* model is decreased when LOF mutant alleles DVAP are expressed [Karsten et al., 2006]. Finally, ALS characteristic symptoms were observed in some FTDP-17 patients [Lomen-Hoerth, 2004]. Thus, hVAPB is involved in typical and atypical ALS.

1.6 *Drosophila* VAPB (DVAP)

Drosophila has three VAPs which are named *farinelli*, *DVAP-33B*, and *DVAP*. They respectively share 39%, 18%, and 40% identity with aVAP-33, respectively [Lloyd et al 2000]. In particular, DVAP is the functional homolog of hVAPB in *Drosophila*, as defects due to DVAP loss-of-function can be rescued by both hVAPB [Chai et al., 2008]. For brevity, DVAP will be known in this thesis as DVAP herein. The *DVAP* gene is located on chromosome X, at cytological position 3F5-6, has seven exons and the encoded protein has a predicted molecular weight of 35 kDa. DVAP protein presents three characteristic structural domains of VAPs the MSP domain, CCD and TMD (Fig. 2A). Interestingly, the TMD does not present the dimerization motif

'GxxxG' that is present in the TMD domain of VAPs in mammals, *C. elegans*, *A. californica* (Fig. 2C) [Lev et al., 2008].

DVAP is ubiquitously expressed through the different developmental stages [Pennetta et al., 2002]. DVAP localizes mainly to the sub-cellular membranes, although some of the protein is also detected in the cytoplasm [Pennetta et al., 2002]. At the NMJ of third instar larvae, DVAP is present at both the pre- and postsynaptic compartments of the glutamatergic synaptic target muscle fibres [Pennetta et al., 2002]. Presynaptically, DVAP is located in the periactive zones where proteins required for synaptic growth are clustered [Pennetta et al., 2002; Sone et al., 2000]. Moreover, during active synaptic bouton budding DVAP redistributes itself in the boutons, becoming enriched at the base of the bud of the newly forming boutons, and at the tip of the incipient bouton at the beginning of bouton budding. In addition, there is association between DVAP and MTs in neurons [Pennetta et al., 2002]. DVAP appears to play a role in connecting MTs to the plasma membrane at the presynaptic compartment, to foster new bouton formation [Pennetta et al., 2002].

1.7 VAP interacting proteins

VAP-interacting proteins can provide clues about the function of VAP proteins in cells [Lev et al., 2008]. However, the interacting partners of VAPs are involved in many diverse intracellular functions that place VAPs at crossroads for different pathways and complicate the dissection of the role of VAP in neurodegeneration. To date, many proteins have been shown to bind to VAP proteins in different organisms [Lev et al., 2008]. The VAPs interacting partners include proteins implicated in a number of cellular functions as it has previously been mentioned in the introduction section [Skehel et al., 2000; Pennetta et al., 2002; Nikawa et al 1995; Kagiwada et al., 2003; Kawano et al., 2006; Brickner, and Walter, 2004; Kanekura et al., 2006; Skehel et al., 1995; Soussan et al., 1999; Loewen et al., 2003].

1.8 Interaction between VAP and proteins involved in lipid metabolism and homeostasis

The interacting partners of VAPs can be classified into four groups according to their subcellular role: MT organization, unfolded protein response (UPR), lipid metabolism and lipid transport, and membrane trafficking [Lev et al., 2008]. These interactions have been identified through a number of *in vitro* binding assays, such as 'yeast two-hybrid', co-immunoprecipitation (Co-IP), *in vitro* pull down, and affinity capture assay [Lev et al., 2008]. Thus, the functional relevance of these interactions needs to be examined. To date, the interactions between VAPs and proteins involved in lipid regulation are the best characterized [Lev et al., 2008].

The proteins involved in lipid metabolism and lipid transport interacting with VAPs include proteins containing a FFAT motif, as well as proteins that do not [Gavin et al., 2002]. The FFAT motif is a consensus sequence (EFFDAxE) that is directly involved in the interaction with VAP proteins [Wyles et al., 2002; Loewen et al., 2003]. Many VAP interacting proteins seem to interact with VAP to localize at the cytoplasmic surface of the ER and at vesicles. The lipids are assembled in the ER, this could explain why the ER is a crucial lipid sensing organelle [Voeltz et al., 2002], and, in turn, why many proteins implicated in lipid synthesis localise to this organelle.

1.8.1 VAP-interacting proteins not containing a FFAT motif in their sequence

The No-FFAT-motif proteins that are involved in lipid metabolism and that interact with VAPs are Sac1 phosphatase and Stt4 kinase. These two enzymes are required for the metabolism of a subgroup of Phosphoinositide phosphates (PIPs): PI4P. The PIPs are phosphorylated derivatives of the phospholipid

phosphatidylinositol, and they recruit molecules to the cytosolic surface of cell organelles and of the plasma membrane [McCrea, and De Camilli, 2009]. These lipid molecules are of considerable interest, as they are involved in a wide variety of processes [Mc Crea, and de Camilli, 2009].

PIPs have an important role in modulating signal transduction at the plasma membrane [Di Paolo and De Camilli, 2006]. PI(4,5)P_2 is a PIP specie that localizes to the PM. This PIP is generated mainly from phosphorylation of 5-OH of PI4P by type I PI-kinases. The PM-PI4P is generated both at specific sites and also by transport from recycling organelles from Golgi membranes by membrane carriers [Odorizzi et al., 2000]. PI(4,5)P_2 can be used as substrate by three different types of enzymes: phospholipases, phosphatases and PI3 kinases. The metabolites that are obtained by the activity of phospholipase C and phospholipase A2 amplify signalling, whereas 5-phosphatases turn off signalling. PI(3,4,5)P_3 obtained by the activity of PI3kinases on PI(4,5)P_2 also propagate signalling [Cantley et al., 2002]. In fact, PI(3,4,5)P_3 recruits effectors to the PM that activate a number of cellular pathways. Signalling pathways including the Tor pathway, are regulated by effectors as PDK and AKT/PKB kinases, whereas the actin cytoskeleton is remodelled by GAP and GEF effectors [Cremona et al., 1999]. In turn, PI(3,4,5)P_3 can face two different dephosphorylation events leading to two outcomes. Dephosphorylation of PI(3,4,5)P_3 by 5-phosphatases induces prolongation of signalling, whereas dephosphorylation of PI(3,4,5)P_3 by 3-phosophatases leads to attenuation of signalling [Majerus et al., 1999].

PIPs regulate different aspects of the actin cytoskeleton: the actin nucleation, the actin filaments elongation and the interaction between actin filaments and the PM [Di Paolo and De Camilli, 2006]. PI(4,5)P_2 in association with Cdc42 GTPase bind and activate Neural-Wiskott Aldrich syndrome protein (N-WASP), that is normally present in an auto-inhibited conformation. Its interaction with PI(4,5)P_2 and Cdc42 induces a conformational change that

allows this protein, in turn, to bind and activate the Actin-Related-Protein (ARP)2/3-mediate the actin polymerization [Pollard et al., 2003; Rohatgi et al., 2000]. In addition, actin filament elongation is facilitated by $PI(4,5)P_2$ that induces the dissociation of CapZ and gelsolin capping proteins at the plus ends of the actin filaments [Yin et al., 2003]. The function of adaptor proteins between actin filaments and membranes are also regulated by $PI(4,5)P_2$ in sites of adhesion between cells or between cells and matrix. $PI(4,5)P_2$ binds a FERM-domain adaptor protein that enhances its affinity for integrins [Di Paolo, and De Camilli, 2006; Ling et al., 2002].

PIPs are implicated in phagocytosis as a consequence of the induction of actin nucleation induced by $PI(4,5)P_2$ as described above. Actin polymerization is required during phagocytosis events because the foreign particle has to be incorporated in the cell by the formation of cell protrusions [Botelho et al., 2004]. PIPs are also implicated in endocytosis, in fact, they bind endocytic factors such as clathrin adaptors and endocytic factors required for the fission reaction [Wenk et al., 2004].

Phosphatidylinositol is synthesised in the ER before being carried to other intracellular membranes by proteins which transfer phospholipids [McCrea and De Camilli, 2009]. Seven PIPs were reported, so far, and they differ from each other depending on the combination of phosphates at three different positions, the 3-OH, the 4-OH and the 5-OH, of their inositol head group. The importance of the position of the inositol head of each PIP is shown by the fact that each phosphatidylinositol phosphate has a specific function and intracellular localization [Volpicelli-Daley and De Camilli, 2007]. Specific PIPs are localised to different intracellular organelles [Mc Crea and de Camilli, 2009]. The addition and removal of the phosphate groups from inositol derivatives is catalysed by lipid kinases and lipid phosphatases, respectively, and Sac1 domain-containing phosphatases are involved in the generation of several of these derivatives [Mc Crea and de Camilli, 2009].

PI4P lipid is mainly generated at the Golgi membranes where it also localizes [Mayinger, 2009]. The Golgi apparatus function depends on PI4P. In particular, in yeast it is implicated in the anterograde trafficking of proteins such as chitin synthases, Hsp150 and invertase, and also in the trafficking from the Golgi to the cell periphery [Walch-Solimena et al., 1999; Audhya et al., 2000; Schorr et al., 2001]. This role of PI4P has been also described in mammals [Walch-Solimena et al., 1999; Hama et al., 1999; Audhya et al., 2000; Schorr et al., 2009]. The proteins that interact with PI4P, bind this lipid molecule through the Pleckstrin homology (PH) domain. The PI4P interacting proteins include two classes of proteins: the first one encompasses no-clathrin-mediated lipid transfer proteins such as FAPP2 (Four-phosphate adaptor protein-2), OSBP (Oxysterol-binding protein) and CERT. The second class of PI4P binding proteins implicated in the clathrin-mediated transport such as Golgi-localized, γ-ear-containing ADP-ribosylation factor-binding proteins (GGAs) and clathrin adaptor protein complex-1 (AP1) [D'Angelo et al., 2008]. The formation of clathrin-coated vesicles is mediated by GGA and AP1 proteins at the endosomes and trans-Golgi network [Hinners, and Tooze, 2003].

All together this evidence supports the idea that PIPs are crucial lipid molecules inside the cell, as they are implicated in a number of cellular functions. This suggests that an alteration in PIP turnover could lead to catastrophic consequences for the cell.

1.8.1.1 Sac1

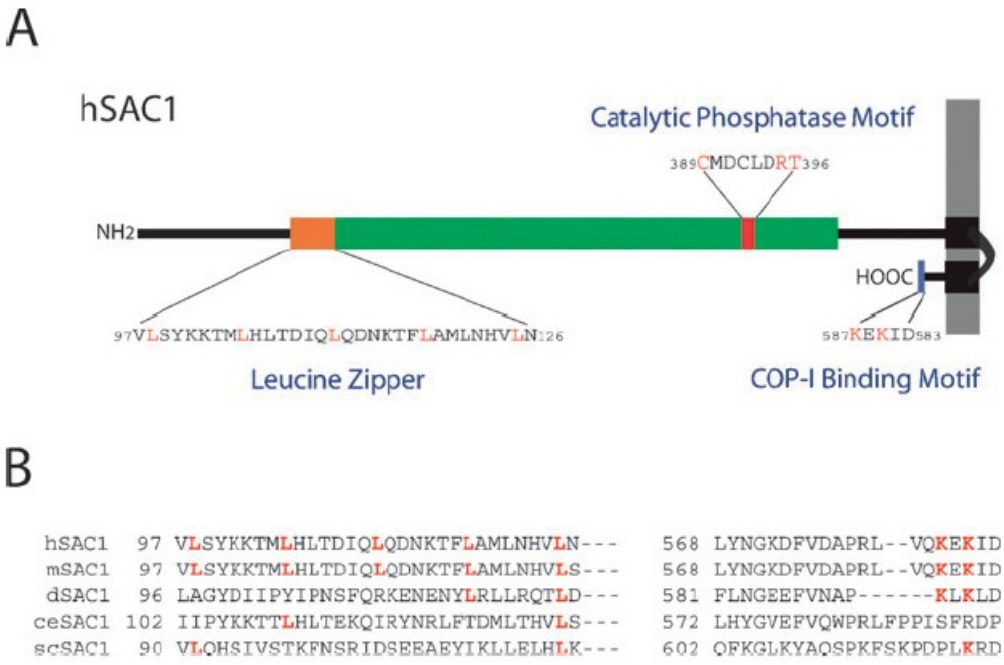

Figure 3. Domain organization of the Sac1 proteins. (**A**) The hSac1 protein present a SAC domain (green) that include seven motifs. The first motif includes a leucine zipper motif (orange, 97-126 aa), whereas the sixth motif includes the phosphatase core (red, 389-396 aa). At the C-terminus of the protein two TM domains allow this protein to be anchored to the membrane. Finally a COP-I binding motif (blue, 587-593) is present at the C-terminal end. (**B**) Alignment among Sac1 proteins from different species shows that the leucine zipper motif is present in the human and murine proteins, but it is not observed in *C. elegans* and *S. cerevisiae*. In *Drosophila* only to leucines of the five leucines in the motif in the mammals Sac1. On the other hand the COP-I binding motif is present in mammals and Drosophila Sac1 proteins but not in *C. elegans* and *S. cerevisiae*. [Blagoveshchenskaya et al., 2008].

Suppressor of actin-1 (Sac1) is a 67 kDa lipid phosphatase and belongs to the Sac1-domain containing protein family [Mayinger et al., 1995]. Other members include Sac2 (also known as INPP5f), Sac3 (also known as FIG4), and Synaptojanin 1 and 2 [Hughes et al., 2000]. Evidence from experiments performed in yeast reported that Sac1 localises to the Golgi complex and to the ER [Whitters et al., 1993; Nemoto et al., 2000]. This phosphatase family is highly conserved across all species and shares a domain, known as SAC

domain, at the N-terminal region. The Sac1 sequence includes also two TM domains at the C-terminus (Fig. 3).

The SAC domain includes seven motifs, where the first one contain the Leucine Zipper motif and the sixth one the catalytic core ($CX_5R(T/S)$) of the protein [Hughes et al., 2000] (Fig. 3A). Intriguingly, there are topological features of Sac1 that are conserved throughout the species such as the presence of the SAC domain and of the two TM domains [Blagoveshchenskaya et al., 2008]. On the other hand, the LZ motif seems to be a characteristic motif of the mammalian Sac1 although two leucines out of five are conserved in the *Drosophila* protein [Blagoveshchenskaya et al., 2008] (Fig. 3B). The LZ motif is required for oligomerization [Blagoveshchenskaya et al., 2008]. Coated protein-I (COP-I) binding motif seems to be present only in mammals (Fig. 3B) and it is required for the interaction with COP-1 [Blagoveshchenskaya et al., 2008].

The $CX_5R(T/S)$ catalytic motif is involved in the removal of a phosphate-group from the position 4 of the inositol-head group of PIPs to regulate the turnover of these lipid molecules [Blagoveshchenskaya et al., 2008]. Nevertheless, *in vitro* Sac1 can also dephosphorylate Phosphoinositide-3-phosphate (PI3P) and Phosphoinositide-3,5-bisphosphate ($PI(3,5)P_2$) [Guo et al., 1999]. In addition, PIPs are also required in priming of vesicles in endocytosis [Wiedemann et al., 1998].

The *Sac1* gene was isolated during a complementation screen performed in *S. cerevisiae* in order to identify suppressor genes of mutations in the actin gene [Novick et al., 1989; Cleves et al., 1989]. Additionally, in yeast, defects in the actin cytoskeleton, caused by *Stt4* null mutations, are partially rescued by *Sac1* null mutations [Gavin et al., 2002]. Moreover, yeast Sac1 has been described to directly interact with Vps74 protein [Wood et al., 2009]. The *Drosophila* Vps74, named GOLPH3, was proposed to act as a bridge between the Golgi complex and the actin cytoskeleton [Dippold et al., 2009]. In addition, yeast

Sac1 is also implicated in controlling the vacuole shape [Foti et al., 2001], and in sphingolipid metabolism *in S. cerevisiae* [Brice et al., 2009].

In *Drosophila* Sac1 functions through the Jun N-terminal kinase (JNK) MAPK signalling pathway to regulate changes in cell shape during gastrulation [Wei et al., 2003]. This process is critical for embryonic development and survival, and loss of Sac1 function results in embryonic lethality [Wei et al., 2003]. In addition, a role for *Drosophila* Sac1 in the modulation of Hedgehog signalling has been reported. In fact, loss-of-function mutations in Sac1 induce localization of Smoothened (SMO) to the plasma membrane. The translocation of SMO to the PM is a step inducing activation of Hh signalling [Yavari et al., 2010].

Phosphoinositide phosphatases are thought to play a role in neurodegenerative processes when their function is impaired [Mc Crea and de Camilli, 2009]. Sac3/Fig4, the molecular cause of ALS11 [Chow et al., 2009], is a phosphatase that dephosphorylates $PI(3,5)P_2$ substrates [Yuan et al., 2007]. A P-element insertion screen performed in *Drosophila* showed that Sac1 enhances the neurodegenerative phenotype in the adult eye caused by overexpression of *Spinocerebellar Ataxia type 8* (*SCA8*) gene in all photoreceptor neurons [Mutsuddi et al., 2004]. The involvement of enzymes that regulate PIP levels in neurodegenerative processes means that these lipid molecules regulate fundamental processes at the nervous system.

Sac1 is expressed in sensory neurons in the peripheral nervous system (PNS) and in Fascilin-II (FasII) positive axons in the central nervous system (CNS) where it was proposed to control axonal path-finding in *Drosophila* embryos [Lee et al., 2011]. FasII is the *Drosophila* orthologue of the synaptic adhesion molecule NCAM (neural cell adhesion molecule). It functions as a bridge between the pre- and postsynaptic membranes at the NMJ [Packard et al., 2003]. The synaptic morphology is perturbed when FasII function is impaired.

Decreased levels of FasII are associated with smaller boutons and shorter and fewer secondary axons [Stewart et al., 1996]. Complete loss-of-function mutations in *fasII* gene lead to retraction of the presynaptic boutons [Schuster et al., 1996]. In addition, Sac1 seems to mediate axon repulsion in the Slit/Robo pathway [Lee et al., 2011].

Finally, preimplantation lethality is observed in the presence of loss-of-function mutations in Sac1 [Liu et al., 2008]. In the same study Sac1 function was studied in HeLa cultured cells and disruption of mitotic spindle and of the Golgi complex was reported when Sac1 levels were decreased by RNAi approach.

A protein-interaction map as a consequence of a high-throughput yeast two-hybrid screen performed by Giot et al., [2003], showed that DVAP binds *Drosophila* Sac1. Interestingly, the *Saccharomyces cerevisiae* VAP proteins (Sc22p and Scs2p) are crucial in regulating the turnover of phosphoinositides-4-monophosphate (PI4P) at contact sites between PM and endoplasmic reticulum (ER) to control Sac1 phosphatase activity *in vitro* and *in vivo* [Stefan et al., 2011].

1.8.1.2 Staurosporine- and temperature sensitive 4 (Stt4) protein

Stt4 kinase is an enzyme that was identified in *Saccharomyces cerevisiae* during a genetic interaction screen designed to identify components of the protein kinase-C (PKC) pathway [Yoshida et al., 1994a]. Stt4 protein presents in its sequence one LKU (lipid kinase unique) domain and a PI4K (PI4-kinase) domain. The topological organization of this protein is conserved from *Saccharomyces cerevisiae* to mammals [Baird et al., 2008].

Although this enzyme has a cytoplasmic localization, it is also required at the plasma membrane where it is anchored to trans-membrane proteins, to generate PI4P lipid from PI [Foti et al., 2001]. The PI4P pool of PM (PM-PI4P) can then

either function in activating transduction-signalling pathways, such as MAP kinase cascade and Hh signalling pathway or it can be further converted to PI(4,5)P_2 by Mss4p (Multicopy Suppressor of Stt4) kinase [Audhya et al., 2000]. The PI4P levels of the PM are modulated by Sac1 phosphatase, which converts PI4P into PI [Foti et al., 2001].

The Stt4 kinase is linked to pathways that are regulated by changes in PM-PI4P levels and in *Saccharomyces cerevisiae*, PI4P pools at the PM are involved in the positive regulation of the MAP kinase cascade [Audhya and Emr, 2002]. Additionally, in *Drosophila*, the PI4P pools generated by Stt4 are involved in activating the Hh signalling pathway [Yavari et al., 2010]. Modulation of the Hh signalling pathway was also observed by studying the murine ortholog of Stt4 protein in mouse fibroblasts [Yavari et al., 2010], indicating that this function is conserved in mammals. The phenotypes in yeast associated with mutations in *Stt4* are altered integrity of wall signalling, that can be rescued by PKC1 over-expression suggesting that Stt4 kinase plays a role in PKC1 pathway [Yoshida et al., 1994a, Yoshida et al., 1994b].

Evidence of the direct interaction between Stt4 kinase and VAP proteins come from a large-scale affinity capture screen carried out in yeast aimed to identify multiprotein complexes carried out in yeast, which provides further evidence that VAP proteins are involved in regulating lipid metabolism [Gavin et al., 2002]. Nevertheless, the interaction between these two proteins needs to be examined *in vivo*.

1.8.2 VAP-interacting proteins containing a FFAT motif in their sequence

In eukaryotes lipids are transferred through the cytosol between different sub-cellular compartments using mechanisms that are independent from vesicular transport [Voelker et al., 2000]. This mode of lipid transfer is directed by lipid binding proteins [Wirtz et al., 1991]. A crucial requirement of these proteins is

their ability to bind to specific sub-cellular organelles. To achieve this, they possess motifs that allow them to interact with resident proteins at specific intracellular membranes. As the synthesis of the majority of lipid molecules occurs in the ER, this organelle has a crucial role in lipid trafficking [Baumann and Walz, 2001]. Additionally, biochemical assays confirmed that the ER compartment is involved in non-vecicular lipid transfer [Vance and Vance, 1990; Voelker, 2000].

The FFAT motif was characterized by studying the residues that are required for the interaction between Scs2p, the VAP yeast homologue, and the transcriptional regulator named Opi1p [Loewen et al., 2003]. The consensus sequence of the FFAT motif was determined as EFFDAXE. Later, VAP proteins were shown to interact with several FFAT-containing proteins that bind and transport lipids. These proteins include human homologues of ceramide transport protein (CERT) [Kawano et al., 2006], oxysterol-binding protein (OSBP) [Wyles et al., 2002], and phosphatidylinositol (PtdIns)/phosphatidylcholine (PtdCho)-transfer protein, Nir2 [Amarilio et al., 2005]. More recently, VAP has been shown to interact with many other proteins involved in lipid metabolism with a "FFAT-like motif", indicating that the consensus sequence may be more variable than previously thought [Mikitova & Levine, 2012].

In *Saccharomyces cerevisiae*, the site in VAPB that recognizes the FFAT motif was identified as a highly conserved 16-amino acid motif in the amino-terminal portion, within the MSP domain [Kaiser et al., 2005]. Surprisingly, MSP proteins do not contain in their MSP domain the FFAT- binding motif [Kaiser et al., 2005]. The crystal structure of the interaction between the FFAT motif and the FFAT-binding motif of the mouse VAPA has been determined [Kaiser et al., 2005]. This model shows that four amino acids (Lys45, Thr47, Lys87 and Lys 118) of the mouse VAPA sequence are responsible for making hydrophobic van der Waals contacts with the aliphatic side chains of the FFAT motif. This

FFAT-binding domain is present also in VAPB, and in addition Thr47, corresponding to Thr46 in human VAPB was found mutated in a group of ALS8 patients [Chen et al., 2010]. Moreover, the capability of the *Saccharomyces cerevisiae VAPB* gene of rescuing the phenotype in *scs2Δ* mutant, is lost when the four residues are mutated [Loewen, and Levine, 2005]. These data support the idea that the FFAT-binding domain of VAPs is crucial for the correct function of this protein [Lev et al., 2008].

1.8.2.1 OSBP

Oxysterol binding protein (OSBP) is a cytoplasmic protein with a molecular weight of 95-110 kDa. It belongs to the OSBP-related protein (ORP) family and was the first member of this highly conserved protein family to be identified [Taylor et al., 1985]. Subsequently, this protein was purified from rabbits and human where the cDNAs of these proteins were cloned [Dawson et al., 1989; Levanon et al., 1990]. Several homologues from different species have been determined for OSBP, as well as for the majority of ORPs [Lehto et al., 2001; Jaworski et al., 2001; Anniss et al., 2002]. ORPs from different species including mouse, rat, *Drosophila*, and *C. elegans*, were identified and characterized, with yeast and human ORPs receiving the most attention [Raychaudhuri et al., 2010]. Humans have 12 ORPs whereas yeast has only 7 ORP members, which are named OSH1-7 [Lehto et al., 2001; Beh et al., 2001].

All these ORPs possess the characteristic ORP motif (EQVSHHPP) as well as an ORP lipid-binding domain [Raychaudhuri et al., 2010]. Additional domains were also identified in the majority of these proteins including pleckstrin homology (PH) and FFAT domains. These two motifs were found conserved in ORPs through various species ranging from yeast to humans [Raychaudhuri et al., 2010].

The PH domain (120 aa) is a domain which has been identified at first in

pleckstrin proteins, and was subsequently reported in many proteins that are associated with microtubules and involved in cell signaling [Haslam et al., 1993; Mayer et al., 1993]. However, the interaction with phosphoinositide phosphate (PIPs) species is a very well studied functional characteristic of all the PH domains [Lemmon et al., 2000]. Each PIP isomer localizes specifically to an intracellular organelle [De Matteis et al., 2002], and PH-domain containing proteins can localize to specific subcellular membranes according to the PIP specie that is recognized by their PH domain [Hanada et al., 2009].

The OSBP protein possesses a PH domain [Ridgway et al., 1992] that specifically interacts with the PIP isomers PI4P and $PI(4,5)P_2$ [Hanada et al., 2003; Levine and Munro, 2002; Godi et al., 2004]. Although OSBP is a cytosolic protein, it can relocate to the Golgi apparatus through the interaction with PI4P in response to an increase in 25-hydroxycholesterol (25-HOC), a cholesterol derivative, levels. The association of OSBP is made possible by the interaction of OSBP with 25-HOC [Lehto and Olkkonen, 2003]. The FFAT domain of OSBP mediates its interaction with VAP proteins [Loewen et al., 2003; Kaiser et al., 2005], which was revealed during a yeast two-hybrid screen aimed at identifying new interactors of OSBP [Wyles et al., 2002].

In yeast, VAPs and ORP1L colocalize at the contact sites between endosomes and ER membranes [Rocha et al., 2009]. VAPs, in association with Oxysterol-binding homology (Osh) proteins, seem to play a role in the regulation of Sac1 PI phosphatase function at the membrane contact sites [Stefan et al., 2011]. Sac1 is a PI4P phosphatase that also interacts with VAP proteins, although the domains responsible for this interaction have yet to be identified. Yeast VAPs seem to positively control the function of Osh3 at the contact sites between plasma membrane and endoplasmic reticulum. The Osh3 function that is regulated by Scs2p senses PI4P pools at the PM, which activates Sac1 at the ER [Stefan et al., 2011].

Two other yeast PI phosphatases, synaptojanin and myotubularin orthologs, named Sjl3 and Ymr1 respectively, are also regulated by the interaction between Scs2p and Osh7 proteins [Parrish et al., 2005]. Stefan et al., [2011] reinforced the idea that Oshs are PIPs sensors and that these proteins have the ability to activate Sac1 phosphatase in response to changes in PIPs levels.

1.8.2.2 CERT

CERT, (also known as Goodpasture antigen binding-protein), is a 68 kDa cytoplasmic protein, that possesses an amino-terminal 120 aa PH domain [Raya et al., 1999; Raya et al., 2000], a central 250 aa serine-repeat (SR) region, a FFAT motif, and, a 230 aa 'steroidogenic acute regulatory protein (STAR)-related' (START) domain in the C-terminal portion of CERT [Ponting et al 1999]. It is a protein implicated in Ceramide transfer [Hanada et al., 2003] and was uncovered because of its ability to restore ceramide transport defects from the ER to the Golgi in a CHO (Chinese Hamster Ovary) mutant cell line [Hanada et al., 2003]. The localization of CERT at the ER depends on the interaction with VAPs, whereas its localization at the Golgi complex membranes depends on its interaction with PI4P through the PH domain. The human CERT protein appears to have a cytoplasmic distribution pattern, but it is enriched at the Golgi compartment [Kawano et al., 2006]. The *Drosophila* counterpart localizes mainly to the ER and to the Golgi apparatus [Rao et al., 2007]. CERT orthologs are found in both invertebrates and vertebrates, but are absent in prokaryotes, unicellular eukaryotes, and plants [Hanada et al., 2009].

The FFAT motif is required for the interaction of human CERT with human VAP-A protein in human (HeLa-S3) and CHO-K1 cultured cells [Kawano et al., 2006]. The 230-aa START domain at the carboxyl-terminal of the protein is required for removing the ceramide molecules from the membranes and delivering them to other membranes (Fig. 4) [Ponting et al., 1999; Hanada et al., 2003; Kumagai et al., 2005].

SR motif phosphorylation is fundamental to regulate the localization of CERT to the ER, Golgi apparatus, and nucleus/cytoplasm. When the SR motif is hyperphosphorylated CERT is distributed to the nucleus/cytoplasm, because the SR motif phosphorylation induces an inhibitory interaction between START domain and PH domain [Kumagai et al., 2007]. Consequently, the PH domain cannot bind PI4P on the Golgi, the START domain cannot transfer the ceramide, and also the FFAT domain is unable to bind VAPs on the ER. When SR motif is dephosphorylated. The PH, START, and FFAT domains can fulfill their function, thus CERT can translocate to the Golgi apparatus or ER. In this context the Ceramide can be transferred from the ER to the Golgi complex [Kumagai et al., 2007].

DCERT null mutant *Drosophila* strains present phenotypes such as decreased lifespan, increased susceptibility to oxidative stress of the plasma membranes, and decreased levels in Ceramide phosphoethanolamine (CPE) [Rao et al., 2007]. CPE is the structural analog of sphingomyelin [Acharya and Acharya, 2005].

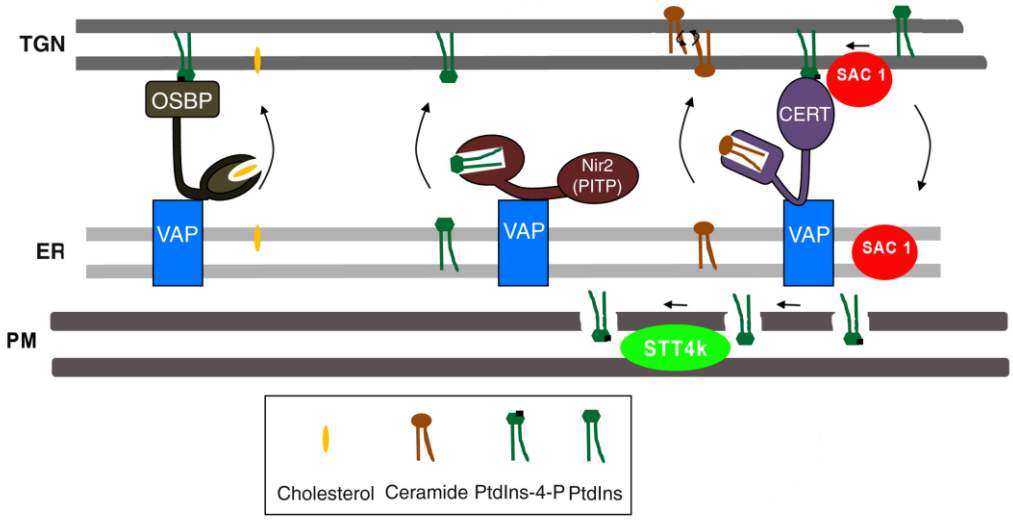

Figure 4. Diagram showing the VAPB interacting partners that are implicated in lipid metabolism. This figure illustrate PI4P being central among the activities of OSBP, Sac1, CERT, VAP, STT4k and Nir2. TGN= Trans-Golgi network. ER= Endoplasmic Reticulum. PM= Plasma Membrane. PtdIns=Phosphoinositide. PtdIns-4-P= Phosphoinositide-4-phosphate. Figure adapted from Bankaitis et al., 2012.

1.9 Aims of the project

The molecular causes of VAPB-induced neurodegeneration in ALS type 8 are still poorly understood. As a number of proteins involved in lipid metabolism were identified as interacting partners of VAPs, it seems that VAPs play an important role in this pathway. It is tempting to hypothesize that the VAP-mediated neurodegenerative process can be caused also by the disruption of some steps in lipid turnover. This hypothesis is reinforced by the fact that other neurodegenerative diseases are caused by alteration of this cellular process. In particular, the Sac1-DVAP interaction has been the starting point of this study. My PhD work has been developed as follows:

1. Characterization of the interaction between Sac1 and DVAP
2. Sub cellular localization of Sac1 and association of Sac1 and DVAP *in vivo*
3. Functional characterization of the Sac1-DVAP interaction at the larval NMJ
4. Involvement of Sac1 phosphatase in VAPB-mediated neurodegeneration

MATERIALS AND METHODS

Chapter 2:

2.1 Materials

2.1.1 *Drosophila melanogaster* stocks

Strain	Source
Canton S	Bloomington *Drosophila* Stock Center
Yw	Bloomington *Drosophila* Stock Center
BG57-Gal4	V. Budnik (University of Massachusetts Medical School, US)
elav^{C155}*-Gal4*	Bloomington *Drosophila* Stock Center
Eyeless–Gal4	Bloomington *Drosophila* Stock Center
ΦX-22A	Bischof lab (Department of Cell Biology and Infection, Institut Pasteur, Paris, France)
DVAP-P58S	G. Pennetta (Centre for Integrative Phisiology, University of Edinburgh, UK)
DVAP-T48I	G. Pennetta (see above)
DVAPRNAi	Vienna *Drosophila* RNAi Center
Sac1^{133A}	G. Pennetta (see above)
Sac1RNAi	Vienna *Drosophila* RNAi Center

Table 2. *Drosophila* strains

2.1.2 General solutions and reagents:

Reagent	Source
Agarose	Melford Cat.9012-36-6
Dithiothreitol (DTT)	Fluka Cat. 43817
Ethylenediaminetetraacetic (EDTA)	ICN Cat. 800683
Sodium Chloride (NaCl)	Fisher Scientific Cat. S/3105/63
Normal Goat Serum Donor Herd (NGS)	Sigma Cat. G6767
Phenylmethylsulfonyl fluoride (PMSF)	Sigma Cat.P7626
Protease inhibitor cocktail tablets (complete Mini, EDTA-free)	Roche Cat. 11 836 170 001
Vectashield medium	Vector Laboratories Cat. 94010
Picric Acid solution	Sigma Cat. P6744
Formaldehyde solution 37-41%	Fisher Scientific Cat. F/1501/PB17
Glacial Acetic Acid	Fisher Scientific Cat. A/0400/PB17
Paraformaldeide	Sigma Cat. P6148
Na pyrophosphate tetrabasic decahydrate, SigmaUltra, minimum 99.0%	Sigma Cat. S6422
Na Fluoride	Sigma Cat. S7920
Na orthovanadate	Sigma Cat. 450243
10X Phosphate-buffered Saline (PBS) (stock solution)	137 mM NaCl, 2.7 mM KCl, 10 mM Na_2HPO_4, 2mM KH_2PO_4 in MilliQH_2O. Dilute to 1X PBS for working solution
PBS-0.1% Triton (PBT)	Dilute 10X PBS to 1X PBS and add 1% triton
Luria Bertani (LB) broth granulated	Melford Cat. GL1704
LB agar granulated	Melford Cat. GL1706
10X Tris EDTA (TE) pH8.0 (stock solution)	100mM Tris-Cl, 10mM EDTA (pH8.0) in total volume of 50 ml.
1X Tris EDTA pH8.0 (working solution)	Dilute the 10X TE to 1X TE with MilliQ H_20

Table 3. General solutions and reagents

2.2 Methods

2.2.1 Cloning procedure

2.2.1.1 Polymerase Chain Reaction (PCR)

In order to amplify DNA using the polymerase chain reaction (PCR) technique, the following reagents were mixed in a 0.5ml tube placed on ice: 26 µl of ddH_2O, 5 µl of Pfu 10x reaction buffer, 5 µl of dNTP (10mM tock), 5 µl of forward primer (10mM tock), 5 µl of reverse primer (10mM tock), 3 µl of DNA template (300 ng), and 1 µl of *Pfu* polymerase enzyme. The total reaction volume was 50 µl. Then, a layer of equal volume of mineral oil was applied on top of the PCR mixture, to avoid evaporation. The tube was, then, placed in a thermo-cycler machine and the following cycling conditions were used;

Step	Time	Temperature (°C)	Cycles
DNA polymerase activation	2 min	95	1
Denaturation	30 sec	95	30
Hybridization	50 sec	60	
Extension	2 min	68	

When the reaction was complete, the layer of mineral oil was discarded and the PCR mixture containing the DNA product was subjected to a phenol-chloroform extraction procedure to remove proteins. 200 µl of 1XTE pH8.0 and 200 µl of Phenol Chloroform-isoamyl alcohol mixture was added to the DNA mixture. After a centrifugation step at 12000xg for 5 minutes, the upper layer containing the DNA was placed into a clean microfuge tube. DNA was precipitated in 500 µl of 100% Ethanol and 20 µl 3M NaAc for 1h at -80°C or over night (O/N) at -20 °C. The next day the precipitated DNA was pelleted by centrifugation at 12000xg for 30 minutes. Excess ethanol was removed and the pellet was air-dried before being dissolved in 1XTE buffer pH 8.0, in 10-50 µl.

Reagents and Solutions:

Reagent	Source
Pfu polymerase enzyme and buffer	Agilent (formerly Stratagene) Cat. 600670
dNTP (10mM tock)	
Mineral oil	Sigma Cat. 8042-47-5
Phenol-Chloroform-isoamyl alcohol mixture	Sigma Cat. 77617
100% Ethanol	AnalaR Normapur Cat. 20821.365

Table 4. Reagents and Solutions for PCR

2.2.1.2 Enzymatic restriction digestion

Plasmid or PCR amplified DNA was subjected to a restriction endonuclease digestion reaction. In a total reaction volume of 40 µl, the following components were added: DNA re-suspended in 30 µl of 1XTE pH8.0, 4 µl of 1XBSA, 4 µl of 10Xbuffer, 1 µl of enzyme 1 and 1 µl of enzyme 2. The digestion reaction was carried out at 37°C for 4 h. If the restriction enzymes buffers were not compatible, then two sequential individual digestion reactions were required. In this case the DNA was precipitated and re-suspended in 23 µl of 1XTE pH8.0, as the total volume of the digestion reaction was 30 µl. The reaction mixture was prepared as follows: DNA re-suspended in 23 µl of 1XTE pH8.0 3 µl of 1XBSA, 3 µl of 10Xbuffer, 1 µl of enzyme. In this case, the digestion reaction mixtures was incubated at 37°C for 2 h.

When all the restriction digestion reactions were completed, DNA was precipitated as previously described and were re-suspended in 10 µl of 1XTE pH8.0.

Reagents:

Restriction enzyme	Source
Bam HI + buffer +10XBSA	NEB Cat. R0136
*Bgl*II + buffer +10XBSA	NEB Cat. R0144
*EcoR*I + buffer +10XBSA	NEB Cat. R0101
*Kpn*I + buffer +10XBSA	NEB Cat. R0142
*Not*I + buffer +10XBSA	NEB Cat. R0189
*Sal*I + buffer +10XBSA	NEB Cat. R0138
*Xba*I+ buffer +10XBSA	NEB Cat. R0145

Table 5. Reagents and Solutions of enzymatic restriction reaction

2.2.1.3 Ligation reaction

DNA fragments purified for cloning into an appropriate vector were digested with an appropriate restriction enzyme to ensure that both insert and vector had compatible ends that could allow the insertion of the DNA fragment in the vector. In order to optimize the ligation reaction outcome it was important to combine the two DNAs following a 1:3 insert: vector molar ratio. The amount of insert and the amount of the DNA molecules was roughly estimated by running 1 µl from each DNA sample on a 1% agarose gel. The reaction mixture had a final volume of 20 µl and it was prepared as follows: 16 µl of DNA insert, 1 µl of DNA vector, 2 µl of 10X ligase buffer, 1 µl of T4 DNA Ligase. The ligation reaction was carried out at 16°C O/N. The next day the DNA constructs was ready for bacterial transformation.

Reagents:

Reagent	Source
T4 DNA Ligase + Buffer	NEB Cat. M020T

Table 6. Reagents and Solutions of ligation reaction

2.2.1.4 Bacterial transformation

Plasmid DNA can be propagated in bacterial cells using a transformation procedure. Briefly, 100 µl of competent bacterial cells were thawed on ice and, after, they were incubated with 1.7 µl of β-Mercaptoethanol (β-ME) for 10 minutes on ice. Super optimal broth (SOB) broth was preheated. 10 µl of the transforming DNA was added to the competent cells and the mixture was incubated on ice for 30 minutes. The transformation mixture was heat-pulsed at 42°C for 45 seconds and immediately incubated for 2 minutes on ice, immediately after. 1 ml Super optimal catabolite repression (SOC) broth was added to the transformation mixture and the tube was incubated for 1 hour at 37°C with shaking at 250 rpm. The transforming mixture was spread over LB agar plates with an appropriate antibiotic selection, depending on the plasmid used. The LB plates were left at 37°C over night. Bacterial colonies will only grow on LB agar plates if they are resistant to the antibiotic selection, which is conferred by an antibiotic resistance cassette that is present in the vector. The DNA from these colonies was extracted in order to check whether the desired construct has been obtained. This protocol was used to transform XL1-blue supercompetent cells, and BL21 (DE3) Competent cells.

Reagents and Solutions:

Bacterial Strain	Source
XL1-blue supercompetent cells + β-ME	Stratagene Cat. 20036
SOB (1litre)	Dissolve in 500 ml of ddH_2O: 20 g of tryptone, 5 g of yeast extract, 0.5 g of NaCl, add MilliQ H_2O to a final volume of 1 liter and autoclave to sterilize. Add 10 ml of sterile 1 M $MgSO_4$ and 10 ml of sterile 1 M $MgCl_2$
SOC (1ml)	1ml of SOB medium, 20 µl of 1M glucose, 10 µl of $MgSO_4$. 5 µl of $MgCl_2$

Table 7. Reagents and Solutions used for bacterial transformation

2.2.1.5 Amplification and extraction of DNA using a boiling protocol

Bacterial cells were prepared by inoculating 2 ml of LB broth containing appropriate antibiotic with a single bacterial colony in a bijoux tube. The 2ml-bacterial cultures were incubated at 37°C O/N with vigorous shaking. The next day 1.5 ml from each inoculate was transferred to a 1.5ml microfuge tube, and the bacteria were pelleted by centrifugation at 12,000xg for 2 minutes at room temperature. The supernatant was discarded and the bacteria were re-suspended in 350 µl of cold STET buffer, the mixture was vortexed for few seconds and 25µl of a lysozyme solution (10mg/ml in 10mM Tris-HCl, pH8.0) was added to the tube. The tubes were heat-shocked for 1 minutes at 95°C and immediately centrifuged at 12,000xg for 10 minutes. The bacterial debris pellet was picked up and trashed, whereas the supernatant was mixed with 40 µl of 2.5 M NaAc pH5.5 and 420 µl of isopropanol. The mixture was incubated for 5 minutes at room temperature, and then centrifuged at 12000xg for 10 minutes. The supernatant was discarded by aspiration and the DNA pellet was re-suspended

in 70% ethanol. The DNA was precipitated by centrifuging at 12000xg for 2 minutes. After pouring off 70% ethanol was the DNA pellet was left to air dry before resuspending the pelleted DNA in 1XTE buffer pH8.0. The DNA obtained from this extraction was analysed by restriction endonuclease digestion to identify the clone of interest.

Reagents and Solutions:

Reagents	**Source**
Isopropyl alcohol	Sigma Cat. I9030
Lysozyme, from chicken egg white	Sigma Cat. L6876
STET buffer	10mM Tris-Cl (pH8.0), 0.1M NaCl, 1mM EDTA (pH8.0), 5%(v/v) Triton X-100

Table 8. Reagents and Solutions of amplification and extraction of DNA by boiling miniprep

2.2.1.6 Large scale preparation of DNA by alkaline lysis

200 µl from the remaining bacterial culture corresponding to the right DNA samples were inoculated in 150 ml of LB broth containing the appropriate antibiotic selection. The culture was grown in a shaking incubator 12-16 hours at 37°C with vigorous shaking (200-250rpm). The DNA extraction was performed in the culture using the Qiagen Maxiprep kit (Qiagen) according to the manufacturer's instructions. 300 µl of 1XTE buffer pH8.0 were used to re-suspend the final DNA pellet. The DNA obtained from this extraction was analysed by restriction endonuclease digestion to double-check that the cDNA has been cloned properly in the vector. Finally, the clone DNA was direct-sequenced to control the exact sequence of the obtained clone.

Reagents:

Antibiotics	Source
Ampicillin	Sigma Cat. A-9518
Kanamycin	Sigma Cat. K-4000
Plasmid Maxi kit.	Qiagen Cat. 12163

Table 9. Reagents and Solutions of clean preparation of DNA by alkaline maxi prep

2.2.2 Generation of *UAS-FLAG-Sac1* transgenic flies:

2.2.2.1 *pUASTattb-FLAG-Sac1* cloning strategy:

To generate a construct encoding *D. melanogaster* Sac1 protein having a FLAG-tag at the N-terminus we amplified 1.7 kb *D. melanogaster Sac1* cDNA by PCR from GH08349 clone. *Bam*HI and *Sal*I restriction sites were incorporated into the primers to generate restriction sites at the 5' and 3' ends of the cDNA, respectively. Sac1 cDNA and *pCMV-Tag2b* (Clontech) (see Appendix 1, Fig. 26) were both cut with *Bam*HI and *Sal*I ligated to produce *pCMV-Tag2b-Sac1*. The sequences of the two primers were the following ones:

*Bam*HI-Sac1-F 5' TATGGGATCCGAAATCATGGACAGCAGG 3'
*Sal*I-Sac1-R 5' CCGCGTCGACTAGCTGCAGAGGTAGTTC 3'
Restriction sites underlined.

The *pUASTattB-FLAG-Sac1* was generated by cloning *FLAG-Sac1* into *pUAST attB* (obtained from A. Jarman, University of Edinburgh, U.K.) (see Appendix 1, Fig. 29) by using *Bgl*II and *Xba*I restriction sites. The *pUAST attB-Flag-Sac1* construct was injected in ΦX-22A flies (*y w M{eGFP.vas-int.Dm}ZH-2A; M{RFP.attP}ZH-22A; +; +*) (Bischof et al., 2007, obtained from A. Jarman, University of Edinburgh, U.K.).

2.2.2.2 *pUAST-FLAG-Sac1* cloning strategy:

The *pUAST-FLAG-Sac1* was generated by cloning *FLAG-Sac1* into *pUAST* (see Appendix 1, Fig. 30) by using *Not*I and *Kpn*I restriction sites.

2.2.2.3 Injection Protocol

Phi-C31 integrase system

The transgenesis performed through Phi-C31 integrase system allows the integration of the heterologous DNA at precise intergenic sites within the fly genome [Bischof et al., 2007]. Thus, several fly strains have been developed containing several landing sites on the four chromosomes besides *attP* sites and Phi-C31 integrase gene [Bischof et al., 2007]. ΦX-22A flies having a landing site on the 2nd chromosome were used in this case. Transgenic flies were generated in our lab by using the following basic injection protocol from Spradling and Rubin [1982]. Briefly, ΦX-22A flies were amplified and placed in an egg laying chamber on grape juice plate with yeast paste. Eggs were collected every 30 minutes to be injected using the FemtoJet/InjectMan NI2 system, according to the manufacturer's instructions (Eppendorf). Embryos were collected from the grape juice plate in a mesh basket using a fine brush and distilled water. Removal of the chorion (dechorionation) from embryos is required before injection to avoid needle breakage. This was performed by washing the embryos in 50% bleach solution for 3 minutes with continual agitation. The bleach solution was removed by using ddH2O. The dechorionated embryos were placed on a square piece of grape juice agar, and one edge of the piece of agar and the micropile used to orient and align the embryos. Embryos were transferred to a coverslip covered with a double-sided 3M Scotch tape strip. The coverslip with embryos was placed on a microscope slide and the embryos were left to dry up in a chamber containing silica gel for 1-3 minutes. The drying timed depended on the room humidity. A drop of

halocarbon oil 700 (Sigma) was added to cover the embryos to prevent them from drying. DNA was loaded into the injection needle (3µl of DNA, 500-600 ng/µl concentration). DNA was injected into the posterior end of the embryo. It was important that the embryos were injected before the cellularization in order to optimize the injection efficiency. Injected embryos were kept in humid chambers overnight. The larvae that survived injection were placed in vial of standard fly food mixed with yeast paste. Adult flies were crossed to *yw* fruit flies. The transformant flies were identified among the off- spring by the presence of a light-orange eye colour. Stocks were established for each individual line identified.

2.2.3 Immunocytochemistry:

2.2.3.2 *MYC- DVAP* cloning strategy:

To generate a construct encoding *D. melanogaster* VAPB (DVAP) protein having a Myc-tag at the N-terminus we amplified 810 bp *DVAP* cDNA by PCR. *Eco*RI and *Not*I restriction sites were added at the 5' and 3' of the cDNA respectively, using the following oligonucleotide primers:

*Eco*RI-DVAP-F 5'GCCAGCGAATTCCCACAATGAGCAAATCAC 3'
*Not*I- DVAP-R 5'ATAGCTGCGGCCGCTCAGAGAAAGAATTTG 3'
Restriction sites underlined

DVAP cDNA and *pCMV-Myc* (Clontech) (see Appendix1, Fig. 27) were digested with *Eco*RI and *Not*I restriction endonuclease enzymes and ligated together to produce *pCMV-Myc-DVAP*.

2.3.3 COS-7 cell transfection and staining:

COS-7 cells were cultured in Dulbecco's Modified Eagle Medium (DMEM) containing 10% of fetal bovine serum (FBS), 1% penicillin/streptomycin, and 1% glutamine. COS-7 cells were plated on BioCoatTM Poly-L-Lysine Coated Glass Coverslips of 12mm (BD Biosciences). Cells were transfected by Liposome transfection using FuGENE Transfection Reagent according to the manufacturer's instructions. COS-7 were incubated for 24 h before being fixed in 4% paraformaldehyde for 20 minutes.

For immunohistochemistry, cells were blocked in 0.1% Triton PBS (PBT) containing 10% normal goat serum (NGS) and, afterwards, stained with 1st antibody **(**αMyc rabbit polyclonal 1:200, and αFlag mouse monoclonal 1:200) in PBT containing 5% NGS for 2h. COS-7 cells were washed 8x15 minutes with PBT and they were incubated with 2nd Ab (Fluorescein isothiocyanate (FITC) αRabbit 1:500, and Cy3 αMouse 1:500) in PBT containing 5% NGS for 2h at room temperature afterwards. The cells were washed 8x15 minutes with PBT. The coverslips were mounted on microscope ground color frosted slides (VWR) in Vectashield medium (Vector laboratories), with the cells facing the slide.

Reagents and solutions:

Reagent	Source
DMEM	Gibco Cat. 21063
Fugene 6 transfection reagent	Roche Cat. 11 815 091 001
Triton X-100	Sigma Cat. T9284
rabbit αMyc polyclonal	Sigma Cat. C3956
mouse monoclonal αFlag	Sigma Cat. F3165
FITC Goat α-Rabbit IgG	Jackson ImmunoResearch Cat. 111-095-003
Cy3 Goat α-Mouse IgG	Jackson ImmunoResearch Cat. 115-165-146

Table 10. Reagents used in Immunocitochemestry

2.2.4 Co-immunoprecipitation (CoIP):

2.2.4.1 Cloning strategy:

Myc-Sac1

In order to generate a construct encoding *D. melanogaster* Sac1 protein having a Myc-tag at the N-terminus end, we amplified 1.7 kb *D. melanogaster Sac1* cDNA by PCR from GH08349 clone. *Sal*I and *Kpn*I restriction sites were added at the 5' and 3' of the cDNA, respectively, using the following oligonucleotide primers:

*Sal*I-Sac1-F5' GATTGTCGACAATCATGGACAGCAGGG 3'
*Kpn*I-Sac1-R 5' GATTGGTACCTGCTAGACGACACTAAC 3'
Restriction sites underlined
Sac1 cDNA and *pCMV-Myc* (Clontech) were digested with *Sal*I and *Kpn*I restriction endonuclease and ligated together to produce *pCMV-Myc-Sac1*.

Flag-DVAP:

To generate a construct encoding *D. melanogaster* VAPB (DVAP) protein having a Flag-tag at the N-terminus we amplified 810 bp *DVAP* cDNA by PCR from their *pBluescript* vectors (G.Pennetta). *Eco*RI and *Sal*I restriction sites were added at the 5' and 3' of the cDNA respectively, using the following oligonucleotide primers:

*Eco*RI-DVAP-F5' ATGCGAATTCGAACAACACCAGGAGCAG 3'
*Sal*I-DVAP-R5' GAGTGTCGACCGTTTATGGCATTCAGAG 3'
Restriction sites underlined
pCMV-Tag2 is a vector that contains a Flag-tag coding region upstream the multiple cloning site. *DVAP* cDNA and *pCMV-Tag2* (Sigma) were digested with *Eco*RI and *Sal*I restriction endonucleases and ligated together to produce *pCMV-Tag2- DVAP.*

Flag-DVAP-P58S

Site-directed mutagenesis on DVAP cDNA was performed using QuikChange Site Directed Mutagenesis Kit (Agilent/Stratagene), according to the manufacturer's instructions [Chai et al., 2008]. The same cloning strategy used to generate *Flag-DVAP* was used to generate a construct encoding *D. melanogaster* VAPB-P58S (DVAP-P58S) protein having a Flag-tag at the N-terminus.

2.2.4.2 COS-7 cell transfection and CoIP:

COS-7 cells were transfected with plasmid DNA as described previously. Two days after transfection, confluent cells were trypsinized and resuspended in DMEM containing the FBS. The cells were centrifuged at 1000xg for 5 minutes, the supernatant was discarded and the cells were re-suspended in PBS.

The cells were centrifuged again as before, the supernatant was discarded and cells were re-suspended in fresh lysis buffer. Cell lysis was performed by incubating cells in 1% digitonin Hepes Buffer [Kawano et al., 2006] for 45 minutes on ice. After the cells were solubilized, an aliquot was removed to use as an input sample. The input sample was kept until loading in 5% β-ME Laemmli sample buffer. The remaining cell lysate was centrifuged at 12000xg for 20 min at 4°C. Pierce Spin Columns were placed in microcentrifuge collection tubes. The supernatant was incubated with the slurry Pierce anti-c-Myc agarose resin (Pierce-c-myc IP/CO-IP kit) in Pierce Spin Columns O/N at 4°C under constant rotation. After incubation, the samples were centrifuged at 2000 rpm? for 5 min in order to separate the beads from the supernatant. The beads remaining in the column, were washed three times with 0.1% digitonin Lysis buffer. 25 µl 2X Non-Reducing Sample Buffer, prepared from the 5X Sample Buffer from the kit, was added to the beads. The column/collection assembly was heated at 95°C for 5 min, pulse centrifuged for 10 s immediately after. β-ME was added at a concentration of 4% to the eluted sample in order to prepare the sample for reducing Sodium-dodecyl-sulfate-polyacrylamide gel electrophoresis (SDS-PAGE).

Reagents and solutions:

Reagent	Source
Digitonin	Sigma Cat. D141
Hepes	Sigma Cat. H4034
Laemmli sample buffer	Biorad Cat. 161-0737
β-ME	Sigma Cat. M3148
Profound c-Myc Tag IP/Co-IP application set	Thermal Scientific Cat. 23622
1X Hepes Lysis Buffer (10ml)	5 ml MilliQH_2O, 5 ml 2X Hepes Lysis Buffer, 20 µl 0.5M DTT, 100 µl 100mM PMSF, 1 tablet protease inhibitors
2X Hepes Lysis Buffer (Lysis Buffer)	50 mM Hepes-NaOH, pH7.4, 1mM EDTA, 50 mM NaCl, 5 mM Na pyrophosphate, 50 mM Na Fluoride, 1 mM Na orthovanadate

Table 11. Reagent and solutions required to perform the Co-IP

2.2.4.3 Western Blot analysis:

The samples obtained by CoIP procedure were analysed by Western Blot. A 12% SDS-PAGE was prepared and the protein samples were loaded together with a molecular weight marker. Samples were resolved by gel electrophoresis at 100 volts for 90 min. The proteins were transferred from the gel onto Hybond-P PVDF membranes (Amersham Biosciences), in order to make them accessible to antibodies for detection. This transferring step was performed by applying an electric field of 120 V for 2 h to the proteins. Later, the membranes, having the proteins on their surface, were incubated in blocking solution over night at 4°C. This solution was made by dissolving ECL Advance Blocking Agent at a 2% in Tris buffered solution with 0.1% Tween (TBS-T). The following day, the membranes were incubated with the primary antibodies diluted in blocking solution for 2 hours at room temperature with gentle shaking. For VAP detection, guinea pig anti-DVAP (GP33, 1:40,000) antibody was added to one membrane in order to detect Flag-DVAP fusion protein, and

rabbit anti-c-Myc (1:10,000) to the other membrane to detect Myc-Sac1 tagged protein. Then, the excess of primary antibody was removed by washing the membranes vigorously with TBS-T for 2 hours changing the buffer every 15 minutes. Membranes were incubated with secondary antibodies at room temperature for 2 hours under gentle agitation. Goat anti guinea pig HRP (1:60,000) was added to bind anti-DVAP, and Ab Goat anti rabbit HRP (1:30,000) was used to bind rabbit anti-c-Myc. Vigorous washes with TBST were performed as. Enhanced chemo-luminescence (ECL) Advance Western Blotting Detection Kit was used to detect signals from the secondary antibodies according to the manufacturer's instructions. The excess of detection solution was drained off from the membrane by using a tissue, and each membrane was wrapped in SaranWrap. The wrapped blots are placed in an X ray film cassette. An autoradiography film is placed on the protein side of the wrapped blot. The membrane was exposed to autoradiography film (Hyperfilm^{TM}ECL) for 60 seconds. The film was then submerged in developer for 30-60 seconds, rinsed in water and then submerged in fixer.

Reagents:

Reagents	Source
2% ECL Advance Blocking Agent	Amersham Bioscience Cat.
SeeBlue Plus2 Pre-stained Standard	Invitrogen Cat. LC5925
EZblue gel staining reagent	Sigma Cat. G1041
Tween-20	Sigma Cat. P5927
HRP Goat anti-GP IgG	Jackson Immunoresearch
HRP Goat anti-Rabbit IgG	Jackson Immunoresearch

Table 12. Reagents used to perform the Western Blot analysis

2.2.5 Generation of anti-Sac1 antibodies:

In order to generate an antibody against *Drosophila* Sac1 protein, a *Drosophila* Sac1 antigen must be produced. The steps regarding the generation of an anti-Sac1 antibody encompass:

1. The generation of a cDNA fragment encoding Sac1 protein or Sac1 protein deletion derivative.
2. The production of the antigen that has to be injected into the animal where the antibody has to be produced.

2.2.5.1 Generation of the sequence encoding the antigen

In order to generate a cDNA sequence encoding the antigen the general cloning procedure has been followed as previously described in this section (paragraph 2.2.1). In order to clone Sac1 cDNA full-length and Sac1 cDNA deletion derivatives in the proper vector specific cloning strategies have been followed, as it is described below.

(His)$_6$-Sac1

To generate a construct encoding Sac1 fusion protein having a His-tag at the N-terminus we amplified 1.7kb Sac1 cDNA by PCR from GH08349 clone. *Bam*HI and *Sal*I restriction site were added at the 5' and 3' of the cDNA respectively. *pET28a* is a vector that contains the His-tag coding region. Sac1 cDNA and *pET28a* (Novagen) (see Appendix 1) were digested with *Bam*HI and *Sal*I restriction endonuclease enzymes and ligated together to produce *pET28a-Sac1*. The sequences of the two primers used in this cloning procedure are:

*Bam*HI-Sac1-F 5'TATGGGATCCGAAATCATGGACAGCAGG 3'

*Sal*I-Sac1-R 5'TTACGTCGACTCATGGGTCTCGAAAGGA 3'

Restriction sites underlined.

(His)$_6$-Sac1 Δ483-594

To generate a construct encoding the Sac1 deletion derivative having a His-tag at the N-terminus we amplified 1.448 kb Sac1 cDNA by PCR from GH08349 clone. *Bam*HI and *Sal*I restriction site were added at the 5' and 3' of the cDNA respectively. Sac1 cDNA and *pET28a* (Novagen) were digested with *Bam*HI and *Sal*I restriction endonuclease enzymes and ligated together to produce *pET28a-Sac1Δ483-594*. The sequences of the two primers used in this cloning procedure are:

*Bam*HI-Sac1Δ483-594-F
5'GTATTGGATCCGAAATCATGGACAGCAGGGAGGAGAAC 3'

*Sal*I-Sac1Δ483-594-R
5'CTCACGTCGACTCATCATCAAGATAGTAGCGCATCAGC 3'

(His)$_6$-Sac1 Δ354-594

To generate a construct encoding the Sac1Δ354-594 deletion derivative having a His-tag at the N-terminus we amplified 1.061kb Sac1 cDNA by PCR from GH08349 clone. *Bam*HI and *Sal*I restriction site were added at the 5' and 3' of the cDNA, respectively. Sac1 cDNA and *pET28a* (Novagen) were both digested with *Bam*HI and *Sal*I restriction endonuclease enzymes and ligated together to produce *pET28a-Sac1Δ354-594*. The sequences of the two primers used in this cloning procedure are:

*Bam*HI-Sac1Δ354-594-F
5'GTATTGGATCCGAAATCATGGACAGCAGGGAGGAGAAC 3'
*Sal*I-Sac1Δ354-594-R
5'GATACGTCGACTCATCATCAAGTATCTTCAGCCGGTCC 3'

(His)$_6$-Sac1Δ1-309

To generate a construct encoding Sac1Δ1-309 deletion derivative having a His-

tag at the N-terminus we amplified 858 bp Sac1 fragment cDNA by PCR from GH08349 clone. *Bam*HI and *Sal*I restriction site were added at the 5' and 3' of the cDNA respectively. Sac1 cDNA and *pET28a* (Novagen) were digested with *Bam*HI and *Sal*I restriction endonuclease enzymes and ligated together to produce *pET28a-Sac1Δ1-309*. The sequences of the two primers used in this cloning procedure are:

*Bam*HI-Sac1Δ1-309-F 5'GCATATGGATCCGATCACAAAGGTGCCGAA 3'
*Sal*I-Sac1Δ1-309-R 5' TTACGTCGACTCATGGGTCTCGAAAGGA 3'

$(His)_6$-Sac1Δ1-267

To generate a construct encoding Sac1Δ1-267 deletion derivative having a His-tag at the N-terminus we amplified 984 bp Sac1 fragment cDNA by PCR from GH08349 clone. *Bam*HI and *Sal*I restriction site were added at the 5' and 3' of the cDNA respectively. Sac1 cDNA and *pET28a* (Novagen) were digested with *Bam*HI and *Sal*I restriction endonuclease enzymes and ligated together to produce *pET28a-Sac1Δ1-267*. The sequences of the two primers used in this cloning procedure are:

*Bam*HI-Sac1Δ1-309-F 5'GCATATGGATCCCTGCCCAATTTGCGCTAT 3'
*Sal*I-Sac1Δ1-309-R 5' TTACGTCGACTCATGGGTCTCGAAAGGA 3'

2.2.5.2 Antigen production

When the clones have been generated, the antigen should be produced and purified from the other proteins of the bacterial host cell. The purified antigen has been quantified in order to inject the required amount of antigen into the host animal.

2.2.5.2.1 Setting up the bacterial culture:

BL21(DE3) competent cells were transformed as described before in this

chapter. Bacterial cells can be induced to generate the target protein of interest. Briefly, a single colony was inoculated in 5 ml of LB broth containing the appropriate antibiotic. This starter bacterial culture was incubated at 37 °C with vigorous shaking (220-250 rpm) until it reached 0.5 OD_{600}. Then, the bacterial culture was stored at 4°C until the next morning. The next day, the bacteria from 1 ml of starter culture were pelleted down at 5000 x g for 30 seconds in micro-centrifuge, and re-suspended in 1 ml of LB broth with the appropriate antibiotic freshly added. This 1ml-culture was inoculated in 50 ml of LB broth plus the appropriate antibiotic, and, the 50-ml-culture was made in duplicate. Incubation of the two bacterial cultures was carry out at 37°C under 220-250 rpm shaking speed until the OD_{600} between 0.6 and 1.0 was reached.

2.2.5.2.2 Synthesis of the heterologous protein:

1ml samples were removed from each bacterial culture and they were used as un-induced samples. Un-induced bacterial controls were spun down by centrifugation at 5000 x g for 5 minutes. At this point the bacteria were ready to be treated in order to induce the expression of $(His)_6$-tag fusion protein. For this, 500 µl of Isopropyl β-D-1-thiogalactopyranoside (IPTG) was added to each bacterial culture in order to obtain a final IPTG concentration of 1mM and the bacterial cultures were incubated for 2 h with vigorous shaking at 37°C. Then, the two bacterial cultures are placed on ice for 5 minutes and the bacteria were harvested by centrifuging them for 5 minutes at 5000 x g at 4°C. The supernatant was discarded and the pellet was stored at -80°C.

2.2.5.2.3 Protein extraction from BL21(DE3) bacteria

Protein extraction was carried out on bacterial pellets from cultures treated with IPTG and from the control bacterial cultures, untreated with IPTG. BugBuster (Novagen) protein extraction reagent was added to each bacterial pellet: 5 ml of the reagent were added per gram of wet pellet weight (=1 volume).

Additionally, 1 µl of benzonase nuclease per ml BugBuster protein extraction reagent was added to the mixture. The cell suspension was incubated for 15 minutes with gently shaking at room temperature (RT). Afterwards, the insoluble debris were removed by centrifuging the bacteria for 20 minutes at a 16000 x g speed at 4°C. The supernatant was transferred to a fresh tube and 2x Laemmli sample buffer, which was previously equilibrated with β-mercaptoethanol, was added to the supernatant sample at a 1:1 ratio, and it was stored at -20°C until loading. The debris pellet was thoroughly re-suspended in 1 volume of Bugbuster protein extraction reagent and in 1KU of rLysozyme solution per ml of Bugbuster protein extraction reagent. Next, the suspension was mixed thoroughly, and incubated at RT for 5 minutes. The Bugbuster protein extraction reagent was diluted 1:10 using deionized water, and 6 volumes of the diluted reagent were added to the mixture. The suspension was vortexed for 1 minute and then centrifuged for 15 minutes at 5000 x g at 4°C. The supernatant was discarded, and the previous two steps, re-suspension and centrifugation, were repeated three times, using half the volume of the original bacterial culture (25 ml) of 1:10 of Bugbuster protein extraction reagent to re-suspend the pellet. The last centrifugation step was carried out at 16000 x g. The supernatant was discarded, and the pellet was re-suspended in 1.5 ml of 1%SDS. The pellet was resuspended in 1%SDS for 2-3 minutes. 20 µl was mixed with an equal volume of 5% β-ME Laemmli sample buffer. The samples were kept at -20°C until use.

2.2.5.2.4 Protein Purification

The pellet from the previous centrifugation was re-suspended in 2.5ml 8M Urea, 1X Binding buffer and incubated in ice for 1h. The protein suspension was centrifuged for 30 min. at 16000 xg at 4°C. The elution, the wash, and the charge buffers together with the columns were prepared for the protein purification step. Once the buffers were arranged 2-3 ml of sterile ddH20 were added to the column. The His-bind resin was gently mixed by inversion to re-

suspend the resin in the storage buffer and 2ml of the suspension were transferred into the column where it passed through by gravity flow. When the storage buffer level went down, the following sequence of washes was used:

- 3 volumes of sterile ddH20 (3ml)
- 5 volumes of Charge Buffer (5ml)
- 3 volumes of Binding Buffer (3ml)

The protein sample was applied to the column and treated by adding the following reagents: 10 volumes of 1X Binding Buffer (10ml), 2 volumes of 1X Wash Buffer, 6 volumes of 1X Elution Buffer. Each ml of 1X Elution buffer exiting the column was saved separately. Each ml corresponds to one elution fraction. All the elution fractions were loaded on a 8% acrylamide gel for Western Blot analysis of the fraction to determine where the majority of the eluted protein was concentrated. The buffers and the $(His)_6$-bind resin are included in $(His)_6$-Bind Purification Kit (Novagen Cat. 70239-3).

2.2.5.2.5 Protein Quantification

The elution fractions containing the majority of the recombinant protein were pooled together and 20μl were loaded for comparison to known BSA dilutions (0.01 μg, 0.1 μg, 1 μg, 5 μg, 10 μg). As the Sac1 fragment appeared to have a concentration close to 1 μg, we made another more precise, quantification comparing our protein to the following BSA dilutions: 0.5 μg, 1 μg, 1.5 μg, and 2 μg. The success of protein extractions from inclusion bodies was tested by loading the protein samples on 8% acrylamide gel. Simultaneously, a protein ladder was loaded on the acrylamide gel together with the samples in order to recognize the Sac1 protein fragment by its size. The acrylamide gel was washed in ddH20 in order to remove the SDS in excess. Next, the gel was incubated in EZ Blue gel staining reagent (Sigma) in order to dye all the proteins on the gel for 45 min. at RT. Excess staining reagent was removed by incubating the gel in ddH20 over night at RT. The next morning the gel was treated with a de-staining solution (20% methanol and 3% glycerol).

Reagents

Reagent	Source
Sodium dodecyl sulphate (SDS)	Sigma Cat. L4509
Benzonase Nuclease	Novagen Cat. 70664-3
BL21 (DE3) Competent cells + β-ME	Stratagene Cat. 200131
BSA fatty acid free low endotoxin	Sigma Cat. A8806
Bugbuster Reagent	Novagen Cat.70584
EZ blue gel staining reagent	Sigma Cat. G1041
IPTG	Sigma Cat. I6758
rLysozyme™ solution	Novagen Cat. 71110-3

Table 13. Reagents used in the process to generate the anti-Sac1 antibody

2.2.6 Immunohistochemistry:

2.2.6.1 NMJ staining and larval muscles staining

Fly crosses were set up for 20-24 h at room temperature before being transferred to a 30°C water-bath. Third instar larvae of the required genotype were dissected in 1XPBS to fillet the larvae. The dissected tissues, usually from 8 animals per set, were fixed in Bouin's fixative for either 5 min or 10 min, according to the antibody that was used. The fixation reaction was stopped by rinsing the tissues with PBT. The fixed preparations were blocked in PBT with 10% NGS for 2h at room temperature under continuous rotation. The preparations were incubated over night with primary antibody at the required concentration in PBT containing 5% NGS, under constant rotation at 4°C. The next morning the tissues were washed 8x15 minutes with PBT, before incubation with 2nd antibody in PBT with 5% NGS for 2 hours at RT under gently shaking. Excess secondary antibody was removed by washing the preparations in PBT 8 times, changing the solution every 15 minutes. Tissues

were mounted on microscope ground colour frosted slides (VWR) using Vectashield medium. An Axiovert Zeiss microscope was used to visualize the larval neuromuscular junctions.

2.2.6.2 Larval brains, larval salivary glands, and larval eye imaginal discs staining

The third instar larvae of the required genotype were dissected in 1XPBS. The dissected tissues, usually from 20 animals per set, were fixed in 4% paraformaldehyde fixative for 10-20 min, accordingly to the antibody that was used. The fixation reaction was stopped by rinsing the tissues with PBT. The preparations were blocked in PBT with 10% NGS for 2h at room temperature under continuous rotation. Preparations were incubated over night with primary antibody at the required concentration in PBT containing 5% NGS, and they were kept under constant rotation at 4°C. The next morning the tissues were washed 8x15 min. with PBT before being incubated with 2^{nd} antibody in PBT with 5% NGS for 2 hours at RT under gently shaking. Excess of secondary antibody was removed by washing the preparations in PBT 8 times, changing the solution every 15 minutes. Tissues were mounted on microscope ground colour frosted slides (VWR) in Vectashield medium. An Axiovert Zeiss microscope was used to visualize the larval brains.

Reagents and Solutions:

Solution	Recipe or Source
4% paraformaldehyde (50 ml)	50 ml PBS, 2g paraformaldehyde
Bouin's fixative	15ml saturated picric acid, 5ml 37% Formaldehyde, 1ml glacial acetic acid
AffiniPure Rabbit α-Horseradish Peroxidase (HRP)	Jackson ImmunoResearch Cat. 323-005-021
Guinea Pig α-DVAP (GP33)	G. Pennetta
Mouse monoclonal α-KDEL	Stressgen Bioreagents Cat. SPA-827
Rabbit α-Sac1	G. Pennetta
Mouse α-DLG	DSHB
Mouse α-HTs1B1	DSHB
α-Boca	(Culi's group)
α-dGM130	Abcam Cat. Ab30637
α-Fustch	DSHB
α-dCSP2	DSHB
Mouse α-Adducin	DSHB
Rabbit α- βspectrin	Cat.
Cy3 Goat α-guinea pig IgG	Jackson ImmunoResearch Cat. 106-165-003

Table 14. Solutions required to perform immunohistochemistry analysis

Primary Antibody dilutions:

Antibody	**Concentration**
α-Boca	1:1000
α-dGM130	1:100
α-Fustch	1:50
α-dCSP2	1:50
Mouse α-Adducin	1:50
Rabbit α- βspectrin	1:500
Mouse α-DLG	1:50

Table 15. Dilutions of the primary antibodies used in immunohistochemical experiments

2.2.7 Adult *Drosophila* Eye paraffin sections:

Adult fruit flies of the appropriate genotype were dissected to leave just the head attached to the abdomen. The proboscis was removed from the head, and the heads together with abdomen were incubated in fixative solution O/N at RT under gently shaking. The next day, fixed heads were moved from the fixative solution to an 80% ethanol solution and they were stored at 4°C. Later, the flies were placed in the "Martin Heisenberg fly collar" whilst they were kept in 80% ethanol solution. Fly heads were dehydrated as follows: incubation in 95% ethanol solution for 5 minutes, incubation in 100% ethanol for 10 minutes. Following the dehydration step, the heads were incubated in a solution of 1:1 100%Ethanol/Xylene for 5 minutes. Heads were incubated in a 1:1 xylene/paraffin solution. The heads were left in 100% paraffin O/N at 65°C. The next day, liquid paraffin was poured into the metal boats and the fly collars with heads were transferred to the metal boats. Once the paraffin block was made the heads were ready for microtome sectioning. The paraffin sections were slice to obtain a thickness of 4μm. The slices were transferred to 'Superfrost^{+} slides'. The samples underwent Haematoxylin + Eosin staining. The samples were examined an Olympus AX70 microscope.

RESULTS

Chapter 3: Sac1 physically associates with DVAP

3.1 Introduction

The relationship between neurodegeneration and the mutations T46I and P56S in the MSP domain of hVAPB has been proved [Chai et al., 2008; Chen et al., 2010]. However, the exact molecular mechanism underlying the ALS8-mediated neurodegeneration is still unclear. To address this issue we decided to look at the interacting partners of the *Drosophila* orthologue of hVAPB protein DVAP-33A or DVAP. Thus, a yeast two-hybrid screen performed by Dr. K. Parry, aimed at identifying interacting partners of DVAP identified a direct interaction between Sac1 phosphatase and DVAP. This interaction has been identified already in yeast during a genome-wide yeast two-hybrid screen by Giot et al., [2003].

The interest in the analysis of this protein-protein interaction in the study of the molecular mechanism underlying ALS 8 comes from a number of reasons. First, a SAC3, also known as FIG4, a protein belonging to the SAC protein family, was found mutated in some ALS cases. SAC3 is a PIP phosphatase which dephosphorylates PI3P specie [Chow et al., 2007]. Second, other neurodegenerative diseases are caused by mutations in gene encoding enzymes involved in PIP metabolism. Mutations in *SAC3* were identified also in Charcot-Marie-Tooth disorder sufferers [Chow et al., 2007]. Charcot-Marie-Tooth disease is a MND. Also same cases of Alzheimer disease were associated to mutations in a PIP phosphatase, synaptojanin 1 [Voronov et al., 2008]. This phosphatase is mainly expressed in neurons where it has $PI(4,5)P_2$ as substrate [Di Paolo and De Camilli, 2006; Gong and De Camilli, 2006]. Lastly, evidence of the implication of VAPB protein in regulating the activity of Sac1 was reported in yeast [Stefan et al., 2011]. All together these pieces of evidence suggest that the characterization of the interaction between dSac1 and DVAP could be used to determine the molecular cause of the VAPB-mediated ALS.

Thus, as a starting point, the dSac1-DVAP association has been confirmed *in vitro*.

3.2 The interaction between DVAP and Sac1 is detected by co-immunoprecipitation

In order to confirm this interaction *in vitro*, the co-immunoprecipitation (Co-IP) assay was used. Firstly, two tagged proteins were generated: Myc-DVAP and Flag-Sac1. Myc-tag has been chosen as it is a small peptide (11 aa with a MW of 1.20 kDa, N-EQKLISEEDL-C) and it is hydrophilic. These two characteristics allow this tag to be placed outside the protein during the proteon folding. Therefore, myc-tag can affect marginally the tertiary structure of DVAP protein, and, thus, DVAP function. In addition, a myc-tagged DVAP fusion protein has been previously generated [Ratnaparkhi et al., 2008]. Similarly, the human orthologue of DVAP (hVAPB) has been fused to the myc peptide [Peretti et al., 2008; Suzuki et al., 2009; Kim et al., 2010], meaning that small tags can be attached to VAP proteins without significantly affecting their function. In addition, the Myc-tag has been successfully used in immunoprecipitation assays [Kipriyanov et al., 1996]. Thus, DVAP was conjugated with a myc-tag and the beads crosslinked with an antibody against myc was used. N-terminal myc-DVAP fusion protein was generated (Fig. 5) by cloning *DVAP* cDNA in *pCMV-Myc* vector that includes a myc-encoding sequence upstream the MCS (see Appendix 1, Fig. 27).

On the other hand, Sac1 protein was conjugated to a different protein tag (flag-tag) (Fig. 5). The flag-tag is also a small (8 aa with a MW of 1.01 kDa, DYKDDDDK) [Hopp et al., 1988] and highly hydrophilic peptide [Terpe et al., 2003]. N-terminal flag-Sac1 tagged protein was generated by cloning Sac1 cDNA in *pCMV-Tag2B* vector, which contains a flag-tag-encoding sequence upstream the MCS (see Appendix 1, Fig. 26). In parallel, the possibility that the

ALS8-causative mutation P56S could affect the interaction between Sac1 and hVAPB was explored. To this end *DVAP* cDNA has been mutagenized in order to express a DVAP protein having the proline-58 that corresponds to the proline-56 in hVAPB, changed to a serine. Then, *DVAP-P58S* cDNA was cloned in *pCMV-Myc* vector in order to generate Myc-tagged DVAP-P58S fusion protein.

Subsequently, COS-7 cells were used as an expression system and, thus, they were transfected as follows: *pCMV-Tag2b-Sac1* together with *pCMV-Myc-DVAP*, and *pCMV-Tag2b-Sac1* together with *pCMV-Myc-DVAP-P58S*. In addition three single transfections with the three constructs (*pCMV-Tag2b-Sac1* alone, *pCMV-Myc-DVAP* alone, and *pCMV-Myc-DVAP-P58S* alone) were used as controls. In fact, flag-Sac1 fusion protein cannot precipitate with the beads in the absence of myc-DVAP. Then, the proteins were extracted from COS-7 cells by using a lysis buffer containing the mild detergent digitonin [Kawano et al., 2006]. Whether a detergent is defined mild or not it depends on its ability to denature proteins. Anti-Myc beads were used to precipitate DVAP-Sac1 complex and the DVAP-P58S-Sac1 complex. The presence of the fusion protein was tested on input, supernatant and pellet fractions from the COS-7 lysates. The input fraction represents the lysate before treatment with the beads crosslinked with the anti-myc antibody. The pellet fraction corresponds to the lysate treated with the beads. The supernatant represents the fraction of the lysate including all the proteins that were not bound by the beads. An antibody against DVAP and an antibody against flag-tag were used to detect the fusion proteins by immunoblot. The antibody against flag-tag gave an unspecific signal for flag-Sac1 in the input fraction of all the lysates (data not shown). However, a specific signal was detected when supernatants and input fractions from all the COS-7 samples were incubated with the same antibody and the anti-DVAP antibody (data not shown). These results suggested the presence of a problem in the precipitation step of Flag-Sac1 fusion protein by using the beads conjugated with the anti-Myc antibody.

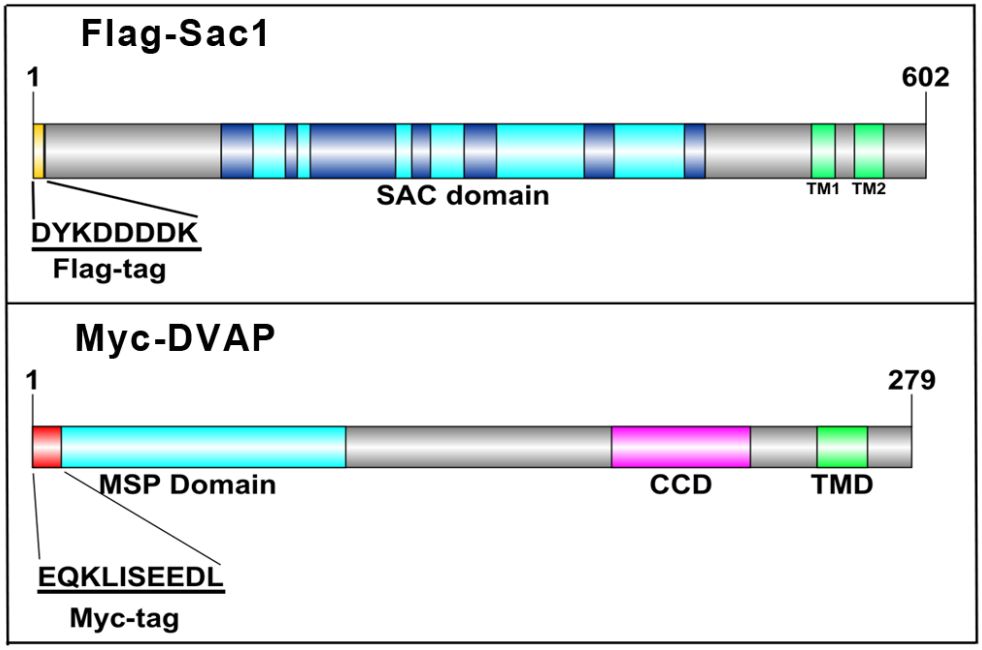

Figure 5. Flag-Sac1 and Myc-DVAP fusion proteins. This figure shows the two fusion proteins that have been generated in the first instance to perform a Co-IP in order to confirm the interaction between DVAP e Sac1. Flag-Sac1 is represented on the top of the figure, whereas myc-DVAP is reported at the bottom of the figure. The relevant domains are represented in each scheme of the protein. Look at the 'Introduction section' for further details about these domains. The protein schemes have been generated using DOG 1.0 software [Ren et al., 2009].

To circumvent the problem described above, COS-7 cells were cotransfected with the following constructs: *pCMV-Myc-Sac1* and *pCMV-Tag2B-DVAP* (Fig. 6A-B). In the cell extracts expressing both Myc-tagged Sac1 and Flag-tagged DVAP, the presence of Myc-Sac1 and Flag-DVAP was tested, also in this case, in the three fractions (input, supernatant and pellet) from COS-7 lysates expressing Myc-Sac1 together with Flag-DVAP, Myc-Sac1 alone, and Flag-DVAP alone (Fig. 6). In this case Myc-Sac1 and Flag-DVAP were detected by anti-Myc and anti-DVAP antibodies by Immunoblot. These results clearly show co-immunoprecipitation of Flag-tagged DVAP together with Myc-tagged Sac1 (Fig. 6C). Instead, Flag-DVAP and Myc-Sac1 were not detected in the pellet fraction from lysates from COS-7 cells transfected with *pCMV-Tag2B-DVAP* (encoding Flag-DVAP) alone (Fig. 6C). In this case Flag-DVAP did not

immunoprecipitate with the beads, as this fusion protein could not bind the beads by itself. In addition, Flag-DVAP was not detected in the pellet fraction from COS-7 cells transfected with *pCMV-Myc-Sac1* (encoding Myc-Sac1) alone. The results from this experiment indicate that Flag-DVAP binds to the beads through the interaction with Myc-Sac1. Thus, the coimmunoprecipitation of Flag-DVAP and Myc-Sac1 shows the interaction between these two proteins, although it does not prove a direct interaction. These data support the idea that Sac1 and DVAP interact. It was observed by yeast two-hybrid.

3.3 The association between Sac1 and DVAP is not affected by ALS8 mutations in DVAP

A Flag-tagged protein for the mutant form of DVAP, DVAP-P58S, was also produced. The construct encoding Flag-DVAP-P58S was generated by cloning *DVAP-P58S* cDNA [Chai et al., 2008] in *pCMV-Tag2B* vector (see Appendix1, Fig. 26). Myc-tagged Sac1 and Flag-DVAP-P58S were co-expressed in COS-7 cells. The analysis of the presence of the fusion proteins was carried out as described in the previous paragraph. The Immunoblot analysis clearly shows the presence of the two proteins in the pellet fraction of the lysates, indicating that the two fusion proteins co-immunoprecipitate (Fig. 6C). Also in this case single transfections with each one of the used constructs, *pCMV-Tag2B-DVAP-P58S* and *pCMV-Myc-Sac1,* have been performed. Coimmunoprecipitation of DVAP-P58S and Myc-Sac1 was not observed in the pellet fractions of the lysates from the single transfected COS-7 cells (Fig. 6C). These data indicate that also the mutant form of DVAP (DVAP-P58S) interact with Sac1. Thus, the ALS causative mutation in DVAP does not disrupt the interaction between DVAP and Sac1 protein.

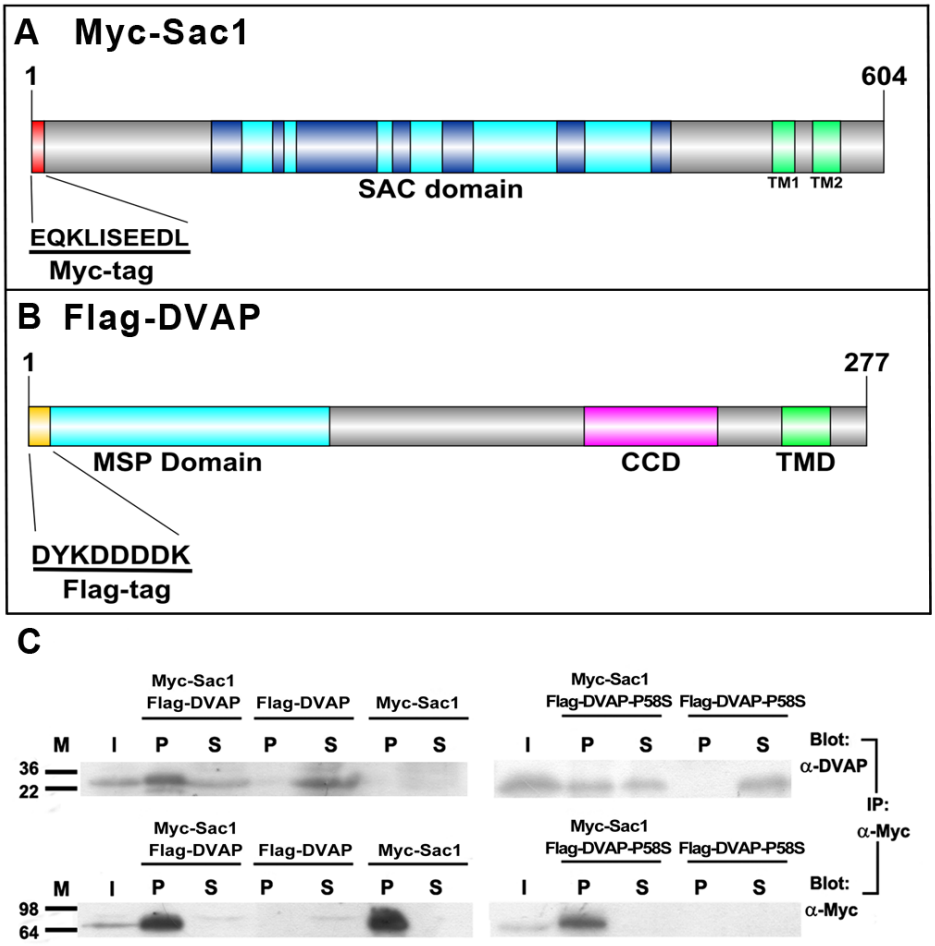

Figure 6. DVAP wt and DVAP-P58S and DVAP-T48I interact with with Sac1 by Co-IP. (**A, B**) represents the schemes of the Flag-Sac1 and Myc-DVAP fusion proteins with respect. The protein schemes have been generated using DOG 1.0 software [Ren et al., 2009]. Constructs encoding these two fusion proteins have been used during the first attempt of Co-IP. Either Flag-DVAP or Flag-DVAP-P58S and Myc-Sac1 fusion proteins were co-expressed in COS-7 cells. In addition, each construct was individually expressed in COS-7 cells and it was used as a control. Cell extracts were immunoprecipitated by using anti-Myc crosslinked with beads. Input (I), pellet (P), and supernatant (S) samples were analyzed by Western Blot by using either anti-DVAP to detect w.t. **(C)**, and mutant DVAP or anti-Myc to detect Sac1 **(C)**.

3.4 Conclusion

In order to investigate whether the analysis of the interaction between dSac1 and DVAP can shed new light on the molecular mechanisms underlying ALS8 pathogenesis, I confirmed this interaction *in vitro* by Co-IP. Interestingly, I observed that the two mutant forms of DVAP (DVAP-P58S and DVAP-T48I) retain their ability to bind Sac1 by Co-IP assay. The same result has been shown by yeast two-hybrid [Forrest et al., 2013]. Moreover, a detailed analysis of the domains of DVAP required for the interaction with Sac1, revealed that the MSP domain is dispensable for that interaction [Forrest et al., 2013]. The P58S and T48I mutations affect two amino acids that are placed in the 'Vap consensus motif inside the MSP domain of VAP proteins [Nishimura et al., 2004]. Forrest et al., [2013] also have shown by yeast two-hybrid, that the TMD of DVAP is required for the interaction with Sac1. These data all together are in agreement with my results showing that P58S and T48I mutations do not affect the association between these two proteins.

Chapter 4: DVAP and Sac1 colocalize at ER membrane

4.1 Introduction

In order to characterize the interaction between DVAP and Sac1 proteins, at first, this association has been confirmed by Co-IP *in vitro* (see Chapter 3 of this thesis). In order to move towards the study of Sac1 function in the nervous system the colocalization between DVAP and Sac1 *in vivo* using *Drosophila melanogaster* tissues and cultured cells. Previously, Sac1 protein was found associated to the ER and the Golgi complex in yeast and mammals [Whitters et al., 1993; Nemoto et al., 2000; Rohde et al., 2003; Tahrovic et al., 2005]. Manford et al.,[2010] suggested a functional model for Sac1. In this model TM1 and TM2 domains of Sac1 allows Sac1 to be anchored to the ER and Golgi membranes. On the other hand, a cationic flexible loop allows the enzymatic site to work in trans to dephosphorylate PIPs on other membranes. Subsequently, Piao and Mayinger [2012] proposed that Sac1 localizes to the Golgi complex when the cell is under starvation condition in mammals and yeast (Fig. 7). When Sac1 translocates to the Golgi dephosphorylates PI4P to PI. The constitutive secretion and translocation of proteins to the PM is reduced when Golgi-PI4P are lowered [Blagoveshchenskaya et al., 2008; Rohde et al., 2003].

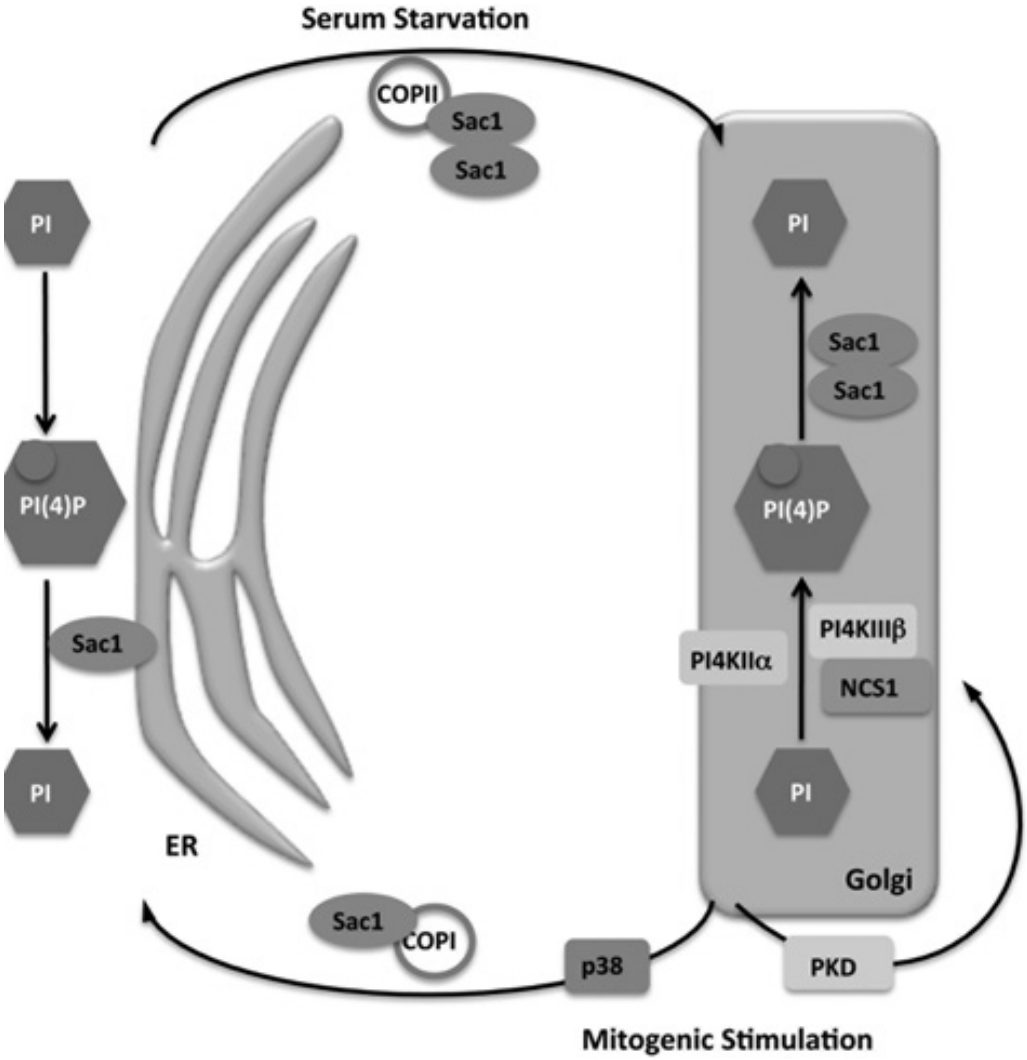

Figure 7. Schematic view of the translocation of Sac1 phosphatase between ER and Golgi. Under mitogenic stimulation Sac1 moves from the Golgi apparatus to the ER. COPI vesicles are implicated in this translocation in mammals. On the other hand, under serum starvation conditions Sac1 phosphatase is brought from ER to Golgi by COPII vesicles. The figure is from Piao and Mayinger, 2012**.**

In order to to assess the subcellular localization of Sac1 two approaches have been followed in parallel: the generation of an antibody against Sac1, and the generation of transgenic flies expressing a tagged form of Sac1.

4.2 Generation of anti-Sac1 antibody: the rationale for the choice of the translation vector and of the hexahistidine tag

In order to generate an antibody recognizing *Drosophila* Sac1, it is crucial that an animal of choice develops a specific immune response against Sac1 protein. Thus, Sac1 protein needs to be produced and then injected into the animal. In order to produce a protein, first, a system where the protein can be expressed has to be chosen; second, the cDNA encoding the protein of interest has to be cloned into an expression vector. pET system has been chosen to produce Sac1 as an antigen. This system allows expressing recombinant proteins in *E. Coli*. So far, *E. Coli* is the cheapest and fastest host cell in which to produce a recombinant protein. In order to maximize production of the recombinant protein a strain that lacks in *lon* and *ompT* proteases was used: BL21 (DE3) strain. In order to choose the expression vector in which to clone the cDNA, two considerations have been made: the need to produce a soluble or insoluble protein and the choice of the peptide to fuse to the protein to express. The need to produce a soluble protein comes from the necessity to have a protein in a native state. An antigen does not need to be in a native state, as in other applications, such as crystallography. On the other hand the production of an insoluble protein that, thus, localizes into cytosolic aggregates presents some advantages. These advantages include that the cytoplasmic aggregates can have a protective effect on the protein against proteolysis, although the bacterial strain in use (BL21 (DE3) strain) lacks two proteases. In addition, the inclusion bodies can be isolated by centrifugation and the protein can be solubilized using a detergent.

The choice of the fusion tag has also been made taking into account the procedures that the produced protein should go through: purification of the protein from the entire pool of proteins of the cell, and the induction of the production of specific antibodies. The His-tag ($(His)_6$) appeared to be a peptide that may be good in all the stages of the generation of an antigen. In fact, first,

the purification of a protein from the inclusion bodies has to be performed under denaturing conditions and the $(His)_6$-tag is a peptide that is not affected by denaturing conditions. Second, the $(His)_6$-tag is a small peptide (only six amino acids with an M.W. of 0.84 kDa) that is not highly antigenic. Although *pET-28* vector contains in its sequence $(His)_6$-tag at both sides of the MCS, the Sac1 cDNA was cloned into this vector in order to express a protein having the His-tag at the N-terminus.

4.2.1 Generation of the expression clone

It is not always possible to express or, at least, to express a certain amount of a full-length recombinant protein to use as an antigen for the production of an antibody. Thus, different constructs encoding fusion proteins containing either the full-length Sac1 protein or Sac1 deletion derivatives were designed and generated in parallel [Graslund et al., 2008]. In expressing Sac1 deletion derivatives, N- and C-terminal boundaries were carefully chosen, as expression levels can be affected due to small differences in the length of the included protein regions [Graslund et al., 2008]. Therefore all Sac1 derivatives were designed by paying attention to the location of the SAC-domain and TM domains in the Sac1 amino acid sequence.

Thus, after these preliminary considerations, a full-length Sac1 cDNA and five *Sac1* deletion derivatives were cloned into the *pET-28a* expression vector. *pET-28* vector exists in three different reading frames (a-c) and we chose the *pET-28a*. The expression cassette of the *pET-28a* expression vector, as in all the *pET* vectors is downstream of the promoter of the T7 RNA polymerase. The lac operator follows this promoter. Thus, the expression of the gene cloned in the expression cassette of this vector is induced when a lactose analog (IPTG) binds the repressor of the lac operator allowing the T7 RNA polymerase to start the transcription [Dubendorff et al., 1991]. The source of T7 RNA polymerase is the bacterial host cell.

Two Sac1 deletion derivatives using cDNA constructs encoding the N-terminal Sac1 portion were generated, and also, three constructs encoding the C-terminal portion of the protein. The two N-terminal Sac1 derivatives comprise the entire SAC-domain ($(His)_6$-Sac1Δ483-594) (Fig. 8B), and the second construct contains the first five motifs of the SAC domain ($(His)_6$-Sac1Δ354-594) (Fig. 8C). All three Carboxyl-terminal Sac1 deletion derivatives include the two TM domains of the Sac1 protein (Fig. 8D-F). The first construct, $(His)_6$-Sac1Δ1-309, comprises motifs six and seven of the SAC domain, in addition to the two TM domains (Fig. 8D). The second construct $(His)_6$-Sac1Δ1-267, includes the fifth, sixth and seventh motifs of the SAC domain and the two TM domains (Fig. 8E). The third construct, $(His)_6$-Sac1Δ1-173, comprises motifs 3-7 of the SAC domain as well as the two TM domains (Fig. 8F).

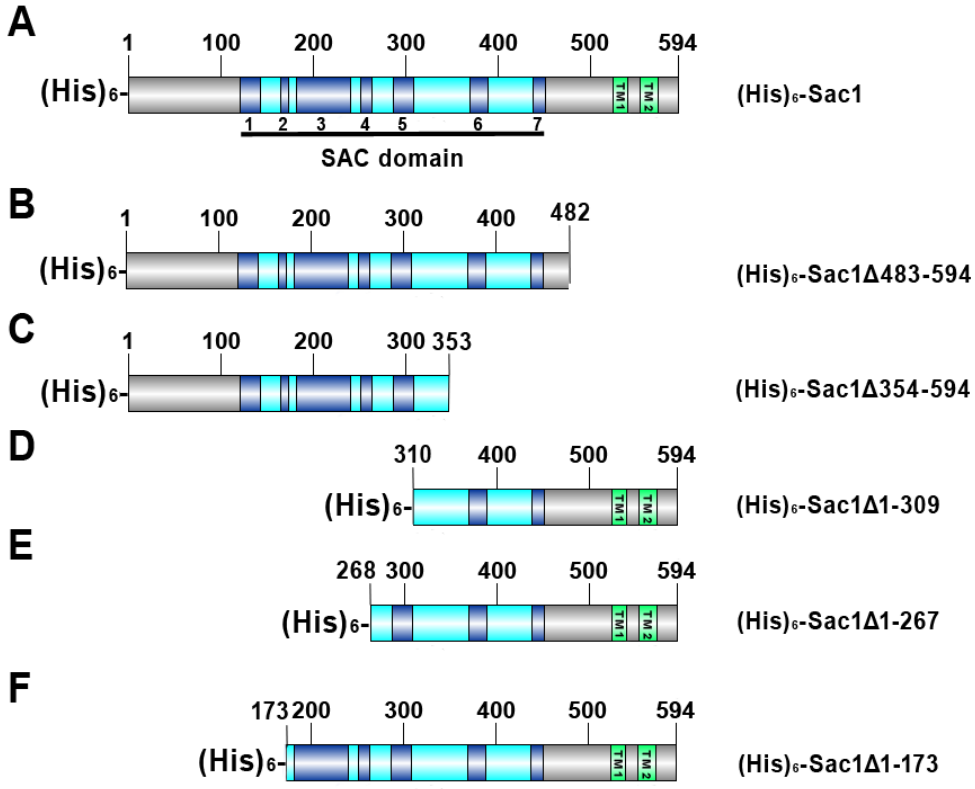

Figure 8. Structure of all the His tag fusion-proteins that were generated to obtain the anti-Sac1 antibody. (A) Structure of the His tag-Sac1 fusion protein which includes the entire *Drosophila* Sac1 enzyme. The domains of Sac1 protein are shown. First, the SAC domain (121-451aa) in light blue. Second, the seven motifs of the SAC domain are in dark blue: motif 1 (121-143 aa), motif 2 (165-173 aa), motif 3 (182-240 aa), motif 4 (251-264 aa), motif 5 (287-309 aa), motif 6 (369-389 aa) and motif 8 (437-451 aa). Then, TM1 (524-540 aa) and TM2 (553-573 aa) domains are showed in green. The structures of the His tagged Sac1 deletion derivatives is also shown: $(His)_6$-Sac1Δ483-594 **(B)**, $(His)_6$-Sac1Δ354-594 **(C)**, $(His)_6$-Sac1Δ1-309 **(D)** $(His)_6$-Sac1Δ1-267 **(E),** and $(His)_6$-Sac1Δ1-173 **(F).** The protein schemes have been generated using DOG 1.0 software [Ren et al., 2009]

4.2.1.1 Expression of the fusion proteins

Five lysates from bacteria expressing the six different fusion proteins were resolved by SDS-PAGE, in order to perform a preliminary characterization of the expression levels of these proteins. The highest expression levels were

obtained with the two C-terminal Sac1 ((His)$_6$-Sac1Δ1-309 and (His)$_6$-Sac1Δ1-267; Fig. 9B,C) deletion derivatives. Both (His)$_6$-Sac1Δ1-309 and (His)$_6$-Sac1Δ1-267 fusion proteins localized to the inclusion bodies (Fig. 9C,E). (His)$_6$-Sac1 (full-length) was not expressed at all (Fig. 9A). The two N-terminal Sac1 fusion proteins and the C-terminal (His)$_6$-Sac1Δ1-173 were not expressed as highly as (His)$_6$-Sac1Δ1-309 and (His)$_6$-Sac1Δ1-267 tagged proteins (data not shown).

The presence of the His-tag fused to the Sac1Δ1-267 fusion protein was checked by Western blot on BL(21)DE3 bacterial lysates using an anti-His antibody. These two proteins alternatively underwent a mild protein extraction from the inclusion bodies. A gentle protein extraction procedure using a mixture of zwitterionic and non-ionic detergents in a Tris buffer was preferred to the mechanical extraction of the protein obtained disrupting the membranes by sonication, to avoid protein disruption.

Metal chelation chromatography approach was used to separate the His-tag fusion protein from the other proteins of the bacterial cell. The eluted His-Sac1Δ1-267 tagged protein from the affinity column was quantified comparing the amount of protein on SDS-PAGE with a number of BSA dilutions (Fig. 9F).

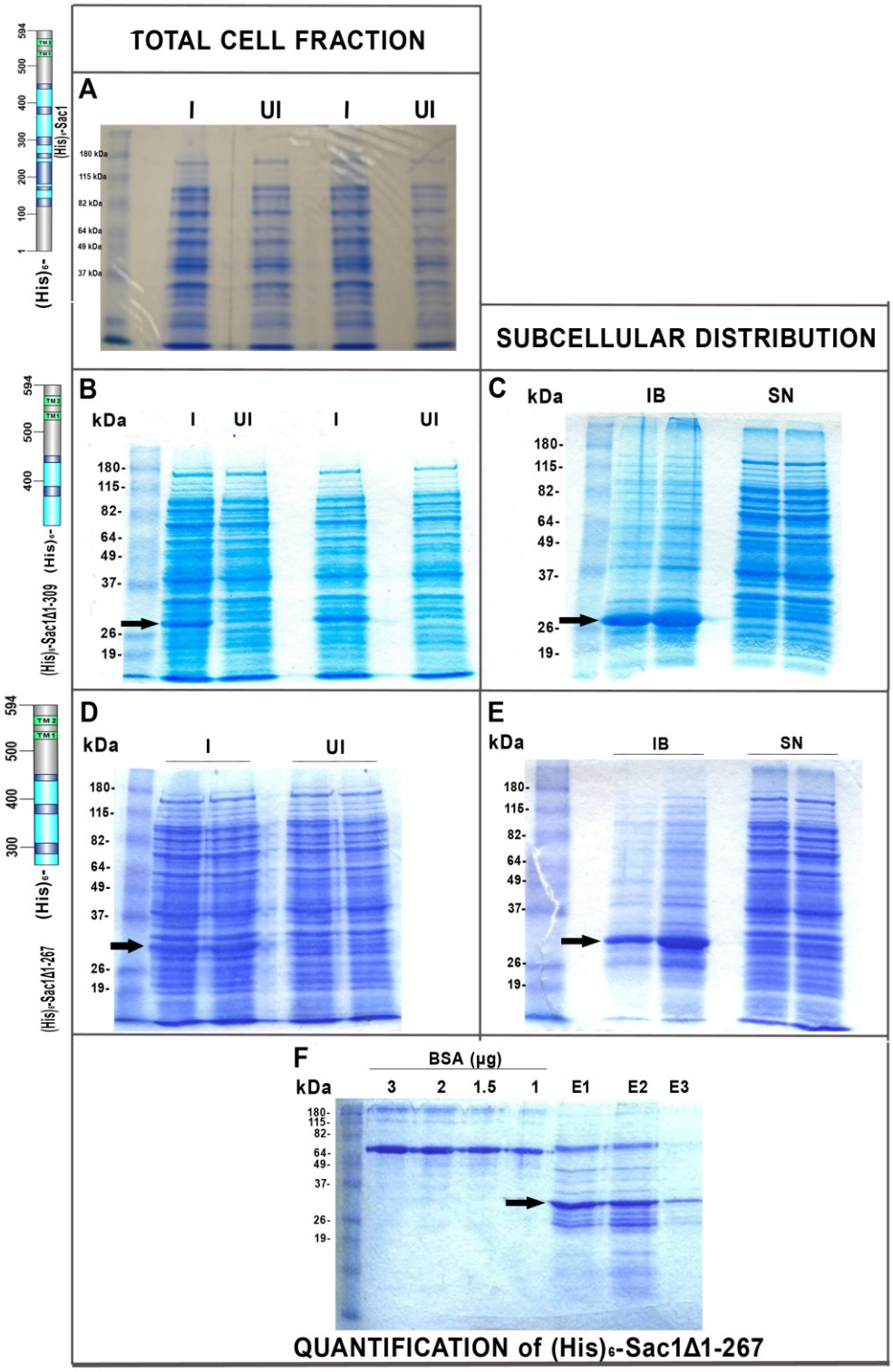
TOTAL CELL FRACTION
SUBCELLULAR DISTRIBUTION
A
I
UI
I
UI
180 kDa
115 kDa
82 kDa
64 kDa
49 kDa
37 kDa
(His)6-Sac1
B
kDa
I
UI
I
UI
180-
115-
82-
64-
49-
37-
26-
19-
(His)6-Sac1Δ1-309
C
kDa
IB
SN
180-
115-
82-
64-
49-
37-
26-
19-
D
kDa
I
UI
180-
115-
82-
64-
49-
37-
26-
19-
(His)6-Sac1Δ1-267
E
kDa
IB
SN
180-
115-
82-
64-
49-
37-
26-
19-
F
BSA (µg)
kDa
3
2
1.5
1
E1
E2
E3
180-
115-
82-
64-
49-
37-
26-
19-
QUANTIFICATION of (His)6-Sac1Δ1-267

Figure 9. Expression of $(His)_6$-Sac1, $(His)_6$-Sac1Δ1-309 and $(His)_6$-Sac1Δ1-267 fusion proteins in BL(21)DE3 bacterial strain. (A) Lysates from BL(21)DE3 bacteria transformed with *pET28a-Sac1* and treated with IPTG to express the fusion protein (I=Induced) and not-treated with IPTG (UI=Uninduced). **(B)** Lysates from BL(21)DE3 bacteria transformed with *Sac1Δ1-309*. **(C)** Inclusion bodies (IB) and supernatant (SN) from lysates expressing His-Sac1Δ1-309 fusion protein. $(His)_6$-Sac1Δ1-309 (M.W.=32,05 kDa) is indicated by an arrow in **(B)** and **(C)**. **(D)** Lysates from BL(21)DE3 bacteria transformed with *pET28a-Sac1Δ1-267* and treated with IPTG to express the fusion protein (I) and not-treated with IPTG (UI). **(E)** IB and SN from lysates expressing His-Sac1Δ1-267 fusion protein. $(His)_6$-Sac1Δ1-267 (M.W.=36.94 kDa) is indicated by an arrow in **(D)** and **(E)**. **(F)** Amount of $(His)_6$-Sac1Δ1-267 protein in the three elution fractions (E1, E2 and E3) were compared with four different BSA dilutions (3μg, 2μg, 1.5 μg and 1μg) $(His)_6$-Sac1Δ1-267 (M.W.=36.94 kDa) is indicated by an arrow in **(c)**, **(d)** and **(E).** The protein schemes have been generated using DOG 1.0 software [Ren et al., 2009]

4.2.1.2 Sac1 protein levels in wild type third instar larvae are under the detection limit for the anti-Sac1 antibodies

The fusion protein was injected in rabbits and guinea pigs for antibody production. The 87-day immunization program was chosen in order to immunize the animal. The antigen was injected four times and four bleeds were collected during the 87 days. This program has been preferred to the 28-days immunization one, because a long immune response of the animal allows the generation of high affinity antisera, for use in immunohistochemistry experiments. In addition, the use of adjuvant compounds in the 28-days immunization program can affect the health of the animal.

The sensitivity and specificity of the antisera in the bleeds collected from the two animals were tested, first, on wild type (*CS*) *Drosophila* embryos, on embryos from one line overexpressing Sac1 (*UAS-Sac1133A*), and, also, on embryos from one line having low levels of Sac1 (*UAS-Sac1RNAi/TM3,Sb,GFP*) when compared to w.t. lines (data not shown). Nevertheless, we are interested in the characterization of the sub-cellular

distribution of Sac1 in particular in the nervous system of third instar larvae. Thus, *Sac1 O.E.* and *Sac1RNAi* transgene expression was targeted to the larval nervous system using the *elav-Gal4* driver [Yao and White, 1994], and the sensitivity and the specificity of these antibodies were tested on brains, eye imaginal discs from *CS*, *elav;Sac1133A* and *elav;Sac1RNAi* larvae. In addition, the two anti-Sac1 antisera were also tested on larval salivary glands from the same genotypes, as *elav-Gal4* driver directs the expression of transgenes also in larval salivary glands [Krueger et al., 2003].

The immunohistochemical analysis revealed that the Sac1 antibody that was generated in guinea pig is able to detect Sac1 protein only in tissues from third instar larvae overexpressing Sac1 (*elav;Sac1133A),* but not from *CS* and *elav;Sac1RNAi* lines. The analysis of the antibody produced in guinea pig by Immunoblot on the same tissues from the three lines (*CS, elav;Sac1133A, and elav;Sac1RNAi*) (Fig. 10) confirmed what observed on the *in vivo* tissues.

The anti-Sac1 antibody that was produced in rabbit, showed a strong background signal both in the immunohistochemical and Western blot analysis (data not shown). The background made it difficult to identify the Sac1 protein in tissues from all three of the analysed lines (*CS*, *elav;Sac1133A, elav;Sac1 RNAi)*. In conclusion, the antibody developed in guinea pig is more specific that the one developed in rabbit, however, it is not sensitive enough for our experimental purposes.

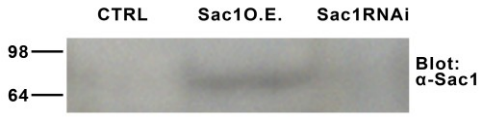

Figure 10. Sac1 levels in a physiological context are under the detection limit of the anti-Sac1 antibody in guinea pig. Larval brains, salivary glands and eye imaginal discs from CTRL, *elav;Sac1133A* and *elav;Sac1RNAi* strains. The lysates were analyzed by Western Blot by using anti-Sac1 in guinea pig to detect Sac1.

4.3 Generation of transgenic flies expressing Flag-Sac1 fusion protein

4.3.1 Use of PhiC31 integration system to generate Flag-Sac1 transgenic flies

As the two anti-Sac1 antisera that were generated lacked both specificity and sensitivity, transgenic flies expressing a tagged form of Sac1 were developed to look at the subcellular localization of Sac1. The PhiC31 integrase system [Bischof et al., 2007] was used for germ-line transformation with a *UAS-Flag-Sac1-attb* construct (Fig. 11).

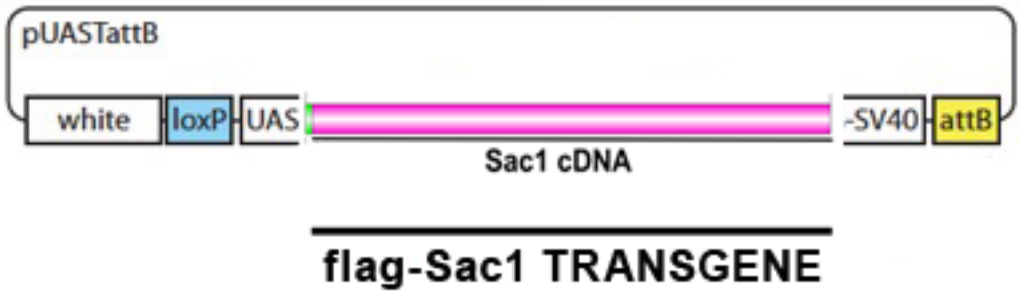

Figure 11. Scheme of the construct that has been used to generate transgenic flies expressing flag-Sac1. The Sac1 cDNA (pink) has a flag-tag encoding sequence (green) upstream in frame. The flag-Sac1 transgene has been cloned in frame into the *pUAST-attB* vector. Figure adapted from Bischof et al., 2007.

When this system is used, the integration of the heterologous DNA into the genome is mediated by a serine integrase, named PhiC31 integrase. PhiC31 integrase is named after the bacteriophage whose genome encodes it. A number of reasons led us to choose this germ-line transformation system. First, this system allows site-specific integration of the transgene carried by the *pUASTattB* vector. The P-element mediated transgenesis which is the first method of transgenesis to be developed [Spradling, 1986] is characterized by transgene integration that is not site-specific. The transgene is often inserted in 5' regulatory regions leading to two major consequences: the local chromosomal environment can affect the expression of the transgene (position

effect) and inactivation of the transgene can occur because it can be inserted close to heterochromatin (position effect variegation) [Venken and Bellen, 2007]. PhiC31 enzyme, on the other hand, catalyses the specific recombination between the 'phage attachment' (*attP*) site and the 'bacterial attachment' (*attB*) site (Fig. 12). Thus, the transgene integrates specifically where the *attP* site is placed in the fly strain genome. In this case, mapping of insertion of transgene is not required [Thorpe et al., 2000].

When the recombination between the *attP* and *attB* sites occurs, the *attB* site is converted into an *attR* site, whereas the *attP* site is converted into an *attL* site. The new sites, *attR* and *attL*, are not recognized by the integrase, thus this enzyme will not mediate a reverse recombination between the two sites [Thorpe et al., 2000]. In addition, the PhiC31 integrase cannot catalyze the integration reaction between *attB* site and either *attR* or *attL* sites [Venken and Bellen, 2007]. Thus, the integration reaction in this system is an irreversible event.

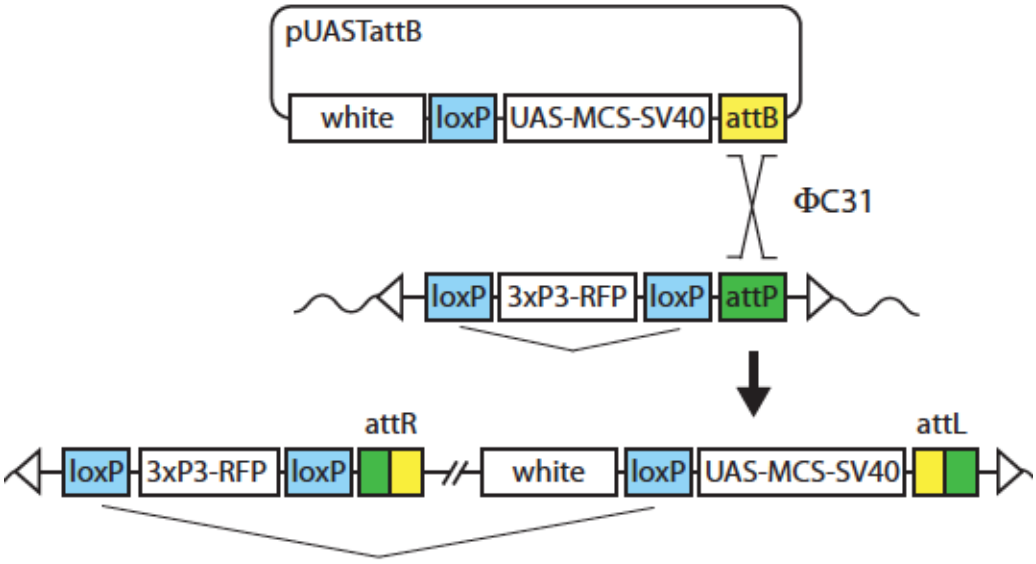

Figure 12 Scheme of the site specific integration of the pUASTattB vector into the *Drosophila* genome. The PhiC31 integrase catalyzes the *attB-attP* combination. When the *attB* and *attP* sites recombinate they change their sequences creating two new sites (*attR* and *attL*) that are not recognized by the PhiC31 integrase. Thus, the transgene into the *pUASTattB* vector will be stably integrated into the specific *Drosophila* strain genome. Figure adapted from Bischof et al., 2007.

The transgene integration in the PhiC31 integration system was described to occur with high frequency (about 42.5%) [Bischof et al., 2007]. This percentage of integration frequency is considerably higher when compared to the one obtained with the P-element based integration frequency (about 1.6%) [Spradling, 1986].

The above described features led to the choice of PhiC31 integrase system to generate transgenic flies expressing Flag-Sac1 fusion protein. Thus, the *Flag-Sac1* was cloned into *pUAST-attB* vector and the insertion *M{3xP3-RFP-attP}ZH-22A* [Bischof et al., 2007] integrated in the *Drosophila* genome (2L; 22A) was designated as the first landing platform to use.

4.3.1.1 Problems encountered using PhiC31 integration system

Flies expressing Flag-Sac1 tagged protein were generated by using PhiC31 integration system, although several disadvantages of these system were observed during the entire procedure.

1. According to our data, the integration frequency was much lower than 42.5%, as the *pUASTattB-UAS-Flag-Sac1* construct was injected in about 4000 embryos (200 embryos/day x 20 days) and only one transformant was generated.

2. The identification of the actual transformant flies through the eye colour was weak and difficult to identify. The eye colour of the transformant *ZH-attP-22A* flies is reported to be light orange three days after eclosion [Bischof et al., 2007]. In addition, the eye color of non-transformant *ZH-attP-22A* flies, usually, turns to pink in about three days time. This characteristic was very problematic when distinguishing between pale orange eyes and pale pink eyes.

3. Lastly, over several generations, the inserted transgene was lost in some flies, this evidence is in contrast with one of the most important hallmark of the PhiC31 integration system. The use of an integrase should avoid the transgene "jumping out" of the insertion site.

All these considerations also led us to generate transgenic flies expressing Flag-Sac1 tagged protein using the standard P-element transformation method. Four independent lines were generated, each one having the *UAS-Flag-Sac1* construct on one chromosome.

4.3.1.2 DVAP and Sac1 associate *in vivo*

In the first instance, *ZH-22A-Flag-Sac1* flies were used to examine *Drosophila* Sac1 subcellular localization *in vivo*, while flag-Sac1 expressing lines were generated using the P-element transformation method by 'Genetic Services, Inc. Drosophila Injections'. In *Drosophila*, it is possible to direct the expression of the transgene of interest in a time- and tissue- specific manner by using the UAS/GAL4 system [Brand and Perrimon, 1995]. To this aim, the expression of *UAS-Flag-Sac1* transgene was driven pan-neuronally and in salivary glands by crossing the *ZH-22A-Flag-Sac1* flies with *elav-Gal4* driver [Yao and White, 1994]. This driver not only directs transgene expression to the nervous system, but also to the salivary glands [Krueger et al., 2003]. DVAP and Flag-Sac1 broadly co-localized in brains, eye imaginal discs, and salivary glands from third instar larvae (Fig.13 A,C,D).

Furthermore, the *UAS-Flag-Sac1* construct was expressed specifically in skeletal muscles using the *BG57-Gal4* driver [Budnik, et al., 1996] where the association of these two proteins was also detected (Fig. 13B). Their distribution displays a peri-nuclear pattern resembling ER/Sarcoplasmic reticulum [Chen et al., 2010]. These results were confirmed by using the transgenic lines

expressing Flag-Sac1 fusion protein (data not shown), which were generated using the standard P-element based integration system.

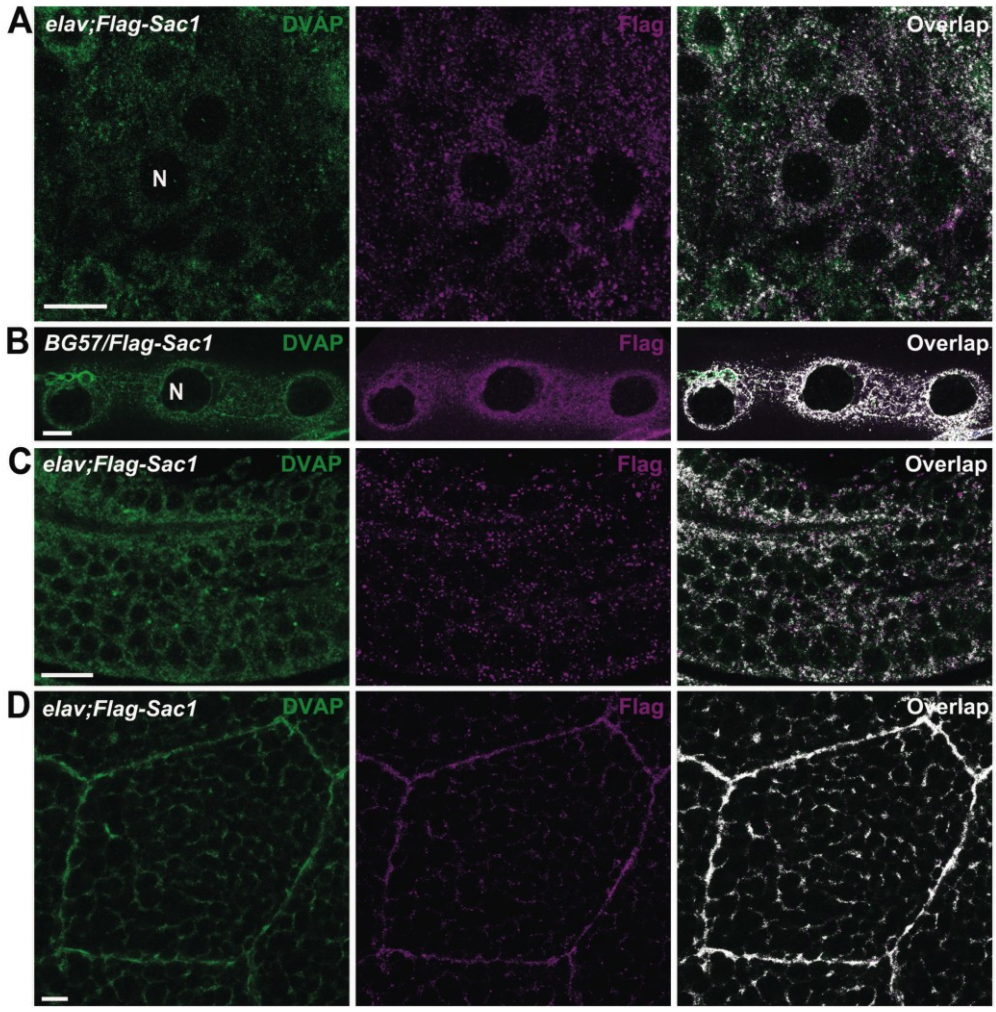

Figure 13. DVAP and Sac1 widely associate in vivo. The *in vivo* colocalization of DVAP and Flag-Sac1 is shown in confocal images of (**A**) brains, (**C**) eye imaginal discs, (**D**) and salivary glands from *elav;Flag-Sac1* (*elav-Gal4/Y;UAS-Flag-Sac1/+ and elav-Gal4/+;UAS-Flag-Sac1/+*) third instar larvae. The association is also detected in (**B**) muscles from BG57/ *Flag-Sac1* third instar larvae. The relevant tissues were stained with anti-DVAP (green) and anti-Flag (magenta) antisera. Image J software was used to analyze the signal from DVAP and Sac1 co-localization. A pseudocolor (white) indicates the co-localization signal. The nuclei are indicated by the white 'N'. Scale bar = 10μm.

4.3 Sub-cellular localization of Sac1 phosphatase in COS-7 cells

In mammals and yeast, Sac1 protein localizes to the ER and Golgi apparatus [Whitters et al., 1993; Konrad et al., 2002]. On the other hand, the yeast VAP-33 homolog (Scs2) is confined to the ER [Kagiwada et al., 1998]. In addition, evidence from *Drosophila* and other experimental models shows that DVAP was found in association with microtubules and membranes [Pennetta et al., 2002]. In particular, in mouse VAPs are associated to microtubules and intracellular vesicles in neurons [Skehel et al., 2000]; in rat VAP-33 homolog is proposed to function in the secretory pathway in the ER and the pre-Golgi compartment [Soussan et al., 1999]. Lastly, a VAP-33 homolog in plants was located mainly to the PM [Galaud et al., 1997; Laurent et al., 2000]. If it is true that Sac1 and DVAP interact *in vivo* they should colocalize. Thus, the intra-cellular distribution of Sac1 was examined in COS-7 cells and it was compared to DVAP localization.

To this aim, myc-DVAP and Flag-Sac1 tagged proteins were expressed in COS-7 cultured cells. The constructs encoding these two fusion proteins were generated as described in the paragraph 3.1 of the Results section. Subsequently, COS-7 cells were co-transfected with both constructs and the two tagged proteins were visualized by fluorescence microscopy. In COS-7 cells myc-tagged DVAP follows an ER-like perinuclear reticular distribution (Fig. 14A) according to previous findings [Chen et al., 2010]. On the other hand, Flag-tagged Sac1 protein presents both an ER distribution, similar to DVAP, as well as a paranuclear Golgi-like pattern (Fig. 14A). These data are in agreement with the sub-cellular localization of Sac1 protein at the Golgi complex reported in yeast [Whitters et al., 1993], in rat [Nemoto et al 2000], in mouse [Liu et al 2008], and in humans [Rohde et al 2003]. No changes in the sub-cellular distribution of both proteins were observed in COS-7 cells that have been cotransfected with flag-tagged Sac1 and myc-tagged DVAP encoding constructs (Fig. 14B). In particular, the merge picture shows an overlapping between the

stainings of the two fusion proteins corresponding to an ER-like perinuclear reticular distribution (Fig. 14B). Additionally, a punctuate staining was observed in a fraction of COS-7 cells coexpressing myc-DVAP and flag-Sac1 (Fig. 14C). These data show that DVAP and Sac1 colocalize.

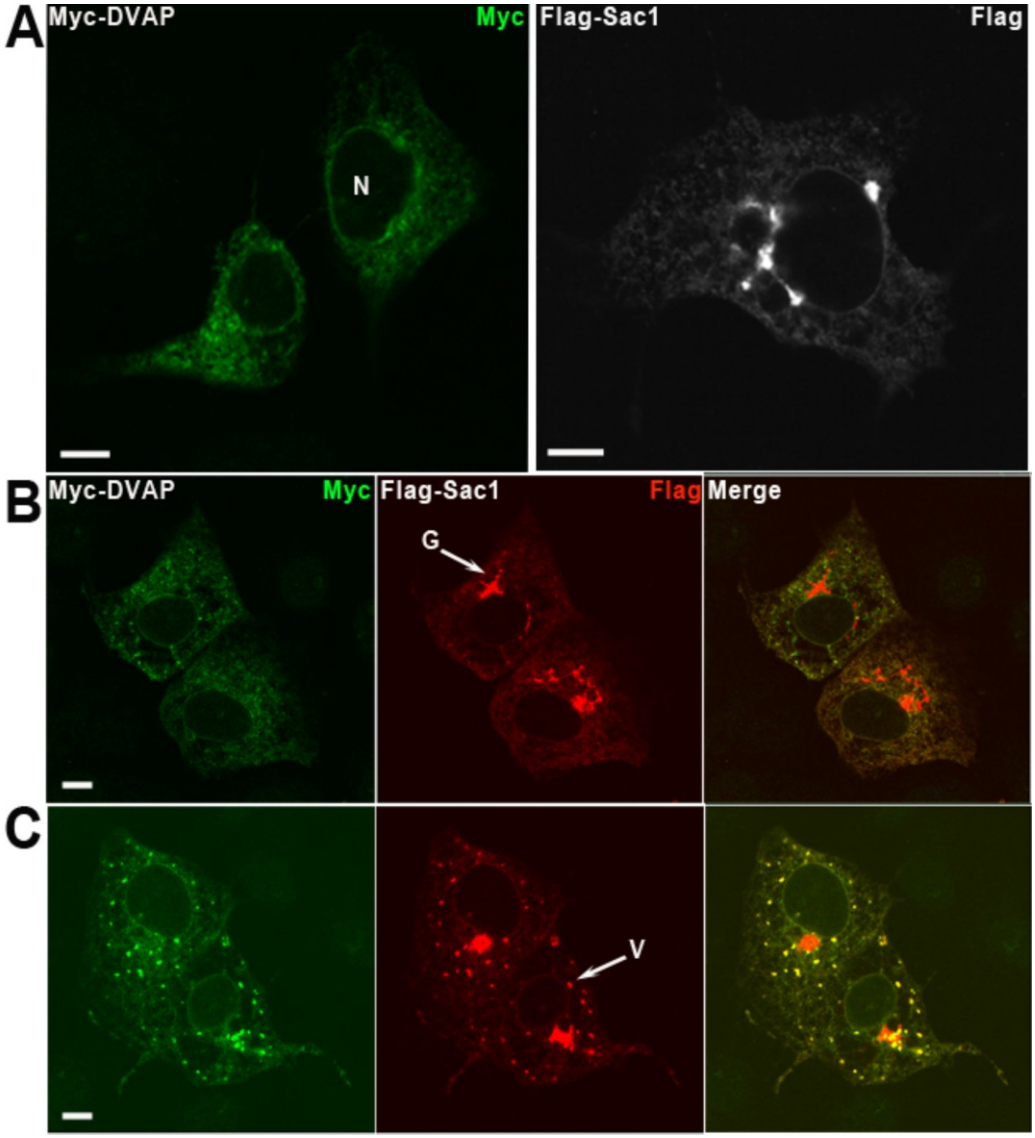

Figure 14. DVAP and Sac1 colocalize in the ER, but not in the Golgi. (A) Images from confocal microscopy of COS-7 cells alternatively transfected with Myc-DVAP and Flag-Sac1. Anti-Myc (green) and anti-Flag (white) antisera were used to visualize the proteins of interest. **(B-C)** Confocal images from COS-7 cells cotransfected with Myc-DVAP and Flag-Sac1. Anti-Myc (green) and anti-Flag (magenta) antisera were used to visualize the proteins of interest. 10 µm scale bar is used. N=Nucleus, G=Golgi apparatus, V= Vesicle-like structure.

4.5 Sac1 localizes to the Golgi in third instar larval salivary gland cells

The intracellular distribution of Sac1 in third instar larvae was examined in salivary gland cells from third instar larvae. The size of salivary gland cells is

much bigger (hundred of times) when compared to the majority of other cells in *Drosophila* [Andrew et al., 2000], thus, these cells are suitable to determine the subcellular localization of a protein. *Flag-Sac1* transgene expression was targeted to the salivary glands by *elav-Gal4* driver [Yao and White, 1994]. As *Drosophila* Sac1 presents a distribution pattern similar to the ER and the Golgi apparatus in COS-7 cells (Fig. 14A-B), Flag-Sac1 staining was compared to the staining pattern of the ER marker Boca [Culi and Mann, 2003], and the cys-cisternal Golgi marker dGM130 (Fig.15B) [Kondylis et al., 2001]. Flag-Sac1 staining largely overlaps with Boca (Fig. 15A) and GM130 stainings (Fig. 15B). This *in vivo* experiment confirmed the results obtained from colocalization experiment in COS-7 cells. Taken together these findings indicate that *Drosophila* Sac1 homolog distributes in the ER and in the Golgi apparatus, as seen in other animal models and that it overlaps with DVAP in the ER.

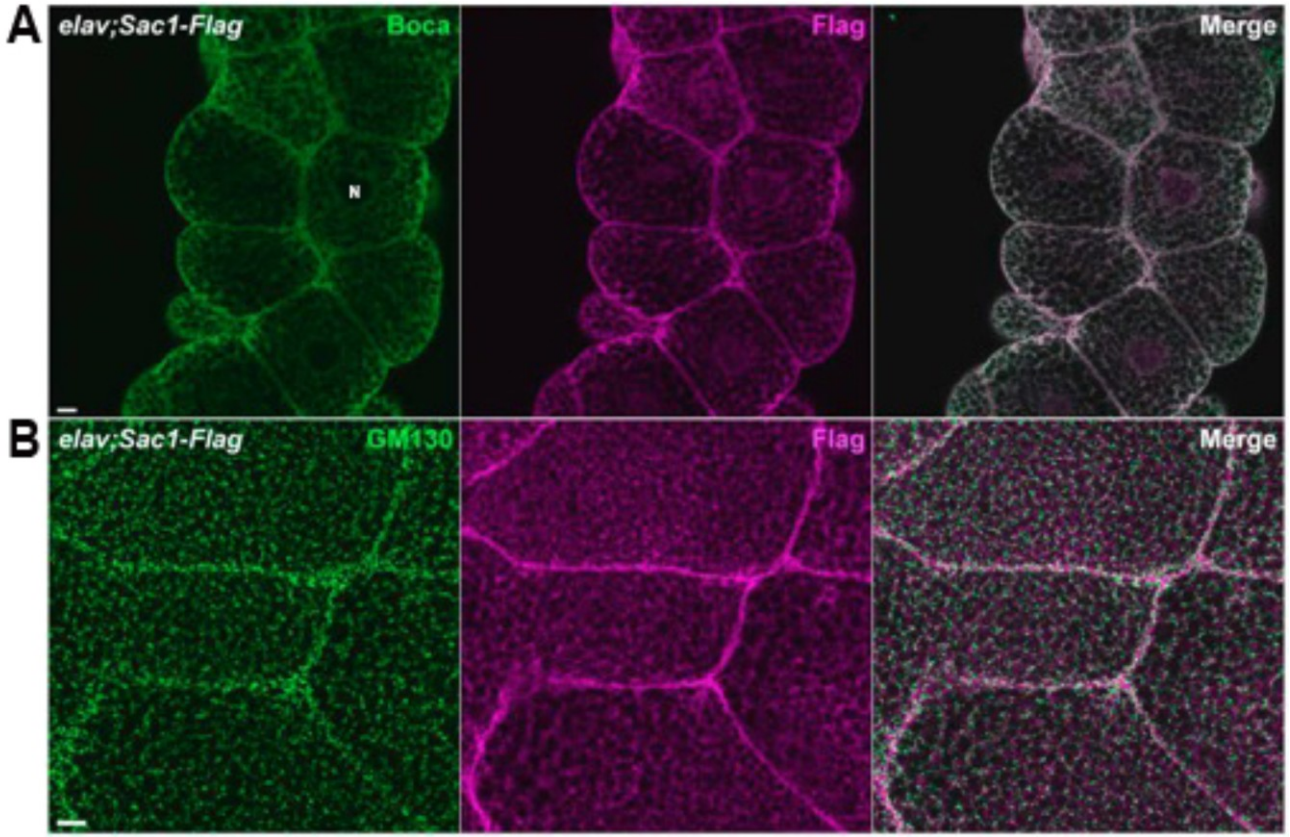

Figure 15. Sub-cellular distribution of Sac1 phosphatase in vivo. Confocal images of salivary gland cells from *elav;Flag-Sac1* (*elav-Gal4/Y;UAS-Flag-Sac1/+ and elav-Gal4/+;UAS-Flag-Sac1/+*) third instar larvae. (**A**) Anti-Boca (green) and anti-Flag (magenta) anti-sera were used to stain the cells. Boca is an ER marker. (**B**) anti-dGM130 (green) and anti-Flag (magenta) antibodies were used to visualize the proteins of interest. dGM130 is a Golgi marker. The N indicates the nucleus. 10 μm scale bar was used.

4.6 Conclusion

The interaction between DVAP and Sac1 is confirmed by the colocalization of these two proteins in several *Drosophila* larval tissues (brains, salivary glands, muscles and eye imaginal discs). However, when *Drosophila* larval tissues are examined, the extent of colocalization between the two proteins depends on the tissue. In fact, the stainings corresponding to DVAP and Flag-Sac1 extensively overlap in larval salivary glands and imaginal discs. On the other hand, Flag-Sac1 and DVAP colocalize only partially in larval brains and eye imaginal discs.

Moreover, the analysis of the subcellular distribution of DVAP and Sac1 in COS-7 cells reveal that these two proteins colocalize at the ER, whereas Sac1 seems to localize also to the Golgi complex. Thus, DVAP and Sac1 may interact at the ER membranes. Previously, an ER and Golgi-like distribution has been reported for Sac1 also in mammalian cells and yeast [Whitters et al., 1993; Konrad et al., 2002; Liu et al., 2008]. Nevertheless, the localization of Sac1 to the Golgi or to the ER apparatus seems to be influenced in yeast by abundance of nutrients or starvation condition. The localization of Sac1 to different sites in the cell allows this phosphatase to control PI4P pools that are generated by different PI4 kinases in different sites of the cell [Faulhammer et al., 2007]. Sac1 localizes at the contact sites between ER and PM when the nutrients are abundant. Here it dephosphorylates the PM-PI4P pool that is generated by Stt4 kinase [Tahirovic et al., 2005]. The enzymatic activity of Sac1 at these membrane contact sites seems to be controlled by its interaction with Scs2p and Osh3 proteins. In fact, Osh3 has a PH domain that can sense PI4P levels directly binding them. Osh3 is an interacting partner of Scsp that stimulate the Sac1 phosphatase activity when Osh3 senses high PM-PI4P levels [Stefan et al., 2011]. Moreover, also VAP proteins present a PIP-binding motif in their sequence that bind PI4P *in vitro* [Kagiwada and Hashimoto, 2007]. This evidence suggests that also VAPs can sense PI4P levels by directly binding

them. Interestingly, this 'PI4P binding motif' partially overlaps with the 'VAP consensus motif', that is required for the interaction with the FFAT motif. This evidence suggests that the binding of PIPs to VAP proteins may affect the interaction with Osh3 that has a FFAT motif in its sequence. On the other hand, Sac1 localizes to the contact sites between ER and Golgi complex under starvation conditions [Faulhammer et al., 2007]. Here it controls Golgi-PI4P pool that is generated by Pik1p [Walch-Solimena et al., 1999]. The anterograde trafficking is down-regulated as a consequence of Sac1 reducing Golgi-PI4P pool. These data suggest that the cell growth conditions affect the trafficking capacity of the Golgi [Piao and Mayinger, 2012].

In addition, we also observed the presence of vesicle-like structures where Sac1 and DVAP localize in the cytoplasm of COS-7 cells transiently expressing two tagged forms of DVAP and Sac1. VAPA has been observed together with OSBP-related-protein 9 (ORP9) in vesicle-like structures in the cytoplasm of mammalian cultured cells [Wyles and Ridgway, 2004]. ORP9 contains a PH domain that binds PI4P [Ngo and Ridgway, 2009]. Moreover, VAP proteins are implicated in the positioning of late endosomes (LE). This happens through the alignment of the LE along the ER membranes. VAPs interact with OSBP-related-protein 1 (ORP1) at the contact sites between ER and LE. These contact sites between ER and LE are transient and depend on the cholesterol levels. When there are low cholesterol levels the FFAT motif of ORP1 is available to interact with VAPs on the ER membrane. As a consequence the interaction between $p150^{Glued}$, that is a subunit of dynactin1, that, in turn, belongs to the dynein complex, and Rab7 interacting lysosomal protein (RILP) on the LE is lost and the LE move towards the positive end of microtubules [Rocha et al., 2009]. Dynein complex moves along the MTs through the interaction between its subunit $p150^{Glued}$ and dynein protein [Muresan et al., 2001]. Dynein complex drives vesicle transport along the motor neuronal axons [Dion et al., 2009]. The vesicle-like structures we observed may be LE. In yeast, Sac1 seem to regulate LE trafficking, through its PI4P phosphatase activity [Tahirovic et al., 2005]. In

addition, in null Sac1 yeast mutant strains PI3P are increased. PI3P is among the phosphoinositides that can be dephosphorylated by Sac1 [Guo et al., 1999]. Moreover, PI3P localizes to endosomal membranes [Gillooly et al., 2000]. However, there are no evidence of the localization of Sac1 to the endocytic compartments, but it may transiently localize to the LE [Tahirovic et al., 2005]. The fact that ORP1 contains a PH domain binding PI4P lipids may suggest that Sac1 activity is implicated in regulating ORP1 function in the positioning of LE.

Chapter 5: Sac1 and DVAP control similar functions at the larval neuromuscular junction

5.1 Introduction

The interaction between Sac1 and DVAP has been showed both *in vitro* and *in vivo*. As I have analysed this interaction in order to elucidate the molecular basis of the motor neuron disease, ALS8, I investigated the functional relevance of this interaction at the site that is major target of motor neuron diseases: the neuronal muscular junction [Ferraiuolo et al., 2011]. Moreover, the *Drosophila* larval NMJ is a site of biological importance to DVAP protein [Pennetta et al., 2002].

Thus, in order to determine whether DVAP and Sac1 are components of the same molecular process, I examined the effects caused alternatively by Sac1 LOF and DVAP LOF at the *Drosophila* larval NMJ pre- and post-synaptically. Subsequently, the phenotypes caused by both LOF have been compared between each other.

5.2 Sac1 and DVAP loss-of-function alleles (LOF) lead to a change in the presynaptic morphology at the NMJ

At first, the possibility that this interaction was functionally relevant at the NMJ was explored. Thus, the genetic interaction between Sac1 and DVAP was studied at the *Drosophila* larval neuromuscular junction. Here, DVAP drives synaptic sprouting by stabilizing microtubules within the boutons. A change in pre-synaptic morphology was observed in the NMJ of loss-of-function mutants for DVAP ($DVAP^{448}$). These larval motor neurons present bigger but fewer boutons [Pennetta et al., 2002].

On the other hand, Sac1 is an essential gene that is required during gastrulation and the early phases of embryonic development. Thus, Sac1 LOF animals die as embryos [Wei et al., 2003], this precludes the possibility of using these LOF mutant animals to study Sac1 function at the NMJ. *Drosophila* NMJ is a highly powerful system to carry out studies on synapse function and development because each component of the synaptic terminal, the motor neuron and muscle cell, forms in a stereotypically consistent manner. In addition to the neuromuscular junction, neuronal arborisation is unique and highly identifiable [Collins et al., 2007].

To bypass the embryonic lethality of Sac1 mutants, a transgenic RNAi approach was employed to reduce the expression levels of *Drosophila* Sac1 phosphatase [Fire et al., 1998]. The lack of a good antibody against *Drosophila* Sac1 did not give me the chance to check the Sac1 protein levels specifically in the tissues where Sac1 levels were decreased. Subsequently, the reduced levels of Sac1 RNA compared to the CS larvae have been reported by Mario Sanhueza [Forrest et al., 2013].

In order to look at the effect of reduced levels of Sac1 on the morphology of the presynaptic compartment of the NMJ, the expression of a *UAS-Sac1RNAi* transgene was driven pan-neuronally by using *elav-Gal4* driver [Yao, and White, 1994]. The larval muscles are organized in a stereotyped manner. Each abdominal segment is made of two specular hemisegments. Each abdominal hemisegment includes 30 skeletal muscles that are innervated by 40 motor neurons [Ruiz-Canada and Budnik, 2006]. The organization of muscles and motor neurons is repeated in each hemisegment [Crossley, 1978] with minor but noticeable differences. Thus, each skeletal muscle in the hemisegment is uniquely identifiable. Each motor neuron makes specific connections with the skeletal muscles in the hemisegment. The pre-synaptic bouton morphology of the NMJ of muscles 12 in the abdominal segment 3 (A3) of 3rd instar larvae was examined. To look at the pre-synaptic shape of the larval NMJ, neurons were

stained with anti-HRP antibody. In *Drosophila*, anti-HRP staining allows to visualize the pre-synaptic arborisation profile (Fig. 16A), as this antiserum binds to carbohydrate lateral chains of several neuronal membrane proteins [Jan and Jan, 1982]. Interestingly, an increase in the size of boutons and a decrease in their number compared to control animals was observed (Fig. 16A-B). This phenotype recapitulates the one, previously reported at the NMJ from third instar larvae lacking DVAP [Pennetta et al., 2002].

In particular, when the surface area in μm^2 of the examined presynaptic boutons from *elav;Sac1RNAi* larvae was compared to control larvae, the bouton size of *elav;Sac1RNAi* larvae is, almost, twice the surface area of boutons from control larvae (Fig. 16C). Control larvae have a presynaptic bouton surface area of 5-10 μm^2 at the NMJ. Moreover, few boutons from control larvae have a surface area of 20-25 μm^2, and no boutons over 25 μm^2. In contrast, *elav;Sac1RNAi* larvae present presynaptic boutons with a surface area of 5-25 μm^2. Boutons with a surface area over 25 μm^2 were consistently detected. Additionally, the quantification of the number of presynaptic boutons in *elav;Sac1RNAi* larvae was half the number of boutons which was observed in w.t. animals (Fig. 16D). The statistical analysis has been made by Mario Sanhueza.

These findings show that when Sac1 phosphatase levels are decreased pre-synaptically, the morphology of the synapse is affected. A similar phenotype was, previously, observed in DVAP loss-of-function ($DVAP^{448}$) [Pennetta et al., 2002].

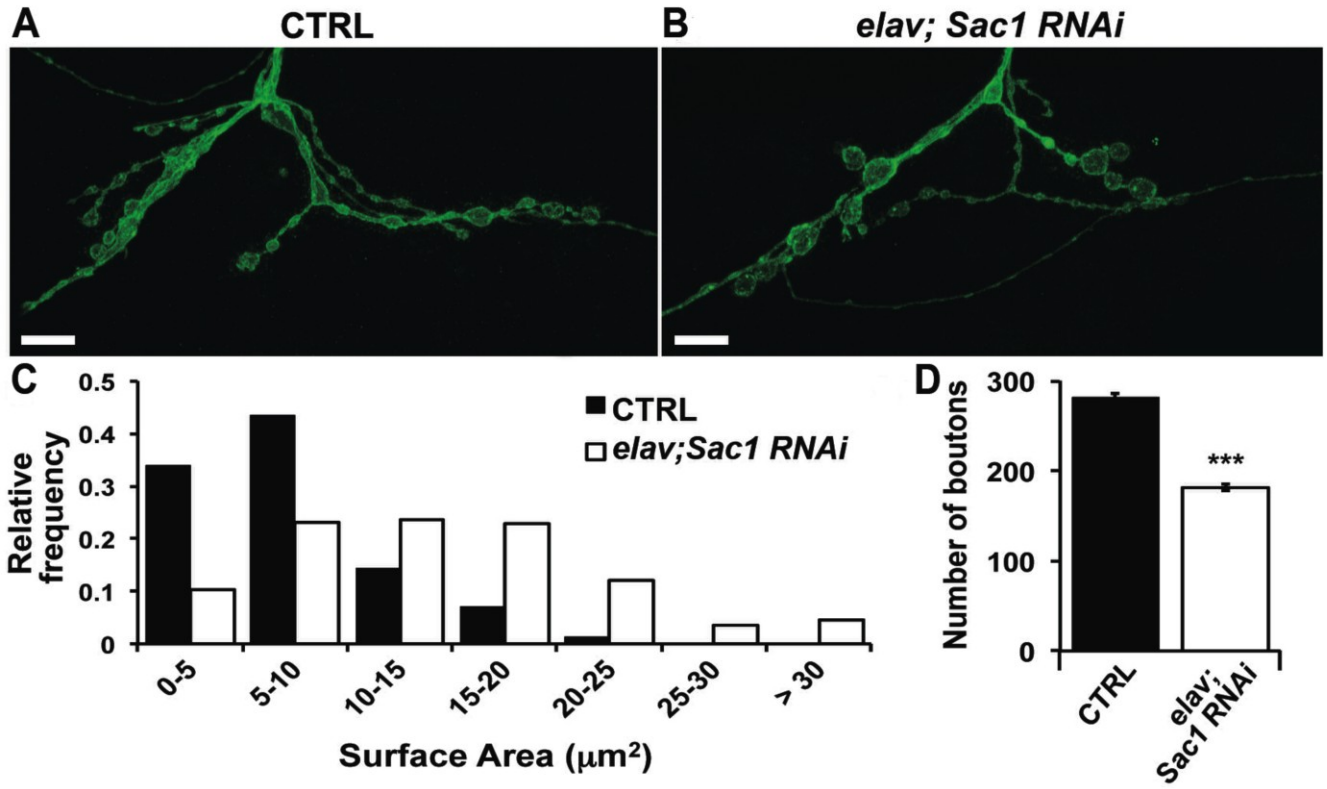

Figure 16. Sac1 and DVAP interaction is functionally relevant. (**A**) Confocal images of muscle 12 from control larvae are compared to (**B**) confocal images of the same muscle from *elav;Sac1RNAi* (*elav-Gal4/+;+/+;UAS-Sac1RNAi/+ and elav-Gal4/Y;+/+;UAS-Sac1RNAi/+*) animals. The pre-synaptic compartment was stained with anti-HRP antiserum. (**C**) Bouton size and (**D**) bouton number were quantified in both controls and *elav;Sac1RNAi* animals. Frequency stands for the ratio between bouton number within a defined range of sizes and the total bouton number. The used scale bar is 10 μm. Error bars = s.e.m. ***P<0.001.

5.2 Sac1 is involved in stabilizing the MT network at the presynapsis of third instar NMJs

The NMJ phenotype of down-regulating Sac1 at the presynaptic compartment (i.e. bigger, but fewer presynaptic boutons) phenocopies the DVAP KO presynaptic phenotype (*DVAP*^{448}) [Pennetta et al., 2002], similar to that seen in *futsch* hypomorphic mutants [Roos et al., 2000]. *Futsch* encodes the *Drosophila* homolog of the Microtubule associated protein-1B (MAP1B) [Hummel et al., 2000]. This protein is associated to microtubules and it is essential for stabilizing the hairpin loop structure that microtubules assume inside the bouton to promote bouton formation in the synapse [Miech et al., 2008; Roos et al., 2000; Hummel et al., 2000]. In addition, either DVAP KO mutations or hypomorphic mutations in futsch present a quite altered MT cytoskeleton inside these bigger boutons. These findings are in agreement with the observation that both proteins directly interact with MT [Pennetta et al., 2002; Roos et al., 2000]. In particular, DVAP was proposed to act as a bridge between MTs and membranes [Pennetta et al., 2002].

As the Sac1 protein is a direct interactor of DVAP, the integrity of the MT cytoskeleton network present in the large presynaptic boutons at NMJs from *elav;Sac1RNAi* larvae was examined. To this aim, *UAS-Sac1RNAi* transgenic construct was selectively expressed in the nervous system, using *elav-Gal4* driver [Yao and White, 1994]. The larval neuromuscular junction was double immunostained with anti-HRP [Jan and Jan, 1982], and anti-Futsch antisera. The anti-Futsch antibody corresponds to the mAb22c10 [Hummel et al., 2000] monoclonal antibody and it detects MAP1B in *Drosophila.* Anti-HRP staining allows the visualization of the change in bouton size and number when Sac1 levels are decreased. Anti-Futsch staining appeared as a filament that runs through the NMJ presynaptic branches in control animals [Godena et al., 2011] (Fig. 17A). When Sac1 expression levels are diminished, the change in presynaptic staining pattern of Futsch is altered (Fig. 17C). The futsch-positive

filaments do not traverse continuously along the presynaptic processes anymore but appear more fragmented and sometimes punctuated, especially in boutons that are more distant from the branching point at the axon terminal (Fig. 17C). Simultaneously, the microtubule organization was examined in the same way in larval NMJs from animals having decreased levels of DVAP in the nervous system (*elav;DVAPRNAi)*. Likewise, big boutons at the NMJ of mutant third instar larvae were associated with MT fragmentation at the presynaptic ramifications (Fig. 17B).

Taken together these results show that the altered presynaptic morphology detected at NMJ from mutant larvae with low Sac1 levels, is associated with an altered presynaptic MT architecture. These findings are in agreement with the results reported earlier in this Results section showing that Sac1 interacts *in vitro* and colocalize *in vivo* with a protein that is associated with MTs.

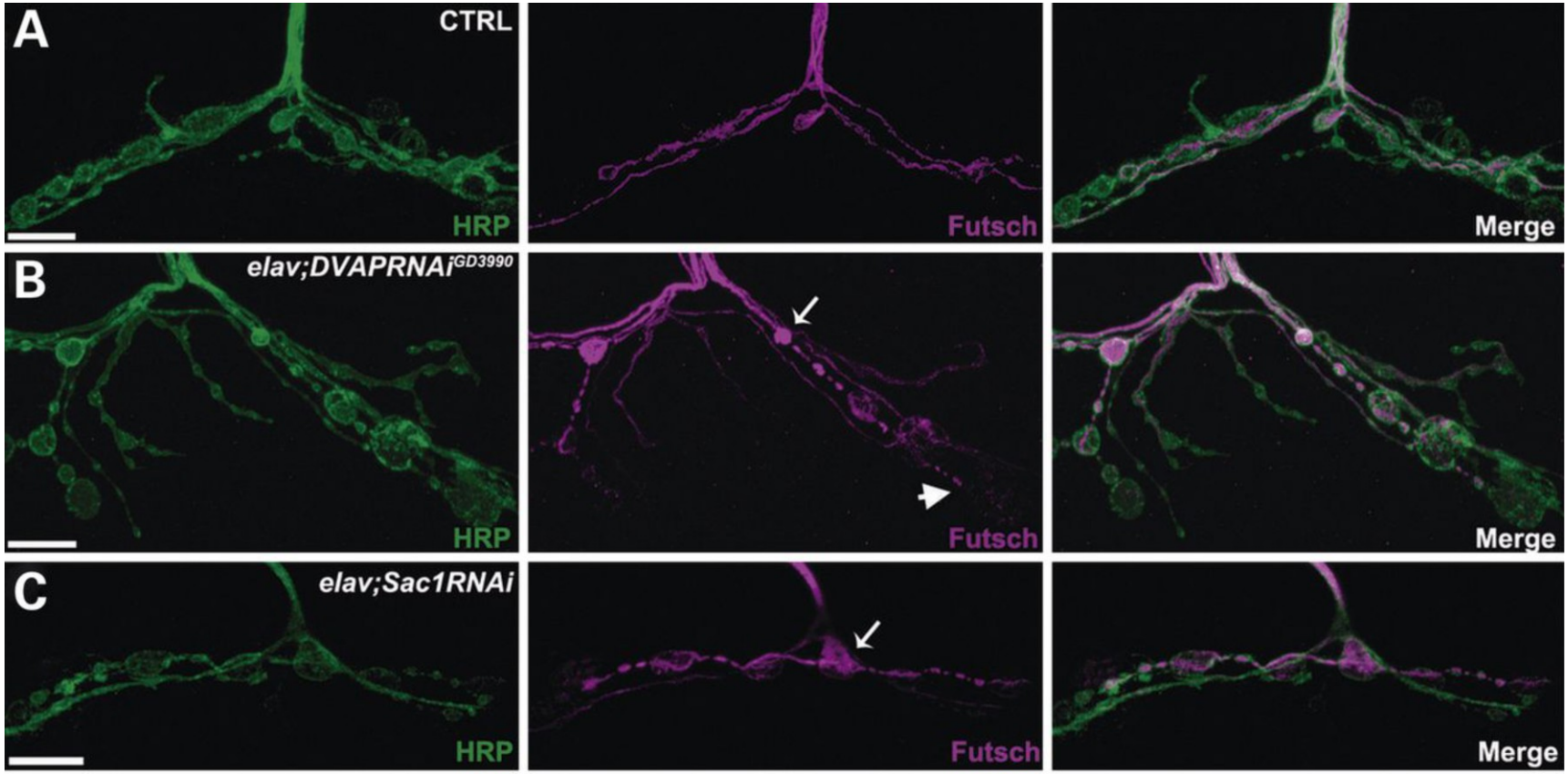

Figure 17. Sac1 has a role in stabilizing microtubules at the NMJ. The confocal images show the synapses of muscle 12 from (**A**) control larvae, (**B**) *elav;DVAPRNAi* (*elav-Gal4/+; +/+;UAS-DVAPRNAi/+ and elav-Gal4/Y; +/+;UAS-DVAPRNAi/+*) larvae, and (**C**) *elav;Sac1RNAi* (*elav-Gal4/+; +/+;UAS-Sac1RNAi/+ and elav-Gal4/Y; +/+;UAS-Sac1RNAi/+*) larvae. The presynaptic compartment was stained with anti-HRP, and anti-Futsch antisera. The arrowheads indicate boutons with punctuate Futsch staining, whereas arrows indicate boutons with Futsch staining accumulation. The scale bar used is 10 μm. Error bars = s.e.m. ***P<0.001.

5.3 Sac1 and DVAP are involved in vesicle trafficking in the axons of motor neurons

MTs are fundamental components of the axon terminal, stabilizing the presynaptic branches and controlling the presynaptic bouton budding [Tanaka et al., 1995]. In particular, the MTs are arranged in bundles with uniform orientation in the axons of motor neurons. In the axons these MT bundles are involved in axonal polarization and axonal growth [Conde and Caceres, 2009].

Given that Sac1 seems to be implicated in preserving the MT network within the presynaptic boutons, the chance that Sac1 has a similar role on the axonal MTs was explored. Moreover, this possibility has never been tested also for DVAP. To answer these questions, the possibility that decreased levels of either Sac1 or DVAP in the nervous system could perturb MT organization in the axons was tested.

Control and *elav;Sac1-RNAi* third instar larval NMJs were stained with both anti-HRP [Jan and Jan, 1982] and anti-Futsch antibodies. A continuous Futsch-positive thread was observed in control larvae running through the axon to the branching point where it divides into several branches. The microtubule organization in the axons did not appear to be affected in *elav;Sac1RNAi* larvae motor neuron (data not shown). In addition, the same experiment was carried out in parallel on *elav;DVAPRNAi* third instar larval NMJs. As with Sac1 down regulation, no differences in axonal microtubule structure were detected in axons from larvae having low DVAP levels in the nervous system (*elav;DVAPRNAi)* (data not shown).

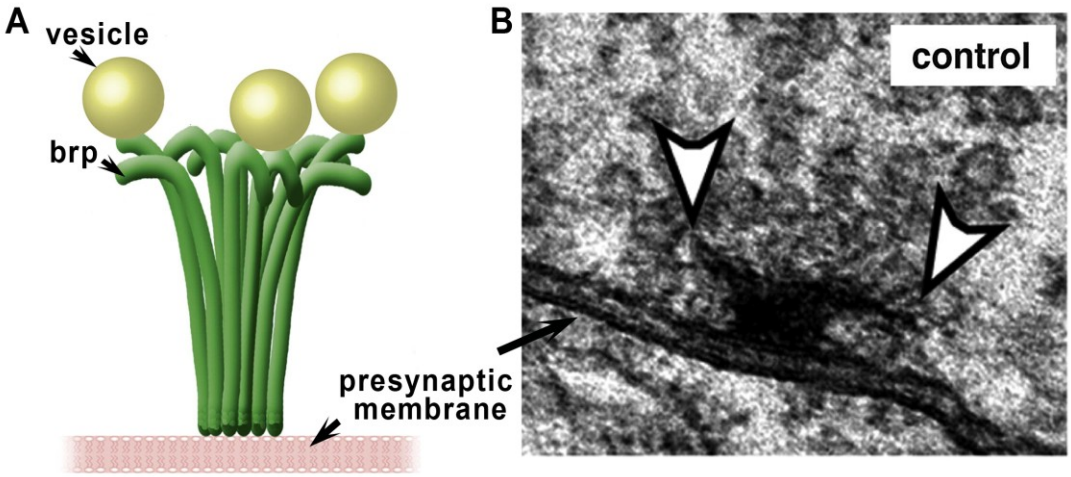

Figure 18. Diagram of T-bars. (A) represents a schematic representation of brp proteins associated to the presynaptic membrane and forming the T-bar together with presynaptic vesicles. (**B**) T-bar is shoed by Scanning Electron Microscopy. The two white arrowheads show the sides of the T-bar. Figure adapted from Toonen and Verhage, 2011

Nevertheless, the effect of low levels of Sac1 or DVAP on axonal vesicle transport was examined by staining NMJs from *elav;Sac1RNAi* and *elav;DVAPRNAi* mutant third instar larvae with the antibody against bruchpilot (brp) protein. Brp is the *Drosophila* homolog of ELK/CAST/ERC protein, which resides in the active zones and binds "T-bars" complex (Fig. 18) [Wagh et al., 2006; Kittel et al., 2006]. T-bars are cytoplasmic projections that facilitate the flow of the presynaptic vesicles to the active zones at synapses, characterized by a high vesicle release [Johnson III et al., 2009]. Some proteins have been identified in these cytoplasmic projections of vertebrates, whereas Brp is the only protein to be known in this site in *Drosophila* [Johnson III et al., 2009]. Sac1 protein was knocked-down by using the *UAS-Sac1RNAi* transgenic construct in the nervous system by using the *elav-Gal4* driver [Yao and White, 1994]. Double staining was carried out on larval motor neuron axons by using anti-HRP [Jan and Jan, 1982] and anti-Brp antisera [Hofbauer et al., 2009]. Brp staining in motor neuron axons from control larvae was virtually absent (Fig. 19A), whereas *elav;Sac1RNAi* transgenic animals showed Brp-positive puncta (Fig. 19C). Analysis of the nerve from *elav;DVAPRNAi* larvae stained with anti-

HRP and anti-Brp showed that although Brp-positive puncta were observed in the axons of NMJs from these transgenic larvae, they were less evident compared to the Brp-positive puncta found in *elav;Sac1RNAi* larvae (Fig. 19B). Moreover, quantification of the Brp signal in axons from control, *elav;DVAPRNAi* and *elav;Sac1RNAi* larvae indicated a big difference between the number of Brp-positive puncta of the mutant larvae and the control larvae (Mario Sanhueza, Fig. 19D).

These data suggest that Sac1 has a role in the transport along the motor neuron axons. In order to explore this hypothesis in depth, motor neuron axons from control, *elav;Sac1RNAi*, and *elav;DVAPRNAi* were stained with an antibody against a protein which has an important role in the transport of vesicles through the axons: Cysteine String Protein (CSP) [Zinsmaier et al., 1994]. NMJs from the three different genotypes were stained with anti-HRP and anti-CSP, and they were compared between each other. *Elav;Sac1RNAi*, and *elav;DVAPRNAi* transgenic larvae presented CSP-positive accumulations in motor neuronal axons (data not shown).

These findings support the hypothesis that the function of both Sac1 and DVAP are important for the transport of synaptic vesicles through the nerve.

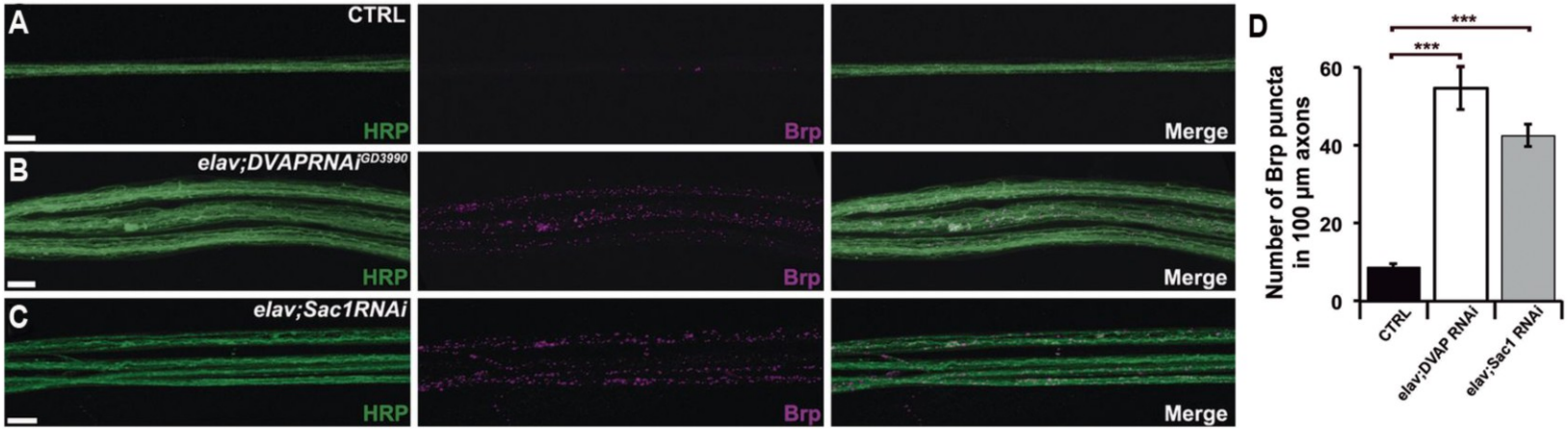

Figure 19. Low Sac1 and DVAP levels induce Brp aggregates in the motor neuron axons. Confocal images of motor neuron axons on muscle 12 from (a) CTRL, (b) *elav;Sac1RNAi* (*elav-Gal4/+; +/+;UAS-Sac1RNAi/+ and elav-Gal4/Y; +/+;UAS-Sac1RNAi/+*), and (c) *elav;DVAPRNAI* (*elav-Gal4/+; +/+;UAS- DVAPRNAI/+ and elav-Gal4/Y; +/+;UAS- DVAPRNAI/+*) larvae. The axons are stained with anti-HRP, and anti-CSP. The scale bar used is 10 µm. (d) Quantification of Brp signal in nerves of the CTRL, *elav;Sac1RNAi* (*elav-Gal4/+; +/+;UAS-Sac1RNAi/+ and elav-Gal4/Y; +/+;UAS-Sac1RNAi/+*), and *elav;DVAPRNAI* (*elav-Gal4/+; +/+;UAS- DVAPRNAI/+ and elav-Gal4/Y; +/+;UAS- DVAPRNAI/+*) larvae. s.e.m.***P<0.001 is symbolized by error bars

5.4 Sac1 and DVAP are required for the proper localization of adducin and β-spectrin

Following the analysis of the interaction between DVAP and Sac1 at the presynaptic compartment of the larval NMJ, Sac1 function was examined also in the postsynaptic compartment of the NMJ. Thus, the effect of reduced Sac1 and DVAP levels on adducin, β-spectrin and DLG proteins that have been well characterized postsynaptically at the *Drosophila* larval NMJ, and have been found implicated in neurodegeneration, was analyzed. These three proteins belong to the spectrin-actin cytoskeleton (Fig. 20) that is placed under the plasma membrane of the post-synaptic compartment supporting the presynaptic compartment of the NMJ.

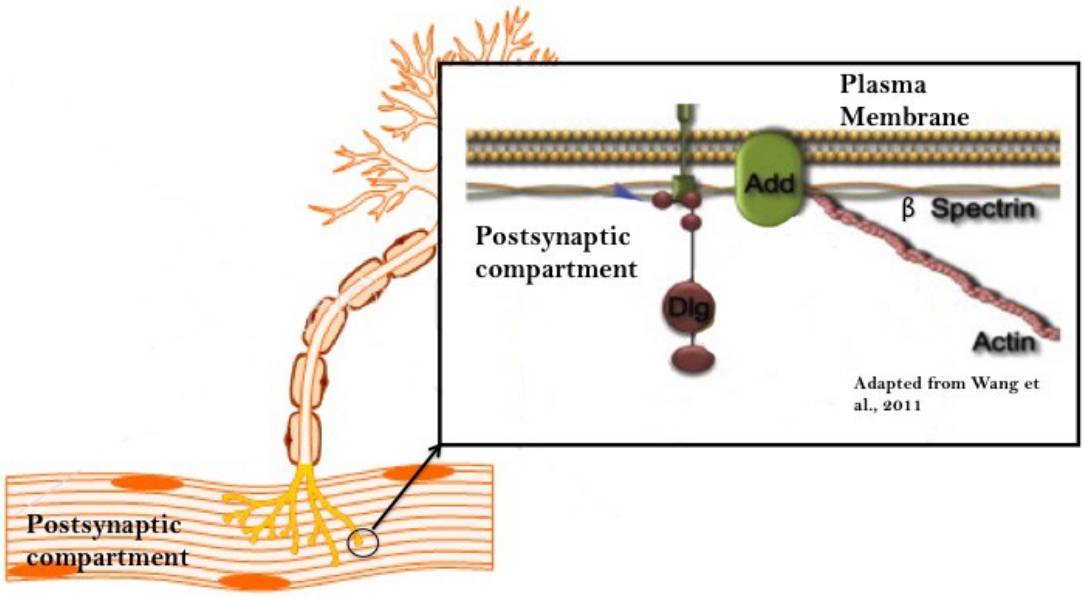

Figure 20. Schematic representation of the Adducin, *β*-spectrin, Dlg and actin in the spectrin-actin cytoskeleton of the post-synaptic compartment. Add = adducin, Dlg = discs large protein. Figure adapted from Wang et al., 2011.

Adducin has an actin-capping activity [Pielage et al., 2011]. In *Drosophila*, one gene (*hu-li tai shao*, also named *hts*) encodes for one adducin protein [Robinson et al., 1994]. In vertebrates three genes encode adducin proteins: *α-adducin*, *β-adducin* and *γ-adducin* [Matsuoka et al., 2000]. The effect of Sac1 and DVAP

functions on adducin distribution pattern was examined for the following reasons. First, impairment in synaptic plasticity and learning was observed in mice where the function of β-adducin was abolished [Shan et al., 2005]. Moreover, adducin has been recently shown to play a key role in synaptic stability in mice and *Drosophila* [Bednarek and Caroni, 2011; Pielage et al., 2011]. Lastly, PKC kinase is required to phosphorylate adducins and high levels of phosphorylated *α-adducin* and *γ-adducin* in association with high levels of PKC were observed in ALS patients [Hu et al., 2003]. Interestingly, PKC activity is induced by a number of lipid molecules including PIPs [Hu et al., 2003].

β-spectrin together with *α*-spectrin and short actin fragments form a network called 'spectrin skeleton' that anchors to the membrane through the interaction with PM-PIPs and PM-proteins [Pielage et al., 2006; Zhang et al 1995]. The interaction of *β*-spectrin is mediated by the PH domain in *β*-spectrin sequence [Zhang et al 1995]. It has been proposed that the spectrin skeleton acts as a frame around the presynaptic compartment [Pielage et al., 2006]. Interestingly, mutations in the domain of *β*-spectrin implicated in the interaction with actin were identified in some Spinocerebellar Ataxia type 5 (SCA5) patients [Ikeda et al., 2006].

In order to analyze the effect of diminished expression levels of Sac1 phosphatase and DVAP on adducin in the postsynaptic compartment at the larval NMJ, the expression of *UAS-Sac1RNAi* and *UAS-DVAPRNAi* transgenes was selectively directed by using the *BG57-Gal4* driver [Budnik et al., 1996]. The NMJ presynaptic compartment profile of wild-type and transgenic larvae was delineated by the use of an antibody against HRP. On the other hand, *Drosophila* adducin in the post-synaptic compartment was visualized through an anti-Hts antiserum (anti-Hts1B1) [Petrella et al., 2007]. In control animals postsynaptic adducin is especially concentrated at the sub-synaptic reticulum (SSR) membrane folds around the presynaptic membrane (Fig. 21A) [Pielage et

al., 2011]. In w.t. animals the anti-HRP antibody delineates the presynaptic membrane that has boutons with regular rounded shape, and they are uniformly arranged along the motor neuron ramification, as "beads on a string" –like organization (Fig. 21A) [Johansen et al., 1989]. In *BG57;DVAPRNAi* larvae the pre-synaptic membrane morphology is highly deformed showing boutons with irregular profile and bigger size. In addition, the adducin distribution pattern is clearly perturbed (Fig. 21B). Likewise, diminished Sac1 levels in the postsynaptic compartment cause a change also in the presynaptic profile, and altered adducin localization (Fig. 21C).

In order to further examine the functional relevance of the association between Sac1 and DVAP, larval NMJs from *BG57;Sac1RNAi* and *BG57;DVAPRNAi* were dissected and double-stained with anti-HRP and anti-*β*-spectrin antisera. As adducin and *β*-spectrin interact with each other to stabilize the spectrin-actin cytoskeleton in the postsynaptic compartment [Bennett et al 1988; Kuhlman et al 1996], wild type larvae displayed a *β*-spectrin staining that closely follows the adducin localization pattern (Fig. 21D). When Sac1 levels were lowered in muscles (*BG57;Sac1RNAi*), larval NMJs presented an unusual diffuse *β*-spectrin distribution when they were compared to control larvae (Fig. 21F). Similarly, an abnormal and irregular *β*-spectrin distribution pattern was detected in *BG57;DVAPRNAi* third instar larval muscles. Also in this case *β*-spectrin staining no longer defines and surrounds the presynaptic membrane (Fig. 21E).

The possibility that Sac1 and DVAP down-regulation in the postsynaptic compartment can affect the distribution of discs large (DLG) was also explored. DLG, the *Drosophila* homolog of PSD (post-synaptic density) -95, is a well-characterized postsynaptic protein and it functions in a complex with adducin and *β*-spectrin, and depends from these two proteins for its proper postsynaptic distribution [Wang et al., 2011; Featherstone et al., 2001; Lahey et al., 1994]. Larval NMJs from *BG57;DVAPRNAi* and *BG57;Sac1RNAi* were double-labeled with anti-HRP and anti-DLG antibodies. Postsynaptic DLG distribution appears

to be altered in both transgenic mutant larvae (Fig. 21G-I), in much the same way as for the previously examined post-synaptic markers.

Nevertheless, besides the changes in the postsynaptic marker distribution patterns, when DVAP and Sac1 are reduced in the postsynaptic compartment of the NMJ, altered bouton shape of the presynaptic compartment is observed (Fig. 21). In control animals, the morphology of boutons consists of a well-defined and oval shape with neuronal process separating the bouton from each other. When the levels of both DVAP and Sac1 are down-regulated, boutons present an abnormal appearance. Intriguingly, they display a bigger size and exhibit protrusions on their surface that are similar to spikes (Fig. 21 B, C, E, F, H, I).

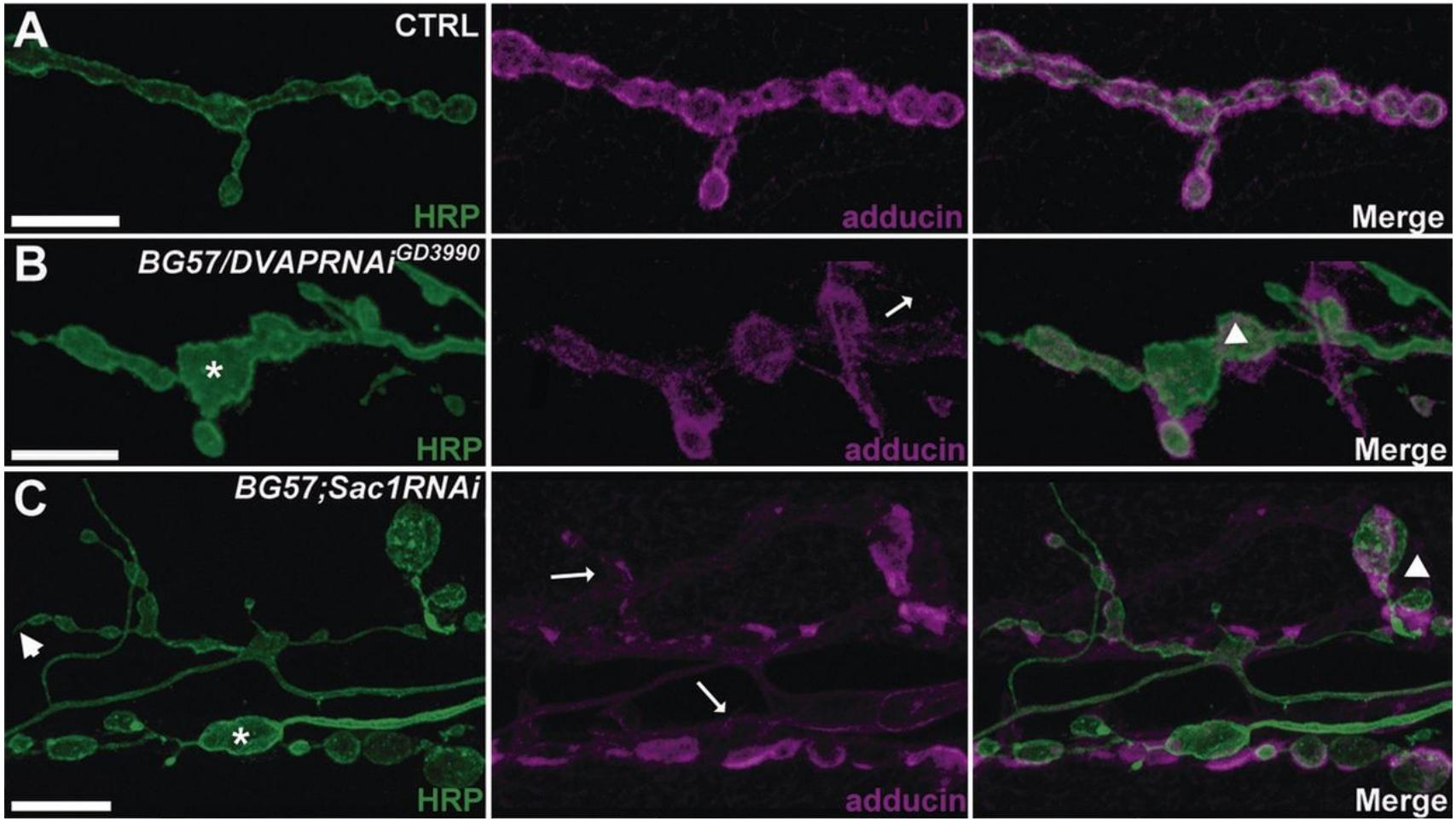
A
CTRL
HRP
adducin
Merge
B
BG57/DVAPRNAi^GD3990
*
HRP
adducin
Merge
C
BG57;Sac1RNAi
*
HRP
adducin
Merge

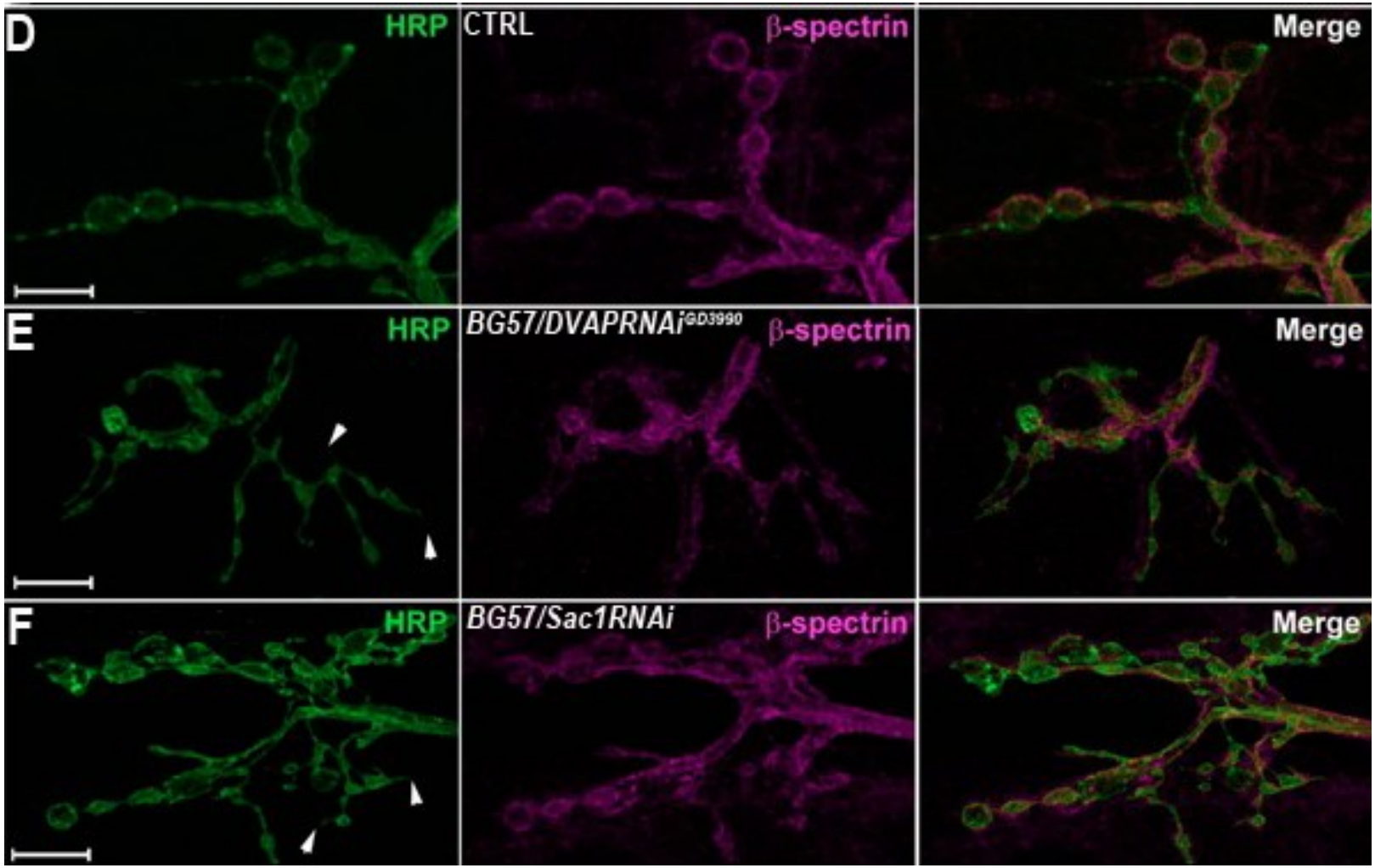
D
HRP
CTRL
β-spectrin
Merge
E
HRP
BG57/DVAPRNAi^GD3990
β-spectrin
Merge
F
HRP
BG57/Sac1RNAi
β-spectrin
Merge

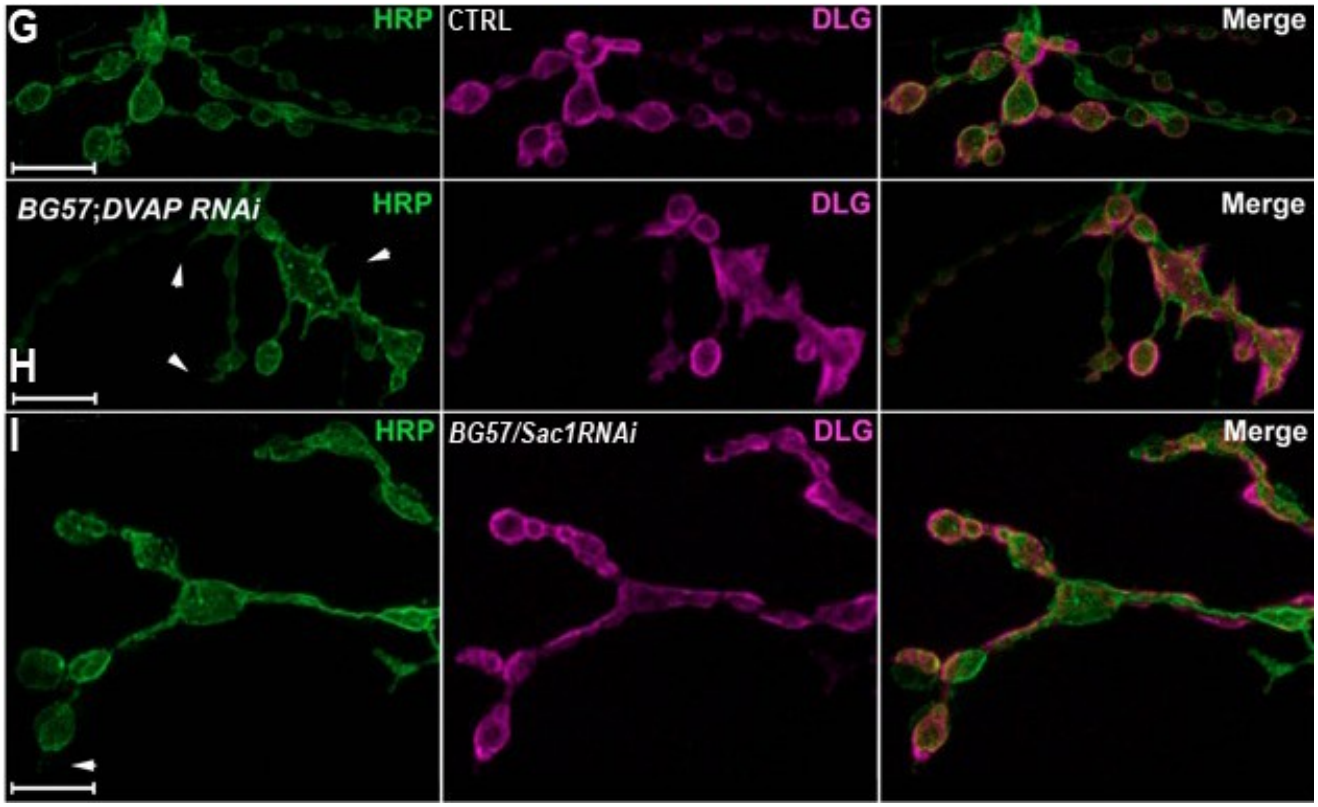

Figure 21. Postsynaptic Adducin, β-spectrin and adducin localization is altered when Sac1 and DVAP are down-regulated selectively in muscles. Confocal images from (**A,D,G**) CTRL, (**B,E,H**) *BG57;DVAPRNAI*^{GD3990} (*BG57-Gal4/+;UASDVAPRNAI/+*), and (**C,F,I**) *BG57;Sac1RNAi* (*BG57-Gal4/+;UAS-Sac1RNAi/+*) larvae. In (**A-C**) third instar larval NMJ were stained with anti-HRP and anti-adducin (anti-HTs1B1) antisera. In (**D-F**) third instar larval NMJ were stained with anti-HRP and anti-β-spectrin antibodies. In (**G-I**) third instar larval NMJ were stained with anti-HRP and anti-DLG antisera. Missing or diffused post-synaptic staining is indicated by arrows, whereas spike-like protrusions are indicated by arrowheads. The scale bar used is 10 μm.

5.5 Conclusion

Sac1 function appears to be fundamental for proper presynaptic membrane shape at the *Drosophila* larval NMJ. Interestingly, low levels of Sac1 at the pre and postsynaptic compartments result in changes of presynaptic membrane shape. On the one hand, the altered PM membrane shape seems to be caused by the altered MT organization in the presynaptic boutons. On the other hand, the delocalization of important components of the spectrin-actin cytoskeleton, such as adducin, β-spectrin and DLG, underlying the postsynaptic PM, also seems to affect the shape of the presynaptic membrane. Both disruption of the MT organization of MT cytoskeleton in the presynaptic boutons, and altered organization of the spectrin-actin cytoskeleton in the muscles are consequences of decreased levels of Sac1 respectively. Nevertheless, the extent of the shape alteration is different according to the compartment of the *Drosophila* larval NMJ where the Sac1 levels where decreased. In fact, when Sac1 was decreased in the presynaptic compartment, the MTs into the boutons were disorganized, and the bouton appeared smaller than wt ones. When Sac1 levels were lowered in the postsynaptic membrane, and, consequently, the adducin, β-spectrin and DLG were mislocalised in the muscles, the presynaptic membrane appeared deformed with spike-like protrusions.

Intriguingly, low levels of Sac1 in the presynaptic membrane are not only associated to altered MT cytoskeleton inside the presynaptic boutons but also to the accumulation of vesicles into the axons of motor neurons. It is not clear which is the relationship between the two phenotypes observed at the presynaptic compartment of the NMJ.

Chapter 6 Sac1 loss-of-function leads to a neurodegeneration

6.1 Introduction

So far, the interaction between DVAP and Sac1 has been examined in vitro and in vivo. The analysis of this interaction in vivo not only has been performed showing the colocalization between the two proteins both in COS-7 cells and *Drosophila* larval tissues, but also looking at the involvement of the functions of DVAP and Sac1 in similar pathways at the larval NMJ. The NMJ is the site that is most severely affected in motor neuron diseases [Ferraiuolo et al., 2011].

Interestingly, Forrest et al., [2013] showed that high levels of PI4P in muscles, brains and salivary glands are associated to both decreased levels of Sac1 and expression of DVAP-P58S in the nervous system. PI4P is the substrate of Sac1 phosphatase, and high levels of PI4P can be associated to an impaired Sac1 activity. Therefore, as both DVAP-P58S and low levels of Sac1 lead to high levels of PI4P, I decided to investigate whether decreased levels of Sac1 as DVAP-P58S could cause neurodegeneration.

6.2 Decreased Sac1 expression levels lead to neurodegeneration

In order to address examine whether Sac1 is implicated in neurodegenerative processes, the levels of Sac1 phosphatase were turned down selectively in the nervous system. Thus, the expression of *UAS-Sac1RNAi* was targeted to the nervous system under the control of the pan-neuronal driver *elav-Gal4* [Yao and White, 1994]. At first, the viability rate (females observed/females expected) of *elav;Sac1RNAi* transgenic animals was recorded. Mutant flies were monitored over the different developmental stages, and the males eclosed into adults at the 50% of the expected Mendelian ratio. This experiment showed that Sac1, as DVAP, affect the developmental process of *Drosophila*. This evidence suggests

that can play a role in neurodegenerative processes and that the amount of Sac1 phosphatase is inversely proportional to neurodegeneration.

Intriguingly, necrotic patches at the legs joints of *elav;Sac1RNAi* transgenic males were also observed (data not shown). It is possible that this patches can make the legs more fragile, and, thus, sensitive to breakage. Moreover, *elav;Sac1RNAi* male flies encounter early death between the 3rd and the 4th day from eclosion. In addition, an obvious degeneration was detected in the eyes of these flies (Fig. 22A); nevertheless, females and males displayed different intensity of this phenotype. In fact, *elav-Gal4/Y;UAS-Sac1RNAi* males present necrotic patches which covered almost the entire area of the eye. The penetrance of this phenotype is 100%, however, the patches of necrosis on the eyes of males displayed differences regarding their extent of damaged tissues and number of patches (Fig. 22A). On the other hand, *elav-Gal4/+;UAS-Sac1RNAi* females present depigmentation all over the eye surface (Fig.22A). The dosage compensation is the reason why such a difference in the phenotype is recorded between males and females [Warrick et al., 1999]. To double check whether the degenerative effect of decreased levels of Sac1 was genuine or the *elav-Gal4* contributed to this phenotype, the appearance of eyes from *elav-Gal4/Y* and *elav-Gal4/+* transgenic flies was examined. In this case, the presence of the driver did not affect the integrity of the eye structure (data not shown).

Evidence about the involvement of Sac1 phosphatase in neurodegeneration was reported as a consequence of the expression of a hypomorphic allele of Sac1 [Wei et al., 2003]. It was not possible to reproduce the degenerative phenotype due to this allele, because this hypomorphic allele is lost and not longer available. However, it has been shown, independently, that decreased levels of Sac1 are associated with neurodegeneration. These data mean that the neurodegeneration observed in flies having lower levels of Sac1 in the nervous system is authentic, and it is not due to off-target effects.

The adult eyes from *elav-Gal4/Y;UAS-Sac1RNAi* transgenic male flies have also been examined by SEM analysis. Thus, it is possible to visualize the architecture of ommatidia that is highly disorganized when compared to the eyes of control flies (Fig. 22B). Additionally, the SEM analysis also showed that mechano-sensory bristles appear sometimes supernumerary and sometimes missing whilst adult eyes are regularly distributed among the ommatidia in *CS* flies (Fig. 22B).

Finally, the extent of the degeneration of the adult *Drosophila* eye from *elav-Gal4/Y;UAS-Sac1RNAi* transgenic male was examined also by looking at the internal structure of the eye by histological analysis. The retina is completely lost, with only few fragments of photoreceptors left (Fig. 22C). On the other hand, an organized array of photoreceptors is visible beneath the eye surface in control flies (Fig. 22C).

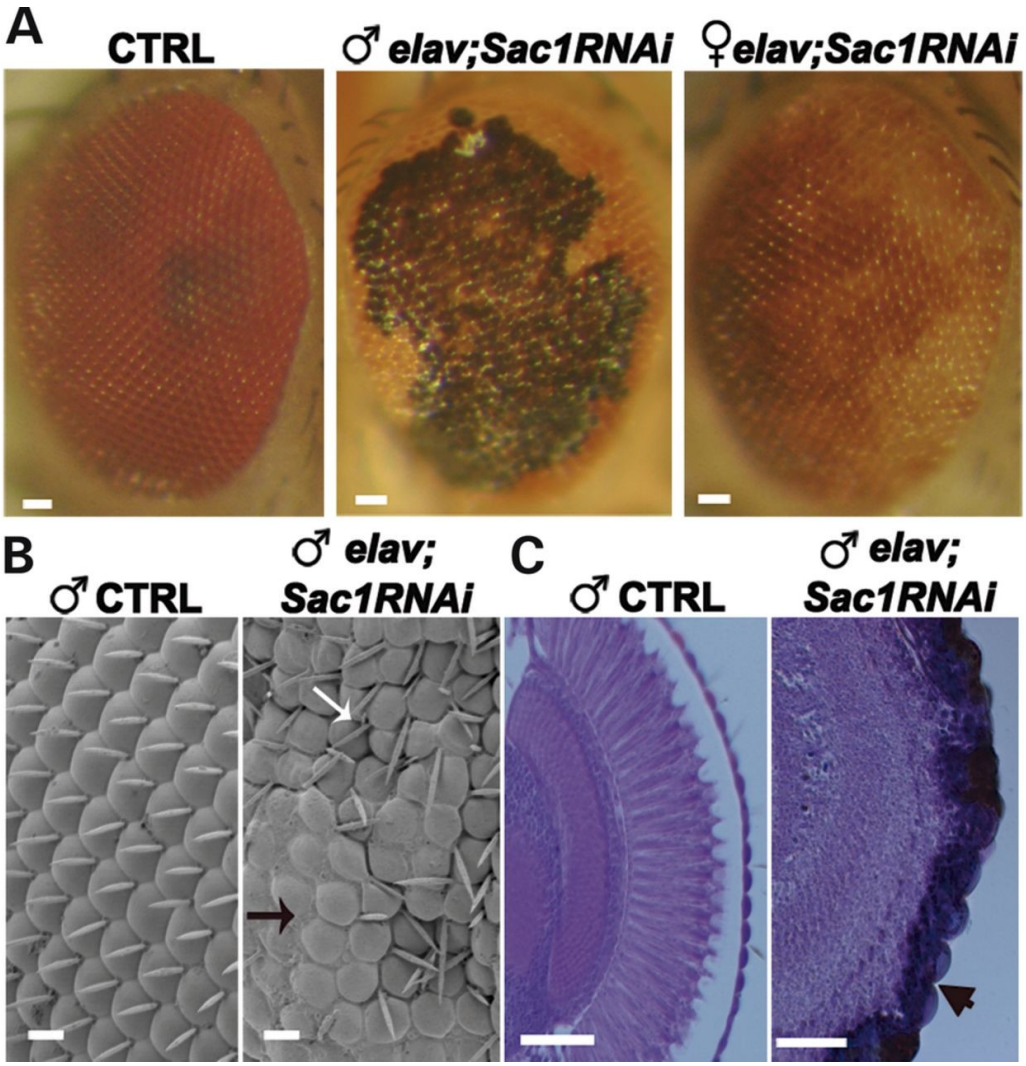

Figure 22. Decreased Sac1 levels cause dosage-dependent neurodegeneration. (**A**) Control, *elav;Sac1RNAi* (*elav-Gal4/Y;+/+;UAS-Sac1RNAi/+)* males and *elav;Sac1RNAi* (*elav-Gal4/+;+/+;UAS-Sac1RNAi*/+) females adult eyes (Stereomicroscope images). (**B**) Control eyes and *elav;Sac1RNAi* transgenic eyes of adult males (SEM images). (**C**) Control eyes and *elav*;*Sac1RNAi* transgenic eyes of adult males (Paraffin sections). 10 μm are represented by scale bars in (**B**) and 50 μm in (**A**) and (**C**).

6.3 Progressive neurodegeneration is observed when Sac1 is lowered in the adult *Drosophila* brain

It has been reported in this thesis that low levels of Sac1 phosphatase in the nervous system are associated with a neurodegenerative phenotype. ALS is a motor neuron disease that is characterized by a progressive worsening of the symptoms [Ferraiuolo et al., 2011]. The possibility that a progressive neurodegeneration was observed when Sac1 levels where lowered selectively in the nervous system was explored. To this aim, the internal structure of the optic lobe from *elav;Sac1RNAi* adult flies was analysed through paraffin sections. In control flies, the structure under the retina is organized showing a tidy organization of the three optic ganglions (Lamina, Medulla, and Lobula) (Fig. 23A). In newly hatched flies expressing *UAS-Sac1RNAi* in the nervous system, an altered structure of the optic lobe is evident (Fig. 23B). The structure of the optic lobe is completely missed in 36-48h old *elav;Sac1RNAi* flies (Fig. 23C). Vacuolisation is also observed in addition to the collapse of the photoreceptor array (Fig. 23C). In conclusion, a progressive neurodegeneration is associated with decreased levels of Sac1 in the nervous system and the adult *Drosophila* eye is a good site in which to study progressive neurodegenerative processes.

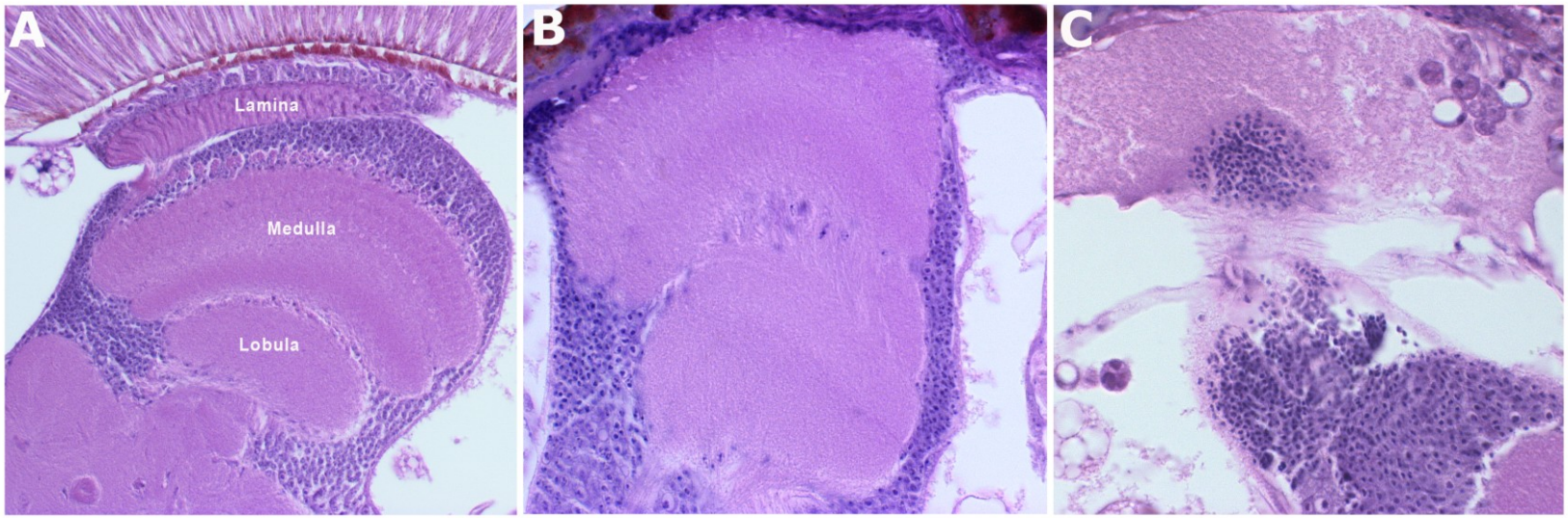

Figure 23. Reduced levels of Sac1 in the nervous system causes progressive neurodegeneration. Histological analysis of the internal structure of the optical lobes was performed on control adult flies (**A**), newly hatched *elav;Sac1RNAi* adult flies **(B),** and 36-48h old *elav;Sac1RNAi* adult flies (**C**).

6.4 Mutant DVAP retains its ability to bind Sac1 *in vivo*

The interaction between the mutant form of DVAP, DVAP-P58S, and Sac1 phosphatase has been shown *in vitro* by yeast two-hybrid assay [Forrest et al., 2013] and by Co-IP [in this thesis]. Moreover, the expression of both DVAP-P58S and DVAP-T48I is associated with the formation of DVAP-positive aggregates *in vitro* as well as *in vivo* [Teuling et al., 2007; Chai et al., 2008; Tsuda et al., 2008; Ratnaparkhi et al., 2008; Chen et al., 2010]. Thus, if the interaction between Sac1 and DVAP is not disrupted by the P58S mutation in DVAP, the possibility that Sac1 localizes into DVAP-positive aggregates has been explored. The expression of *UAS-Flag-Sac1* transgenic construct was directed to the eyes by using the *ey-Gal4* driver in a DVAP-P58S background. Eye imaginal discs from *Ey;UAS-DVAP-P58S/Flag-Sac1* third instar larvae were double-stained with anti-DVAP and anti-Flag antisera (Fig. 24A). Likewise, when *UAS-Flag-Sac1* construct was expressed specifically in the nervous system by using *elav-Gal4 driver* [Yao and White, 1994] in the presence of DVAP-P58S (*elav;DVAP-P58S;Flag-Sac1)*, Sac1 was captured into the DVAP-positive cytosolic aggregates (Fig. 24B). These data further confirm that Sac1 is mislocalised when DVAP-P58S is expressed as it is trapped into cytoplasmic aggregates that are caused by the expression of the mutant DVAP.

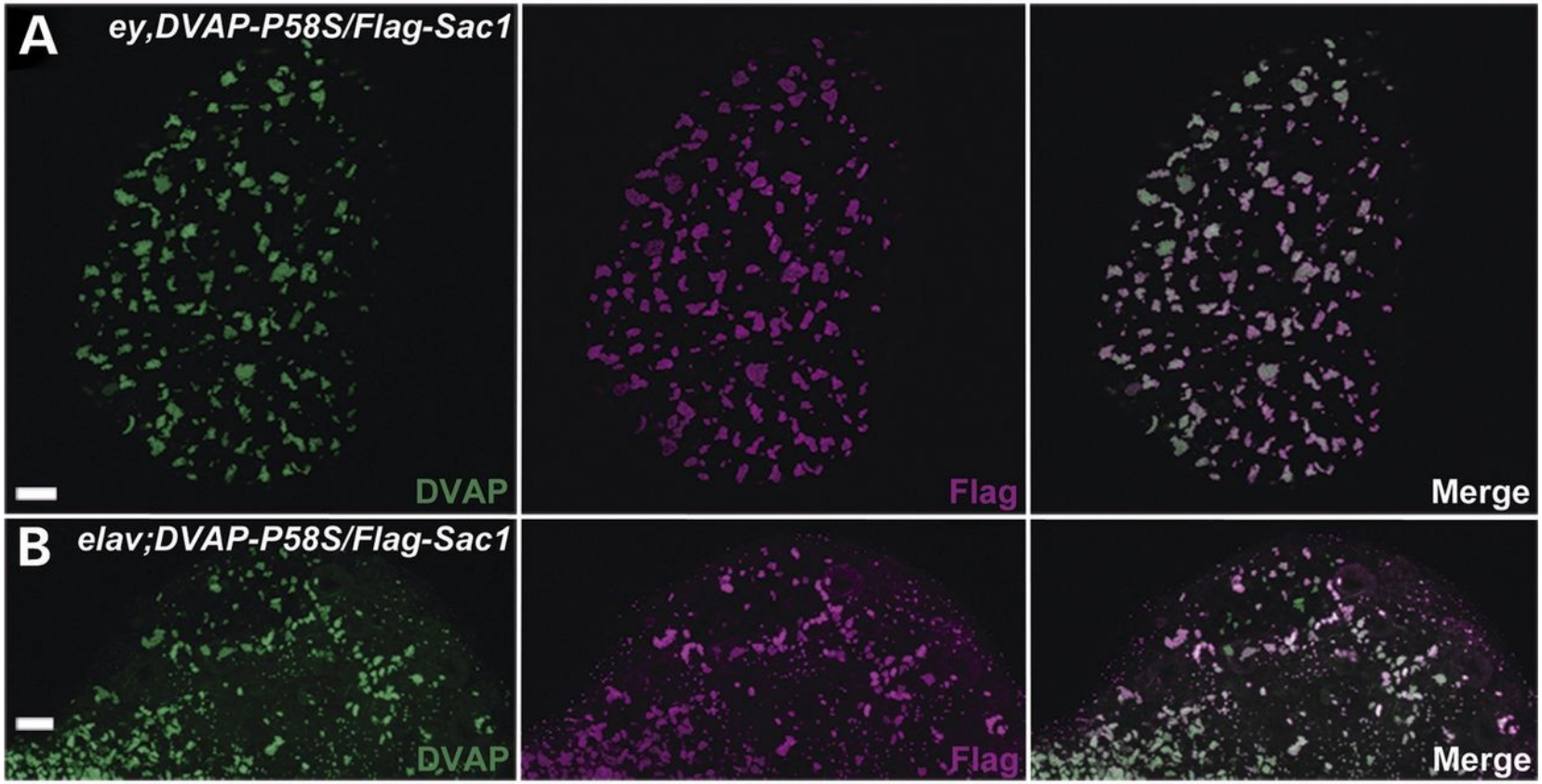

Figure 24. **Sac1 is recruited in DVAP cytoplasmic inclusions.** (**A**) Eye imaginal discs from *Ey;UAS-DVAP-P58S/Flag-Sac1* third instar larvae were. (**B**) Brains from third instar *elav;DVAP-P58S;Flag-Sac1* larvae. Both DVAP and DVAP-58S are stained with an anti-DVAP antibody, whereas Flag-Sac1 fusion protein has been stained with an anti-Flag antibody. The bar corresponds to 10µm.

6.5 Conclusion

When Sac1 levels are decreased in the nervous system a progressive neurodegenerative phenotype is observed in third instar larvae. This evidence suggests that the altered developmental process observed in flies having low levels of Sac1 in the nervous system can be a consequence of the neurodegeneration. The fact that Sac1 has been detected into DVAP-P58S positive aggregates both in larval eye imaginal discs and brains, suggests a molecular mechanism underlying DVAP-P58S mediated neurodegeneration [Chen et al., 2010]. Sac1 maybe trapped into the aggregates caused by the expression of DVAP-P58S, and, thus, a context characterized by low levels of Sac1 can be mimic. This hypothesis is supported by the fact that DVAP-P58S mutant protein interacts with Sac1 phosphatase. Moreover, increased levels of PI4P, the substrate of Sac1 are detected in DVAP-P58S and Sac1RNAi-contexts.

DISCUSSION AND, FUTURE QUESTIONS AND EXPERIMENTS

Chapter 7: Discussion

7.1 Introduction

Flies expressing mutant alleles of DVAP that cause ALS8 in humans present the major characteristics of the disease, such as neuronal death, formation of aggregates in the motor neurons, locomotion defects and neurodegeneration [Chai et al., 2008; Chen et al., 2010]. Moreover, the phenotypes associated to the expression of DVAP-P58S are rescued by the transgenic expression of hVAPB [Chai et al., 2008]. This means that the function of VAP proteins is evolutionary conserved, and, thus, studying the cellular processes in which DVAP is implicated can be useful in understanding the cellular functions of hVAPB. This information can be used to understand the molecular mechanisms underlying the pathogenesis of ALS8 in humans.

In this PhD thesis I focused on the cellular pathways at the larval *Drosophila* NMJ that are regulated by the interaction between DVAP and Sac1, and on the role of this interaction in ALS8 pathogenesis. Initially, the interaction between these two proteins was identified during a genome-wide yeast two-hybrid assay by Dr. Katherine Parry and it has been thoroughly confirmed by co-immunoprecipitation, and colocalization *in vivo* between these two proteins. Moreover, when DVAP levels or Sac1 levels are decreased, similar phenotypes are observed. The similarity in the phenotypes suggests that the two genes control the same pathways. In yeast, VAP proteins stimulate the enzymatic activity of Sac1 *in vivo* and *in vitro* [Stefan et al., 2011], supporting the hypothesis that these two proteins are implicated in the same pathways.

7.2 DVAP and Sac1 control the stabilization of the MT scaffold in the presynaptic boutons at the NMJ

At the presynaptic compartment low levels of Sac1 as low levels of DVAP alter synaptic morphology and the MT organization inside the synaptic boutons. The

role of DVAP in maintaining the synaptic morphology as a consequence of its role in stabilizing the interaction of MTs to the plasma membrane inside the synaptic boutons has been previously shown in DVAP null *Drosophila* larvae [Pennetta et al., 2002]. Evidence in the literature shows the involvement of PIs in MT stabilization and disassembly. In particular, MT structure is destabilized by PIs-enriched micelles *in vitro* [Yamauchi and Purich, 1987]. These micelles have a negative charge around their surface and that reduces the interaction between Microtubule-associated-protein 2 (MAP-2) proteins and MT [Yamauchi and Purich, 1987]. MAP-2 is a protein family that is abundantly expressed in the nervous system and that binds MTs [Sanchez et al., 2000]. MT nucleation and stabilization are among the cellular functions that MAP-2 is needed for [Sanchez et al., 2000]. If PIs may reduce the association of MAP-2 to the MT filaments, and, in turn, MT may become less stable in the presence of high levels of PIs. Moreover, low levels of Sac1 in cultured cells perturbed the MT filaments of the mitotic spindle in cultured cells. In fact, the mitotic spindle presents many poles as a consequence of many MT nucleation sites [Liu et al., 2008].

PIPs are implicated in the stabilization of MTs to particular area of the plasma membrane during the cell motility process. Rafts containing $PI(4,5)P_2$ and the small GTPase, Cdc42, recruit the positive ends of MT filaments to the PM. The recruitment of this MT filament further promotes the formation PIP-enriched rafts [Golub and Caroni, 2005]. Interestingly, synapses formation seems to present similarities at the phenomenological level and sometimes at the molecular levels with the cell motility process [Weston et al., 2000].

In addition, the actin cytoskeleton is required for the structural integrity of MT cytoskeleton [Lin and Forscher, 1993] and growth cones of motor neurons are characterized by the presence not only of the MT filaments, but also of actin scaffolds [Schaefer et al., 2002]. Several aspects of the actin cytoskeleton organization (actin nucleation, actin filament elongation, and interaction

between actin filaments and membrane) are controlled by PIPs [Di Paolo and De Camilli, 2006]. PI(4,5)P_2 is required for the recruitment of actin to the PM [Pollard et al., 2003]. The same PIP induces the dissociation of actin-capping proteins from the actin filaments stimulating filament elongation [Yin et al., 2003]. Then, PI(4,5)P_2 also enhances the affinity between adhesion proteins of the PM and FERM-domain adaptor proteins [Di Paolo and De Camilli, 2006]. The FERM domain binds PIPs and the proteins containing this domain are implicated in the association between actin filaments and PM [Hamada et al., 2000]. PI4P is required for the generation of PI(4,5)P_2, thus, Sac1 enzymatic activity can control the MT cytoskeleton through the stabilization of actin filaments. Thus, when Sac1 function is impaired, the destabilization of MT cytoskeleton can depend on destabilization of actin filaments.

The importance of MT scaffold is also shown by the fact that many neurodegenerative diseases present problems regarding microtubules or the proteins that stabilize microtubules [De Vos et al., 2008; Saxena and Caroni, 2007]. Moreover, one of the early pathogenic mechanisms in neurodegeneration seems to be the synaptic dysfunction, meaning that the control of MT scaffold in the presynaptic boutons is a fundamental function [Plowey and Chu, 2011].

7.3 DVAP and Sac1 control the vesicular trafficking in the axons of motor neurons

We observed that low levels of DVAP and Sac1 selectively in the nervous system disrupt vesicular trafficking in the axons of motor neurons. In this compartment of the cell the MT structure does not appear to be perturbed, but the axonal accumulation of vesicles is reported. Problems regarding axonal transport are reported in many human neurodegenerative diseases [De Vos et al., 2008]. Some cases of motor neuron diseases are associated to mutations in genes encoding proteins involved in vesicle transport on MTs, such as $p150^{Glued}$ [Dion et al., 2009]. $p150^{Glued}$ forms a complex, called dynactin, interacting with

other motor proteins. A model where $PI(4,5)P_2$ molecule together with other acidic phospholipids is required to recruit dynein complex to specific organelles was proposed in squid [Muresan et al., 2001].

Interestingly, $PI(3,5)P_2$ is involved in the trafficking of endosomal vesicles to the tran-Golgi complex. $PI(3,5)P_2$ levels are modulated by Sac3/Fig4 PI5 phosphtase that has been found mutated in a form of ALS [Chow et al., 2004].

7.5 DVAP and Sac1 regulate the organization of the spectrin-actin cytoskeleton at the postsynaptic compartment of the *Drosophila* larval NMJ

I observed DVAP and Sac1 also participate together to the correct localization of the components of the spectrin-actin cytoskeleton in the postsynaptic compartment of the NMJ. Small filaments of actin together with eterotetramers of α- and β-spectrin create a reticulum that acts as a framework under the PM surrounding the presynaptic boutons [Pielage et al., 2006]. The spectrin-actin cytoskeleton seems to contain and support the boutons in the post-synaptic compartment [Pielage et al., 2006]. In agreement with this model the delocalization of β-spectrin in the post-synaptic compartment that is observed when DVAP and Sac1 levels are knocked down in the muscles, is accompanied by an alteration of the presynaptic morphology. In particular the synaptic membrane presents protrusion similar to spikes. Another protein involved in the correct organization of this cytoskeleton has been found mislocalised in muscles with low levels of Sac1 and DVAP: the adducin. Adducin acts as an actin-capping protein and it is required for the recruitment of spectrin to the actin filament ends [Hu et al., 2003]. The mislocalization of β-spectrin and adducin can indicate that the spectrin-actin cytoskeleton is quite disorganized.

Interestingly β-spectrin has a PH domain that mediates the interaction with $PI(4,5)P_2$ [Das et al., 2008]. The PH domain is required for spectrin assembly [Das et al., 2008], meaning that the binding to PIPs is required for the spectrin-actin scaffold. Maybe altered PI4P levels can lead to an altered spatial distribution of β-spectrin, as PI4P is a precursor of $PI(4,5)P_2$.

Adducin binds PIPs through its myristoylated alanine-rich C-kinase substrate (MARCKS) domain, and the interaction of adducin with these lipid molecules induces the dissociation of adducin from the actin-spectrin cytoskeleton [Barkalow et al., 2003]. Moreover, the actin-capping and the spectrin-recruiting activities of adducin are blocked when this protein is phosphorylated by PKC [Matsuoka et al., 1998]. High levels of PKC in association with high levels of phosphorylated adducin have been reported in ALS sufferers and ALS-SOD1 murine models [Hu et al., 2003; Shan et al., 2005].

7.6 DVAP-T48I and DVAP-P58S have a dominant negative effect on Sac1

Our data showed that decreased levels of Sac1 cause neurodegeneration, and the same was observed for DVAP-T48I and DVAP-P58S [Chen et al., 2008]. These results suggest that the interaction between Sac1 and DVAP is kept but Sac1 function is impaired. Thus, these two mutant alleles of DVAP have a dominant negative effect on Sac1. DVAP-T48I and DVAP-P58S cause the formation of cytoplasmic aggregates, where these two mutant proteins localize [Chai et al., 2008; Chen et al., 2010]. The dominant negative effect of these two mutant proteins on the wt DVAP is a consequence of the fact that wt DVAP keeps its ability to interact with the mutant DVAP, thus, it is trapped into the aggregates. wt DVAP cannot fulfil its function because it is mislocalised [Ratnaparkhi et al., 2008].

I observed that Sac1 is trapped into cytosolic aggregates induced by the expression of DVAP-P58S. These data suggests that Sac1 localized into the

aggregates cannot function properly, thus, DVAP-P58S has a dominant negative effect also on Sac1. The dominant negative effect of DVAP-P58S on wt DVAP and Sac1 leads these two proteins to not function properly. Thus, altered synaptic morphology, destabilization of MT in the synaptic boutons, altered vesicle trafficking in the motor neuron axons, that we observed when DVAP and Sac1 are decreased in the nervous system, should resemble the phenotypes associated with the expression of DVAP-P58S. The expression of DVAP-T48I also induce the formation of aggregates in larval skeletal muscles [Chen et al., 2010], very likely Sac1 gets trapped in the mutant DVAP-mediated aggregates also in skeletal muscles. The mislocalization of Sac1 in skeletal muscles can alter the organization of the actin-spectrin scaffold at the post-synaptic compartment of the NMJ.

7.7 ALS8 disease is associated altered PI4P metabolism

If Sac1 function is impaired one would expect that PI4P levels are increased as Sac1 phosphatase is the only PI4P phosphatase [Blagoveshchenskaya and Mayinger, 2009]. Our data support the hypothesis that ALS8 is associated with high PI4P levels. Many cellular functions are regulated by different classes of PIPs [Di Paolo and De Camilli, 2006]. They include signal transduction and stabilization of the actin and MT cytoskeleton. In turn, the regulation of this last aspect implicates the regulation of cell migration, phagocytosis, endocytosis, cell-cell and cell-matrix adhesion [Di Paolo and De Camilli, 2006]. The concentration of all PIP species is finely regulated suggesting the altered turnover of one of these lipid molecules very likely can have an impact on the majority of the cellular functions just mentioned.

Forrest et al., [2013] showed that PI4P levels are increased when DVAP-P58S is expressed as well as when Sac1 levels are decreased. These data suggest that the expression of DVAP-P58S is associated with Sac1 impaired function. This is in agreement with the dominant negative effect of DVAP-P58S on Sac1.

Chapter 8: Future questions and experiments

8.1 Introduction

The results obtained from the analysis of the interaction between DVAP and Sac1, firstly, confirmed that DVAP and Sac1 interact; secondly, it pointed out the functional relationship between Sac1 phosphatase activity and DVAP at the *Drosophila* larval NMJ; and lastly, it linked Sac1 to neurodegeneration. In addition, the data reported by Forrest et al., [2013] showed the expression of DVAP-P58S mutant protein in the nervous system of third instar larvae is associated to high levels of PI4P. Moreover, the neurodegenerative phenotype observed in the adult eye of *Drosophila* strains expressing the DVAP-P58S mutant protein, is rescued when PI4P levels are brought back to wt levels. All together this evidence suggest that PI4P metabolism has a relationship with neurodegeneration, but still it is not clear the exact mechanism through which the levels of this lipid molecule can induce neurodegeneration. It is possible that the neurodegeneration is the consequence of altered pathways at the NMJ. In fact, I observed that low levels of Sac1 lead not only to neurodegeneration, but also to a number of phenotypes both at the pre- and postsynaptic compartments of the larval NMJ. However, it is still undefined the exact mechanism through which altered levels of PI4P lipid molecule affect some NMJ compartment functions, and they cause neurodegeneration. Therefore, on the one hand my data highlighted the involvement of PIPs in ALS8-mediated neurodegeneration, on the other hand raised important questions about the relationship between PIP metabolism and neurodegenerative diseases, and PIP metabolism and some important cellular functions of the *Drosophila* larval NMJ.

8.2 How MT stability in the motor neurons can be affected by altered levels of PI4P?

The evidence reported in this thesis show some cellular mechanisms where DVAP and Sac1 proteins cooperate, including MT stability inside the presynaptic boutons. In order to investigate whether PI4P levels control either directly or indirectly the MT cytoskeleton inside the presynaptic compartment few hypothesis have been considered.

The growth cone of motor neurons contains a cytoskeletal structure made of MT and actin chains that are in intimate association between each other (fig. 25)[Lowery and Van Vactor, 2009]. Mutations in yeast Sac1 protein have been showed to suppress the phenotypes associated to actin mutations [Novick et al., 1989; Cleves et al., 1989]. Therefore, it seems that Sac1 has an effect on actin in yeast. The possibility that Sac1 phosphatase activity can be crucial for the maintaining of MT structure in the presynaptic boutons of Drosophila larvae can be explored looking at the distributions of actin protein in the boutons in larvae having decreased levels of Sac1 in the nervous system.

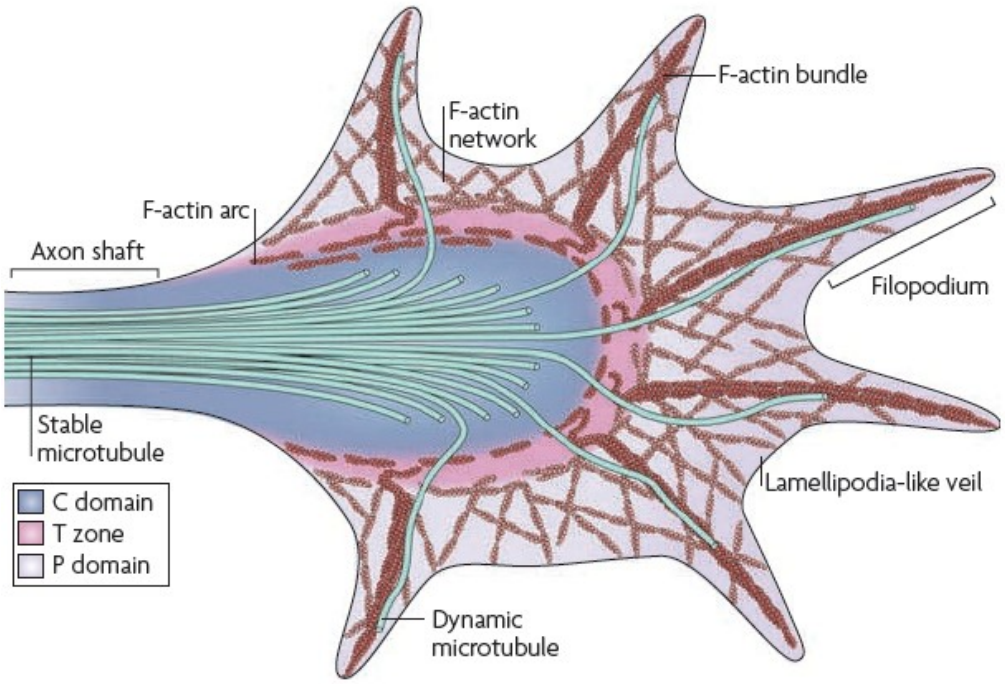

Figure 25. Schematic view of the growth cone of a motor neuron. Dynamic MT filaments directly associate with the actin network. Figure from Lowery and Van Vactor,[2009].

8.3 Which is the cause of vesicle accumulation in axons of motor neurons?

I showed in my thesis that when either Sac1 or DVAP levels are alternatively lowered into the nervous system, accumulation of important components of presynaptic vesicles, is observed into the axons of motor neurons. The cause of this accumulation is unclear. Is there a problem in the assembling of vesicles at the presynaptic boutons? To address this question it would be interesting to look at the distribution of brp and CSP proteins inside the presynaptic boutons. Additionally, the accumulation of brp and CSP proteins in the axons could be a consequence of the altered MT structure inside the presynaptic boutons? To examine this hypothesis the *CS* larvae can be treated with vinblastine. Vinblastine is a microtubule destabilizing drug leading to the capping of MT ends [Dhamodharan et al., 1995]. The brp and CSP protein accumulation will be checked after the treatment.

Can we exclude that a problem in the transport of vesicle is the cause of the accumulation of these organelles into the axons of motor neurons? Two genes encoding two proteins implicated in axonal transport have been associated to ALS: *DCTN1* (dynactin-1) and *NEFH* (neurofilament heavy polypeptide) [Munch et al., 2004; Figlewicz et al., 1994]. To address this point the kinetics of Brp and CSP can be followed in the axons of motor neurons of larvae having low levels of Sac1 in the nervous system.

Lastly it is not clear whether presynaptic vesicles the only organelles that accumulate in a knock-down Sac1 or knock-down DVAP context. To address this point the markers of organelles that usually are transported through the axon to the presynaptic boutons, such as mitochondria, can be checked in the axons of motor neurons from Drosophila larvae, where either Sac1 levels are decreased.

8.2 Do ALS8 mutations in DVAP affect cellular functions controlled by interacting partners others than Sac1?

hVAPB, as well as its *Drosophila* orthologue, has a number of interacting partners besides Sac1, most of them are proteins and enzymes involved in lipid transport and metabolism. It would be important to examine the effect of the expression of mutations in hVAPB on the functions controlled by its interacting partners. The possibility that the phenotypes associated with decreased levels of DVAP are only due to the lack of Sac1 stimulation can be explored. To this aim, *Drosophila melanogaster* can be used ones more as model organism. A mutant form of DVAP that is unable to interact with Sac1 should be overexpressed in loss-of-function background for DVAP. If the OE of the mutant form of DVAP, that is unable to interact with Sac1, rescues the phenotypes associated to DVAP LOF, the entity of this rescue should be quantified and compared to the rescue obtained by DVAP OE. Complete rescue of the phenotype should mean that the phenotype caused by decreased

levels of DVAP is independent from the activity of Sac1. A partial rescue of the phenotype should mean that the phenotype is not only due to the inactivation of Sac1. Finally, no rescue should mean that the observed phenotype is completely dependent on the interaction between DVAP and Sac1.

8.3 Is PIP metabolism altered in cases of the FTDP-17 tauopathy?

High levels of VAPB were found associated with a form of tauopathy called FTDP-17. In particular, high levels of VAPB were found in a murine model of FTDP-17 [Karsten et al., 2006] and the neurodegeneration in a *Drosophila* model of FTD was reduced by knocking down the function of DVAP. The possibility that high levels of VAPB can play a role in the pathogenesis of tauopathies affecting PI4P metabolism, can be explored. Thus, the levels of PI4P can be analysed in *Drosophila* strains expressing the mutant form of tau in the nervous system. In particular, PI4P can be checked in the larval brains, eye imaginal discs, and salivary glands. If the PI4P levels are increased compared to control larval nervous system, the possibility that the neurodegeneration in the *Drosophila* model of FTD is affected by altering Sac1 phosphatase activity, can be examined. In fact, the PI levels could be changed because increased levels of VAPB can have an affect on Sac1 phosphatase activity.

8.4 Is Sac1 also trapped into DVAP-P58S-associated aggregates in muscles?

During my PhD work the localization of Sac1 in the DVAP-P58S-induced aggregates was reported in the nervous system. The formation of DVAP positive cytosolic aggregates was reported as a consequence of the expression in the postsynaptic compartment of another pathogenic mutation of DVAP:

T48I [Chen et al., 2010]. The possibility that also the selective expression of DVAP-P58S to the muscles causes the formation of aggregates in the postsynaptic compartment of the NMJ, and that Sac1 is trapped into these aggregates can be explored. This experiment would suggest that the phenotypes of the postsynaptic compartment associated with decreased levels of Sac1 in that compartment are also present in ALS8 genetic background.

8.5 Does the V234I mutation in hVAPB affect the hVAPB-Sac1 interaction?

Recently, a third mutation has been identified into hVAPB gene leading to an amino acid substitution (V234I) in the TMD of hVAPB protein [van Blitterswijk et al., 2012]. Forrest et al.,[2013] shows that the TMD domain of the *Drosophila* orthologue of hVAPB (DVAP) is involved in the interaction with *Drosophila* Sac1 by yeast two-hybrid. As the V234 is a conserved amino acid, the possibility that this amino acid between humans and *Drosophila*, is required for the interaction of DVAP with Sac1 can be explored. To this aim the Valine in the position 260 of DVAP that corresponds to the Valine234 in hVAPB, can be changed into an isoleucine mutagenizing the DVAP cDNA by site-directed mutagenesis. The capability of DVAP-V260I to bind Sac1 can be examined by yeast two-hybrid assay and, subsequently, can be confirmed by Co-IP assay. If the interaction between DVAP and Sac1 is lost as a consequence of the V260I mutation, PI4P levels when DVAP-V260I is expressed can be checked to investigate whether the phenotypes associated with this mutation is caused by altered PI4P levels.

8.6 Human genetics analysis of *Sac1* gene and of genes encoding enzymes implicated in PIP metabolism

If the hypothesis that Sac1 is trapped in hVAPB-P56S positive aggregates, ALS8 is associated to a context where Sac1 function is impaired. Thus, it would be interesting to analyse ALS patients that resulted negative to mutation analysis to the known ALS-associated genes for mutations in *Sac1* gene. In fact, a mutation that negatively affects Sac1 phosphatase activity can cause the same phenotype reported in ALS8 cases. In addition, mutations in enzymes directly implicated in lipid metabolism can be searched.

Moreover, Sac1 expression levels can be checked in spinal cords from ALS8-patient and motor neurons of the *Drosophila* models of ALS8 in order to check whether neurons from spinal cords expressing ALS8-associated hVAPB mutant proteins, try to overcome the lack of functional Sac1 in its proper subcellular site.

8.7 Is the association between DVAP and its interacting partners, other than Sac1, altered in ALS8?

During my PhD work, I focused on the analysis of the interaction between DVAP and Sac1, where Sac1 does interact with the TMD of DVAP [Forrest et al., 2013]. Some VAP protein interacting partners, including CERT, that bind to VAPs through their FFAT motif and VAP's MSP domain. What does it happen to these interactions? How do P56S and T46I mutations affect them? The analysis of the interaction between these two mutant forms of DVAP and these proteins can be performed. This analysis can reveal whether these protein-protein interactions are kept in an ALS8 disease context. Consequently, additional cellular functions that are altered in ALS8 NMJ can

be identified. These data will shed new light on the mechanisms causing ALS8 phenotypes.

8.8 Conclusion

Although, my PhD study contributed to elucidate the mechanisms underlying the neurodegenerative phenotype associated to ALS8, it raised up a number of questions. Indeed, *Drosophila melanogaster* genetics can be used to answer the majority of them, but also approaches of cell biology and biochemistry can be employed. In conclusion, on the one hand, my study can be considered the final step of a short ride, such as the time of a PhD, but on the other hand, the launch pad of a number of interesting research projects.

Appendix 1. Vector maps

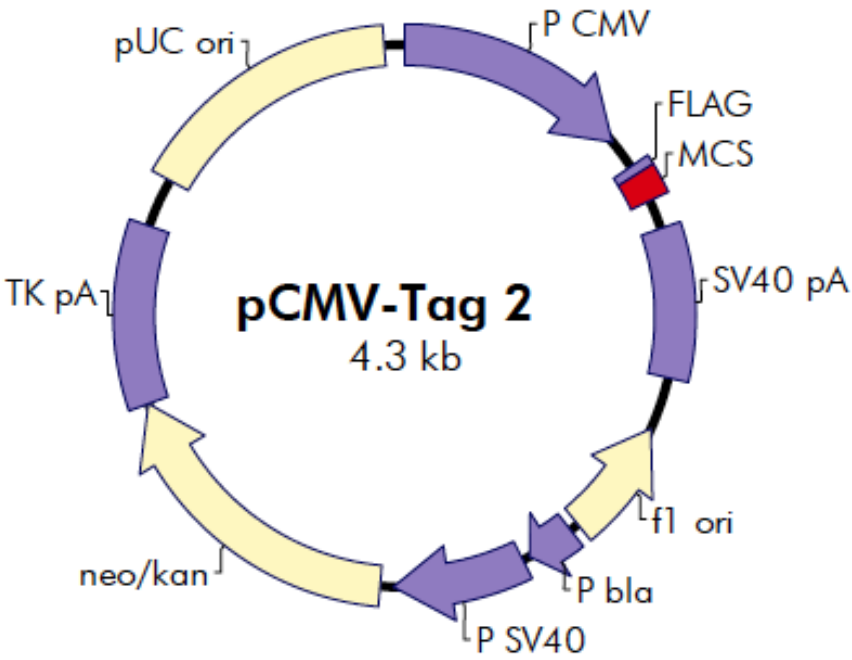

Figure 26. ***pCMV-Tag 2*** **Vector Map from Clontech.**

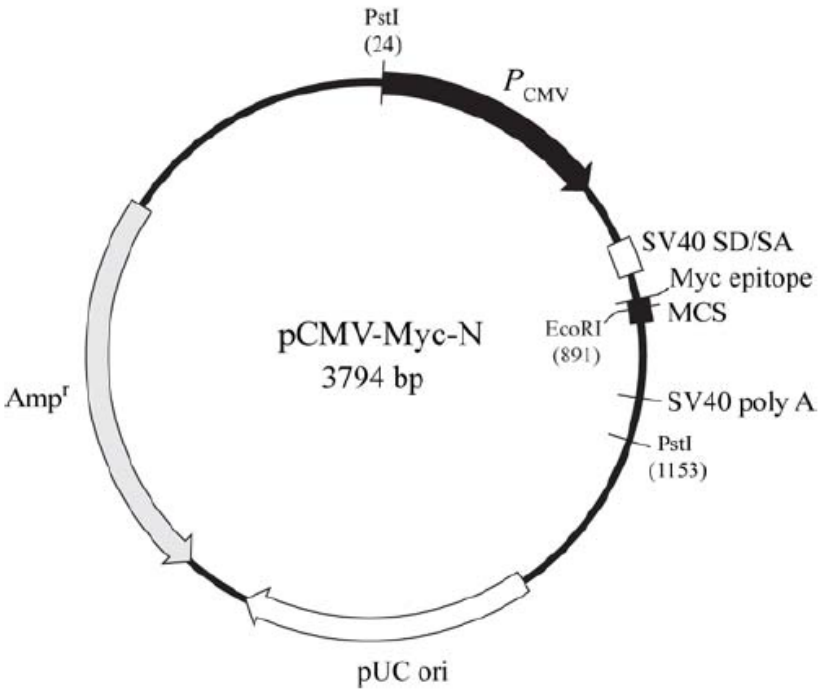

Figure 27. ***pCMV-Myc-N*** **Vector Map from Clontech.**

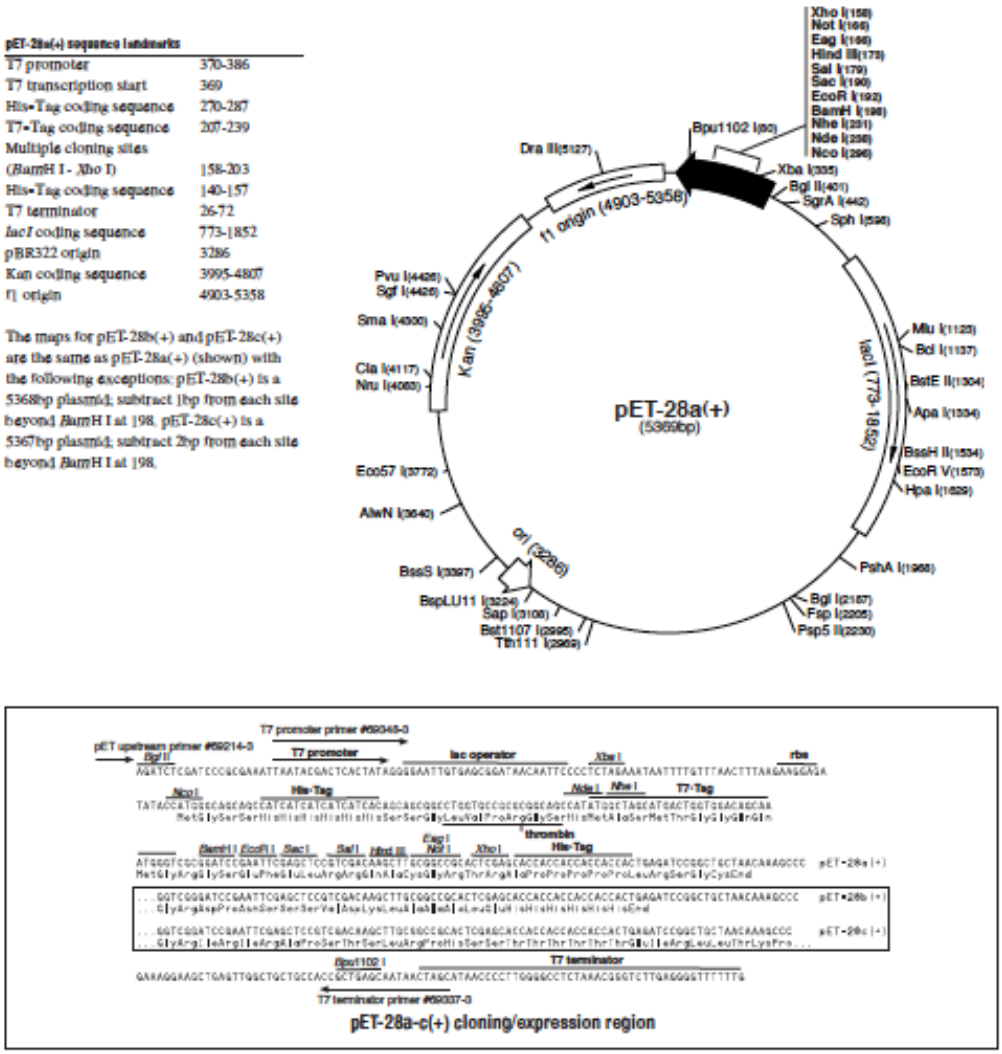

Figure 28. ***pET-28a*** **Vector Map from Novagen**

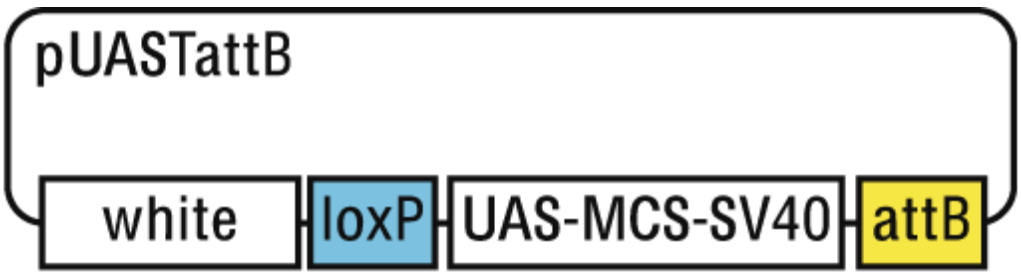

Figure 29. ***pUASTattb*** **Vector Map.** Figure adapted from Bischof et al., 2007.

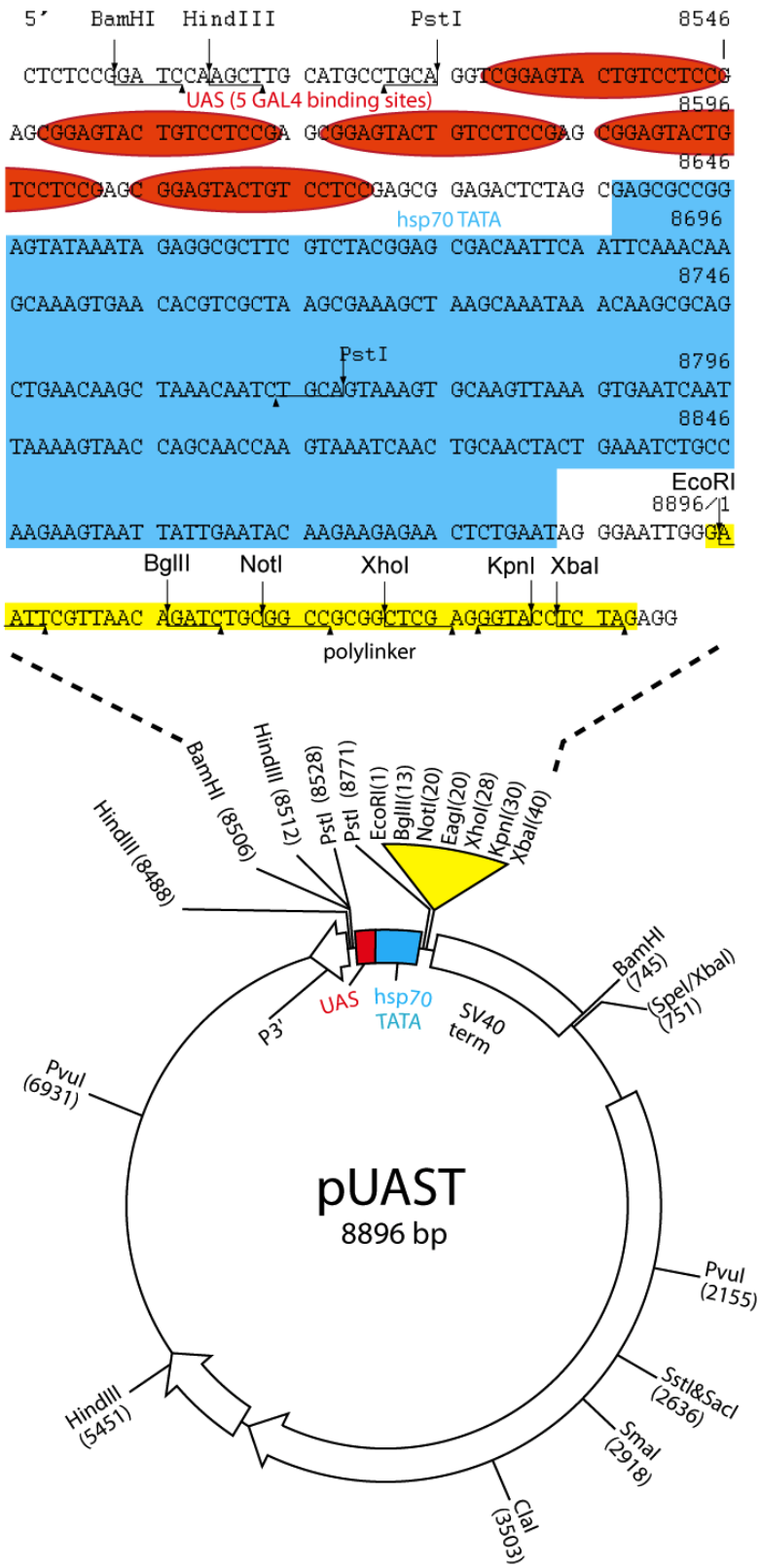

Figure 30. ***pUAST*** **Vector Map.** Figure from Brand Lab website.

BIBLOGRAPHY

Acharya, M. M., and S. S. Katyare. "Structural and Functional Alterations in Mitochondrial Membrane in Picrotoxin-Induced Epileptic Rat Brain." *Experimental neurology* 192.1 (2005): 79-88. Print.

Acharya, U., and J. K. Acharya. "Enzymes of Sphingolipid Metabolism in Drosophila Melanogaster." *Cellular and molecular life sciences : CMLS* 62.2 (2005): 128-42. Print.

Agapite, J., Steller S. "Neuronal Cell Death. In Molecular and Cellular Approaches to Neuronal Development." W.M. Cowan, T.M. Jessell, and S.L. Zipursky, eds.New York: Oxford University Press (1997): 264-89. Print.

Al-Saif, A., Al-Mohanna, F. and Bohlega, S. "A Mutation in Sigma-1 Receptor Causes Juvenile Amyotrophic Lateral Sclerosis." *Annals of neurology* 70.6 (2011): 913-9. Print.

Amarilio, R., Ramachandran, S., Sabanay, H., and Lev, S. "Differential Regulation of Endoplasmic Reticulum Structure through Vap-Nir Protein Interaction." *The Journal of biological chemistry* 280.7 (2005): 5934-44. Print.

Andrew, D. J., Henderson, K. D. and Seshaiah, P. "Salivary Gland Development in Drosophila Melanogaster." *Mechanisms of development* 92.1 (2000): 5-17. Print.

Anniss, A. M., J. Apostolopoulos, S. Dworkin, L. E. Purton, and R. L. Sparrow. "An Oxysterol-Binding Protein Family Identified in the Mouse." *DNA and cell biology* 21.8 (2002): 571-80. Print.

Atasoy, H. T., Nuyan, O., Tunc, T., Yorubulut, M., Unal, A. E. and Inan, L. E. "T2-Weighted Mri in Parkinson's Disease; Substantia Nigra Pars Compacta Hypointensity Correlates with the Clinical Scores." *Neurology India* 52.3 (2004): 332-7. Print.

Audhya, A., and S. D. Emr. "Stt4 Pi 4-Kinase Localizes to the Plasma Membrane and Functions in the Pkc1-Mediated Map Kinase Cascade." *Developmental cell* 2.5 (2002): 593-605. Print.

Audhya, A., Foti, M. and Emr, S. D. "Distinct Roles for the Yeast Phosphatidylinositol 4-Kinases, Stt4p and Pik1p, in Secretion, Cell Growth, and Organelle Membrane Dynamics." *Molecular biology of the cell* 11.8 (2000): 2673-89. Print.

Baird, D., C. Stefan, A. Audhya, S. Weys, and S. D. Emr. "Assembly of the Ptdins 4-Kinase Stt4 Complex at the Plasma Membrane Requires Ypp1 and Efr3." *The Journal of cell biology* 183.6 (2008): 1061-74. Print.

Bankaitis, V. A., R. Garcia-Mata, and C. J. Mousley. "Golgi Membrane Dynamics and Lipid Metabolism." *Current biology : CB* 22.10 (2012): R414-24. Print.

Barkalow, K. L., Italiano, J. E., Jr., Chou, D. E., Matsuoka, Y., Bennett, V. and Hartwig, J. H. "Alpha-Adducin Dissociates from F-Actin and Spectrin During Platelet Activation." *The Journal of cell biology* 161.3 (2003): 557-70. Print.

Baumann, O., and B. Walz. "Endoplasmic Reticulum of Animal Cells and Its Organization into Structural and Functional Domains." *International review of cytology* 205 (2001): 149-214. Print.

Bednarek, E., and P. Caroni. "Beta-Adducin Is Required for Stable Assembly of New Synapses and Improved Memory Upon Environmental Enrichment." *Neuron* 69.6 (2011): 1132-46. Print.

Beh, C. T., Cool, L., Phillips, J. and Rine, J. "Overlapping Functions of the Yeast Oxysterol-Binding Protein Homologues." *Genetics* 157.3 (2001): 1117-40. Print.

Bennett, V., K. Gardner, and J. P. Steiner. "Brain Adducin: A Protein Kinase C Substrate That May Mediate Site-Directed Assembly at the Spectrin-Actin Junction." *The Journal of biological chemistry* 263.12 (1988): 5860-9. Print.

Bischof, J., R. K. Maeda, M. Hediger, F. Karch, and K. Basler. "An Optimized Transgenesis System for Drosophila Using Germ-Line-Specific Phic31 Integrases." *Proceedings of the National Academy of Sciences of the United States of America* 104.9 (2007): 3312-7. Print.

Blagoveshchenskaya, A., F. Y. Cheong, H. M. Rohde, G. Glover, A. Knodler, T. Nicolson, G. Boehmelt, and P. Mayinger. "Integration of Golgi Trafficking and Growth Factor Signaling by the Lipid Phosphatase Sac1." *The Journal of cell biology* 180.4 (2008): 803-12. Print.

Blagoveshchenskaya, Anastasia, and Peter Mayinger. "Sac1 Lipid Phosphatase and Growth Control of the Secretory Pathway." *Molecular bioSystems* 5.1 (2009): 36-42. Print.

Bonini, N. M., and M. E. Fortini. "Human Neurodegenerative Disease Modeling Using Drosophila." *Annual review of neuroscience* 26 (2003): 627-56. Print.

Bossy-Wetzel, E., Schwarzenbacher, R. and Lipton, S. A. "Molecular Pathways to Neurodegeneration." *Nature medicine* 10 Suppl (2004): S2-9. Print.

Botelho, R. J., Scott, C. C. and Grinstein, S. "Phosphoinositide Involvement in Phagocytosis and Phagosome Maturation." *Current topics in microbiology and immunology* 282 (2004): 1-30. Print.

Brand, A. H. and Dormand, E. L. "The Gal4 System as a Tool for Unravelling the Mysteries of the Drosophila Nervous System." *Current opinion in neurobiology* 5.5 (1995): 572-8. Print.

Brand, A. H., and N. Perrimon. "Targeted Gene Expression as a Means of Altering Cell Fates and Generating Dominant Phenotypes." *Development* 118.2 (1993): 401-15. Print.

Brice, S. E., Alford, C. W. and Cowart, L. A. "Modulation of Sphingolipid Metabolism by the Phosphatidylinositol-4-Phosphate Phosphatase Sac1p through Regulation of Phosphatidylinositol in Saccharomyces Cerevisiae." *The Journal of biological chemistry* 284.12 (2009): 7588-96. Print.

Brickner, J. H., and Walter, P. "Gene Recruitment of the Activated Ino1 Locus to the Nuclear Membrane." *PLoS biology* 2.11 (2004): e342. Print.

Brown, R. H., Jr. "Sod1 Aggregates in Als: Cause, Correlate or Consequence?" *Nature medicine* 4.12 (1998): 1362-4. Print.

Bruijn, L. I., M. K. Houseweart, S. Kato, K. L. Anderson, S. D. Anderson, E. Ohama, A. G. Reaume, R. W. Scott, and D. W. Cleveland. "Aggregation and Motor Neuron Toxicity of an Als-Linked Sod1 Mutant Independent from Wild-Type Sod1." *Science* 281.5384 (1998): 1851-4. Print.

Budnik, V., Y. H. Koh, B. Guan, B. Hartmann, C. Hough, D. Woods, and M. Gorczyca. "Regulation of Synapse Structure and Function by the Drosophila Tumor Suppressor Gene Dlg." *Neuron* 17.4 (1996): 627-40. Print.

Caldwell, J. C., Miller, M. M., Wing, S., Soll, D. R., and Eberl, D. F. "Dynamic Analysis of Larval Locomotion in Drosophila Chordotonal Organ Mutants." *Proceedings of the National Academy of Sciences of the United States of America* 100.26 (2003): 16053-8. Print.

Cantley, L. C. "The Phosphoinositide 3-Kinase Pathway." *Science* 296.5573 (2002): 1655-7. Print.

Cauchi, R. J., and M. van den Heuvel. "The Fly as a Model for Neurodegenerative Diseases: Is It Worth the Jump?" *Neuro-degenerative diseases* 3.6 (2006): 338-56. Print.

Chai, A., J. Withers, Y. H. Koh, K. Parry, H. Bao, B. Zhang, V. Budnik, and G. Pennetta. "Hvapb, the Causative Gene of a Heterogeneous Group of Motor Neuron Diseases in Humans, Is Functionally Interchangeable with Its Drosophila Homologue Dvap-33a at the Neuromuscular Junction." *Hum Mol Genet* 17.2 (2008): 266-80. Print.

Chen, H. J., Anagnostou, G., Chai, A., Withers, J., Morris, A., Adhikaree, J., Pennetta, G. and de Belleroche, J. S. "Characterization of the Properties of a Novel Mutation in Vapb in Familial Amyotrophic Lateral Sclerosis." *The Journal of biological chemistry* 285.51 (2010): 40266-81. Print.

Chen, Y. Z., C. L. Bennett, H. M. Huynh, I. P. Blair, I. Puls, J. Irobi, I. Dierick, A. Abel, M. L. Kennerson, B. A. Rabin, G. A. Nicholson, M. Auer-Grumbach, K. Wagner, P. De Jonghe, J. W. Griffin, K. H. Fischbeck, V. Timmerman, D. R. Cornblath, and P. F. Chance. "DNA/Rna Helicase Gene Mutations in a Form of Juvenile Amyotrophic Lateral Sclerosis (Als4)." *American journal of human genetics* 74.6 (2004): 1128-35. Print.

Chow, C. Y., Landers, J. E., Bergren, S. K., Sapp, P. C., Grant, A. E., Jones, J. M., Everett, L., Lenk, G. M., McKenna-Yasek, D. M., Weisman, L. S., Figlewicz, D., Brown, R. H. and Meisler, M. H. "Deleterious Variants of Fig4, a Phosphoinositide Phosphatase, in Patients with Als." *American journal of human genetics* 84.1 (2009): 85-8. Print.

Cleves, A. E., Novick, P. J. and Bankaitis, V. A. "Mutations in the Sac1 Gene Suppress Defects in Yeast Golgi and Yeast Actin Function." *The Journal of cell biology* 109.6 Pt 1 (1989): 2939-50. Print.

Collins, C. A., and A. DiAntonio. "Synaptic Development: Insights from Drosophila." *Current opinion in neurobiology* 17.1 (2007): 35-42. Print.

Conde, C., and A. Caceres. "Microtubule Assembly, Organization and Dynamics in Axons and Dendrites." *Nature reviews. Neuroscience* 10.5 (2009): 319-32. Print.

Couillard-Despres, S., Q. Zhu, P. C. Wong, D. L. Price, D. W. Cleveland, and J. P. Julien. "Protective Effect of Neurofilament Heavy Gene Overexpression in Motor Neuron Disease Induced by Mutant Superoxide Dismutase." *Proceedings of the National Academy of Sciences of the United States of America* 95.16 (1998): 9626-30. Print.

Cremona, O., G. Di Paolo, M. R. Wenk, A. Luthi, W. T. Kim, K. Takei, L. Daniell, Y. Nemoto, S. B. Shears, R. A. Flavell, D. A. McCormick, and P. De Camilli. "Essential Role of Phosphoinositide Metabolism in Synaptic Vesicle Recycling." *Cell* 99.2 (1999): 179-88. Print.

Crossley, C.A. "The Morphology and Development of the Drosophila Muscular System." *Ashburner, M., Wright, T.R.F., The Genetics and Biology of Drosophila,* 2b.Academic, New York (1978): 499-599. Print.

Culi, J., and R. S. Mann. "Boca, an Endoplasmic Reticulum Protein Required for Wingless Signaling and Trafficking of Ldl Receptor Family Members in Drosophila." *Cell* 112.3 (2003): 343-54. Print.

D'Angelo, G., M. Vicinanza, A. Di Campli, and M. A. De Matteis. "The Multiple Roles of Ptdins(4)P -- Not Just the Precursor of Ptdins(4,5)P2." *Journal of cell science* 121.Pt 12 (2008): 1955-63. Print.

Das, A., C. Base, D. Manna, W. Cho, and R. R. Dubreuil. "Unexpected Complexity in the Mechanisms That Target Assembly of the Spectrin Cytoskeleton." *The Journal of biological chemistry* 283.18 (2008): 12643-53. Print.

Dawson, P. A., Ridgway, N. D., Slaughter, C. A., Brown, M. S. and Goldstein, J. L. "Cdna Cloning and Expression of Oxysterol-Binding Protein, an Oligomer

with a Potential Leucine Zipper." *The Journal of biological chemistry* 264.28 (1989): 16798-803. Print.

De Matteis, M., A. Godi, and D. Corda. "Phosphoinositides and the Golgi Complex." *Current opinion in cell biology* 14.4 (2002): 434-47. Print.

De Vos, D., Y. Xu, T. Aerts, F. Van Petegem, and J. J. Van Beeumen. "Crystal Structure of Sulfolobus Acidocaldarius Aspartate Carbamoyltransferase in Complex with Its Allosteric Activator Ctp." *Biochemical and biophysical research communications* 372.1 (2008): 40-4. Print.

DeJesus-Hernandez, M. et al. "Expanded Ggggcc Hexanucleotide Repeat in Noncoding Region of C9orf72 Causes Chromosome 9p-Linked Ftd and Als." *Neuron* 72.2 (2011): 245-56. Print.

Deng, H. X., W. Chen, S. T. Hong, K. M. Boycott, G. H. Gorrie, N. Siddique, Y. Yang, F. Fecto, Y. Shi, H. Zhai, H. Jiang, M. Hirano, E. Rampersaud, G. H. Jansen, S. Donkervoort, E. H. Bigio, B. R. Brooks, K. Ajroud, R. L. Sufit, J. L. Haines, E. Mugnaini, M. A. Pericak-Vance, and T. Siddique. "Mutations in Ubqln2 Cause Dominant X-Linked Juvenile and Adult-Onset Als and Als/Dementia." *Nature* 477.7363 (2011): 211-5. Print.

Dhamodharan, R., M. A. Jordan, D. Thrower, L. Wilson, and P. Wadsworth. "Vinblastine Suppresses Dynamics of Individual Microtubules in Living Interphase Cells." *Molecular biology of the cell* 6.9 (1995): 1215-29. Print.

Di Paolo, G., and De Camilli, P. "Phosphoinositides in Cell Regulation and Membrane Dynamics." *Nature* 443.7112 (2006): 651-7. Print.

Dion, P. A., H. Daoud, and G. A. Rouleau. "Genetics of Motor Neuron Disorders: New Insights into Pathogenic Mechanisms." *Nature reviews. Genetics* 10.11 (2009): 769-82. Print.

Dubendorff, J. W., and F. W. Studier. "Controlling Basal Expression in an Inducible T7 Expression System by Blocking the Target T7 Promoter with Lac Repressor." *Journal of molecular biology* 219.1 (1991): 45-59. Print.

Dupuis, L., Corcia, P., Fergani, A., Gonzalez De Aguilar, J. L., Bonnefont-Rousselot, D., Bittar, R., Seilhean, D., Hauw, J. J., Lacomblez, L., Loeffler, J. P., and Meininger, V. "Dyslipidemia Is a Protective Factor in Amyotrophic Lateral Sclerosis." *Neurology* 70.13 (2008): 1004-9. Print.

Dupuis, L., Oudart, H., Rene, F., Gonzalez de Aguilar, J. L., and Loeffler, J. P. "Evidence for Defective Energy Homeostasis in Amyotrophic Lateral Sclerosis: Benefit of a High-Energy Diet in a Transgenic Mouse Model." *Proceedings of the National Academy of Sciences of the United States of America* 101.30 (2004): 11159-64. Print.

Dupuis, L., Pradat, P. F., Ludolph, A. C. and Loeffler, J. P. "Energy Metabolism in Amyotrophic Lateral Sclerosis." *Lancet neurology* 10.1 (2011): 75-82. Print.

Faulhammer, F., Kanjilal-Kolar, S., Knodler, A., Lo, J., Lee, Y., Konrad, G. and Mayinger, P. "Growth Control of Golgi Phosphoinositides by Reciprocal Localization of Sac1 Lipid Phosphatase and Pik1 4-Kinase." *Traffic* 8.11 (2007): 1554-67. Print.

Featherstone, D. E., W. S. Davis, R. R. Dubreuil, and K. Broadie. "Drosophila Alpha- and Beta-Spectrin Mutations Disrupt Presynaptic Neurotransmitter Release." *The Journal of neuroscience : the official journal of the Society for Neuroscience* 21.12 (2001): 4215-24. Print.

Ferraiuolo, L., Kirby, J., Grierson, A. J., Sendtner, M., and Shaw, P. J. "Molecular Pathways of Motor Neuron Injury in Amyotrophic Lateral Sclerosis." *Nature reviews. Neurology* 7.11 (2011): 616-30. Print.

Figlewicz, D. A., A. Krizus, M. G. Martinoli, V. Meininger, M. Dib, G. A. Rouleau, and J. P. Julien. "Variants of the Heavy Neurofilament Subunit Are Associated with the Development of Amyotrophic Lateral Sclerosis." *Human molecular genetics* 3.10 (1994): 1757-61. Print.

Fire, A., S. Xu, M. K. Montgomery, S. A. Kostas, S. E. Driver, and C. C. Mello. "Potent and Specific Genetic Interference by Double-Stranded Rna in Caenorhabditis Elegans." *Nature* 391.6669 (1998): 806-11. Print.

Forrest, S., A. Chai, M. Sanhueza, M. Marescotti, K. Parry, A. Georgiev, V. Sahota, R. Mendez-Castro, and G. Pennetta. "Increased Levels of Phosphoinositides Cause Neurodegeneration in a Drosophila Model of Amyotrophic Lateral Sclerosis." *Human molecular genetics* (2013). Print.

Fortini, M. E., Skupski, M. P., Boguski, M. S. and Hariharan, I. K. "A Survey of Human Disease Gene Counterparts in the Drosophila Genome." *The Journal of cell biology* 150.2 (2000): F23-30. Print.

Foti, M., A. Audhya, and S. D. Emr. "Sac1 Lipid Phosphatase and Stt4 Phosphatidylinositol 4-Kinase Regulate a Pool of Phosphatidylinositol 4-Phosphate That Functions in the Control of the Actin Cytoskeleton and Vacuole Morphology." *Molecular biology of the cell* 12.8 (2001): 2396-411. Print.

Galaud, J. P., V. Laval, M. Carriere, A. Barre, H. Canut, P. Rouge, and R. Pont-Lezica. "Osmotic Stress Activated Expression of an Arabidopsis Plasma Membrane-Associated Protein: Sequence and Predicted Secondary Structure." *Biochimica et biophysica acta* 1341.1 (1997): 79-86. Print.

Gavin, A. C., M. Bosche, R. Krause, P. Grandi, M. Marzioch, A. Bauer, J. Schultz, J. M. Rick, A. M. Michon, C. M. Cruciat, M. Remor, C. Hofert, M. Schelder, M. Brajenovic, H. Ruffner, A. Merino, K. Klein, M. Hudak, D. Dickson, T. Rudi, V. Gnau, A. Bauch, S. Bastuck, B. Huhse, C. Leutwein, M. A. Heurtier, R. R. Copley, A. Edelmann, E. Querfurth, V. Rybin, G. Drewes, M. Raida, T. Bouwmeester, P. Bork, B. Seraphin, B. Kuster, G. Neubauer, and G. Superti-Furga. "Functional Organization of the Yeast Proteome by Systematic Analysis of Protein Complexes." *Nature* 415.6868 (2002): 141-7. Print.

Gillooly, D. J., Morrow, I. C., Lindsay, M., Gould, R., Bryant, N. J., Gaullier, J. M., Parton, R. G. and Stenmark, H. "Localization of Phosphatidylinositol 3-Phosphate in Yeast and Mammalian Cells." *The EMBO journal* 19.17 (2000): 4577-88. Print.

Giot, L., Bader, J. S., Brouwer, C., Chaudhuri, A., Kuang, B., Li, Y., Hao, Y. L., Ooi, C. E., Godwin, B., Vitols, E., Vijayadamodar, G., Pochart, P., Machineni, H., Welsh, M., Kong, Y., Zerhusen, B., Malcolm, R., Varrone, Z., Collis, A., Minto, M., Burgess, S., McDaniel, L., Stimpson, E., Spriggs, F., Williams, J., Neurath, K., Ioime, N., Agee, M., Voss, E., Furtak, K., Renzulli, R., Aanensen, N., Carrolla, S., Bickelhaupt, E., Lazovatsky, Y., DaSilva, A., Zhong, J., Stanyon, C. A., Finley, R. L., Jr., White, K. P., Braverman, M., Jarvie, T., Gold, S., Leach, M., Knight, J., Shimkets, R. A., McKenna, M. P., Chant, J., and Rothberg, J. M. "A Protein Interaction Map of Drosophila Melanogaster." *Science* 302.5651 (2003): 1727-36. Print.

Godena, V. K., Romano, G., Romano, M., Appocher, C., Klima, R., Buratti, E., Baralle, F. E. and Feiguin, F. "Tdp-43 Regulates Drosophila Neuromuscular Junctions Growth by Modulating Futsch/Map1b Levels and Synaptic Microtubules Organization." *PloS one* 6.3 (2011): e17808. Print.

Golub, T., and P. Caroni. "Pi(4,5)P2-Dependent Microdomain Assemblies Capture Microtubules to Promote and Control Leading Edge Motility." *The Journal of cell biology* 169.1 (2005): 151-65. Print.

Gong, L. W., and De Camilli, P. "Regulation of Postsynaptic Ampa Responses by Synaptojanin 1." *Proceedings of the National Academy of Sciences of the United States of America* 105.45 (2008): 17561-6. Print.

Graslund, S., P. Nordlund, J. Weigelt, B. M. Hallberg, J. Bray, O. Gileadi, S. Knapp, U. Oppermann, C. Arrowsmith, R. Hui, J. Ming, S. dhe-Paganon, H. W. Park, A. Savchenko, A. Yee, A. Edwards, R. Vincentelli, C. Cambillau, R. Kim, S. H. Kim, Z. Rao, Y. Shi, T. C. Terwilliger, C. Y. Kim, L. W. Hung, G. S. Waldo, Y. Peleg, S. Albeck, T. Unger, O. Dym, J. Prilusky, J. L. Sussman, R. C. Stevens, S. A. Lesley, I. A. Wilson, A. Joachimiak, F. Collart, I. Dementieva, M. I. Donnelly, W. H. Eschenfeldt, Y. Kim, L. Stols, R. Wu, M. Zhou, S. K. Burley, J. S. Emtage, J. M. Sauder, D. Thompson, K. Bain, J. Luz, T. Gheyi, F. Zhang, S. Atwell, S. C. Almo, J. B. Bonanno, A. Fiser, S. Swaminathan, F. W. Studier, M. R. Chance, A. Sali, T. B. Acton, R. Xiao, L. Zhao, L. C. Ma, J. F. Hunt, L. Tong, K. Cunningham, M. Inouye, S. Anderson, H. Janjua, R. Shastry, C. K. Ho, D. Wang, H. Wang, M. Jiang, G. T. Montelione, D. I. Stuart, R. J. Owens, S. Daenke, A. Schutz, U. Heinemann, S. Yokoyama, K. Bussow, and K. C. Gunsalus. "Protein Production and Purification." *Nature methods* 5.2 (2008): 135-46. Print.

Greenway, M. J., P. M. Andersen, C. Russ, S. Ennis, S. Cashman, C. Donaghy, V. Patterson, R. Swingler, D. Kieran, J. Prehn, K. E. Morrison, A. Green, K. R. Acharya, R. H. Brown, Jr., and O. Hardiman. "Ang Mutations Segregate with Familial and 'Sporadic' Amyotrophic Lateral Sclerosis." *Nature genetics* 38.4 (2006): 411-3. Print.

Griffith, L. C. and Budnik, V. "Plasticity and Second Messengers During Synapse Development." *International review of neurobiology* 75 (2006): 237-65. Print.

Guo, S., L. E. Stolz, S. M. Lemrow, and J. D. York. "Sac1-Like Domains of Yeast Sac1, Inp52, and Inp53 and of Human Synaptojanin Encode Polyphosphoinositide Phosphatases." *The Journal of biological chemistry* 274.19 (1999): 12990-5. Print.

Hama, H., E. A. Schnieders, J. Thorner, J. Y. Takemoto, and D. B. DeWald. "Direct Involvement of Phosphatidylinositol 4-Phosphate in Secretion in the Yeast

Saccharomyces Cerevisiae." *The Journal of biological chemistry* 274.48 (1999): 34294-300. Print.

Hamada, K., T. Shimizu, T. Matsui, S. Tsukita, and T. Hakoshima. "Structural Basis of the Membrane-Targeting and Unmasking Mechanisms of the Radixin Ferm Domain." *The EMBO journal* 19.17 (2000): 4449-62. Print.

Han, S. M., Tsuda, H., Yang, Y., Vibbert, J., Cottee, P., Lee, S. J., Winek, J., Haueter, C., Bellen, H. J., and Miller, M. A. "Secreted Vapb/Als8 Major Sperm Protein Domains Modulate Mitochondrial Localization and Morphology Via Growth Cone Guidance Receptors." *Developmental cell* 22.2 (2012): 348-62. Print.

Hanada, K., K. Kumagai, N. Tomishige, and T. Yamaji. "Cert-Mediated Trafficking of Ceramide." *Biochimica et biophysica acta* 1791.7 (2009): 684-91. Print.

Hanada, K., Kumagai, K., Yasuda, S., Miura, Y., Kawano, M., Fukasawa, M., and Nishijima, M. "Molecular Machinery for Non-Vesicular Trafficking of Ceramide." *Nature* 426.6968 (2003): 803-9. Print.

Hart, W. S., Heuzenroeder, M. W., and Barton, M. D. "A Study of the Transfer of Tetracycline Resistance Genes between Escherichia Coli in the Intestinal Tract of a Mouse and a Chicken Model." *Journal of veterinary medicine. B, Infectious diseases and veterinary public health* 53.7 (2006): 333-40. Print.

Haslam, P. J., S. J. Proctor, T. H. Goodship, and J. Zouvani. "Immune Complex Glomerulonephritis, Myasthenia Gravis and Compensated Hypothyroidism in a Patient Following Allogeneic Bone Marrow Transplantation." *Nephrology, dialysis, transplantation : official publication of the European Dialysis and Transplant Association - European Renal Association* 8.12 (1993): 1390-2. Print.

Hinners, I., and S. A. Tooze. "Changing Directions: Clathrin-Mediated Transport between the Golgi and Endosomes." *Journal of cell science* 116.Pt 5 (2003): 763-71. Print.

Hofbauer, A., T. Ebel, B. Waltenspiel, P. Oswald, Y. C. Chen, P. Halder, S. Biskup, U. Lewandrowski, C. Winkler, A. Sickmann, S. Buchner, and E. Buchner. "The Wuerzburg Hybridoma Library against Drosophila Brain." *Journal of neurogenetics* 23.1-2 (2009): 78-91. Print.

Hopp, T. P., Prickett K.S., Price V.L., Libby R.T., March C.J., Cerretti D.P., Urdal D.L., and Conlon P.J. "A Short Polypeptide Marker Sequence Useful for Recombinant Protein Identification and Purification." *Nature Biotechnology* 6 (1988): 1204 - 10. Print.

Hosler, B. A., T. Siddique, P. C. Sapp, W. Sailor, M. C. Huang, A. Hossain, J. R. Daube, M. Nance, C. Fan, J. Kaplan, W. Y. Hung, D. McKenna-Yasek, J. L. Haines, M. A. Pericak-Vance, H. R. Horvitz, and R. H. Brown, Jr. "Linkage of Familial Amyotrophic Lateral Sclerosis with Frontotemporal Dementia to Chromosome 9q21-Q22." *JAMA : the journal of the American Medical Association* 284.13 (2000): 1664-9. Print.

Hu, J. H., H. Zhang, R. Wagey, C. Krieger, and S. L. Pelech. "Protein Kinase and Protein Phosphatase Expression in Amyotrophic Lateral Sclerosis Spinal Cord." *Journal of neurochemistry* 85.2 (2003): 432-42. Print.

Hughes, W. E., F. T. Cooke, and P. J. Parker. "Sac Phosphatase Domain Proteins." *The Biochemical journal* 350 Pt 2 (2000): 337-52. Print.

Hummel, T., K. Krukkert, J. Roos, G. Davis, and C. Klambt. "Drosophila Futsch/22c10 Is a Map1b-Like Protein Required for Dendritic and Axonal Development." *Neuron* 26.2 (2000): 357-70. Print.

Ikeda, Y., K. A. Dick, M. R. Weatherspoon, D. Gincel, K. R. Armbrust, J. C. Dalton, G. Stevanin, A. Durr, C. Zuhlke, K. Burk, H. B. Clark, A. Brice, J. D. Rothstein, L. J. Schut, J. W. Day, and L. P. Ranum. "Spectrin Mutations Cause Spinocerebellar Ataxia Type 5." *Nature genetics* 38.2 (2006): 184-90. Print.

Ince, P. G., J. Tomkins, J. Y. Slade, N. M. Thatcher, and P. J. Shaw. "Amyotrophic Lateral Sclerosis Associated with Genetic Abnormalities in the Gene Encoding Cu/Zn Superoxide Dismutase: Molecular Pathology of Five New Cases, and Comparison with Previous Reports and 73 Sporadic Cases of Als." *Journal of neuropathology and experimental neurology* 57.10 (1998): 895-904. Print.

Jackson, G. R., Salecker, I., Dong, X., Yao, X., Arnheim, N., Faber, P. W., MacDonald, M. E., and Zipursky, S. L. "Polyglutamine-Expanded Human Huntingtin Transgenes Induce Degeneration of Drosophila Photoreceptor Neurons." *Neuron* 21.3 (1998): 633-42. Print.

Jan, L. Y. and Jan, Y. N. "Antibodies to Horseradish Peroxidase as Specific Neuronal Markers in Drosophila and in Grasshopper Embryos." *Proceedings of the National Academy of Sciences of the United States of America* 79.8 (1982): 2700-4. Print.

Jaworski, C. J., E. Moreira, A. Li, R. Lee, and I. R. Rodriguez. "A Family of 12 Human Genes Containing Oxysterol-Binding Domains." *Genomics* 78.3 (2001): 185-96. Print.

Johansen, J., M. E. Halpern, K. M. Johansen, and H. Keshishian. "Stereotypic Morphology of Glutamatergic Synapses on Identified Muscle Cells of Drosophila Larvae." *The Journal of neuroscience : the official journal of the Society for Neuroscience* 9.2 (1989): 710-25. Print.

Johnson, E. L., 3rd, Fetter, R. D. and Davis, G. W. "Negative Regulation of Active Zone Assembly by a Newly Identified Sr Protein Kinase." *PLoS biology* 7.9 (2009): e1000193. Print.

Johnson, J. O., J. Mandrioli, M. Benatar, Y. Abramzon, V. M. Van Deerlin, J. Q. Trojanowski, J. R. Gibbs, M. Brunetti, S. Gronka, J. Wuu, J. Ding, L. McCluskey, M. Martinez-Lage, D. Falcone, D. G. Hernandez, S. Arepalli, S. Chong, J. C. Schymick, J. Rothstein, F. Landi, Y. D. Wang, A. Calvo, G. Mora, M. Sabatelli, M. R. Monsurro, S. Battistini, F. Salvi, R. Spataro, P. Sola, G. Borghero, G. Galassi, S. W. Scholz, J. P. Taylor, G. Restagno, A. Chio, and B. J. Traynor. "Exome Sequencing Reveals Vcp Mutations as a Cause of Familial Als." *Neuron* 68.5 (2010): 857-64. Print.

Kagiwada, S., and Hashimoto, M. "The Yeast Vap Homolog Scs2p Has a Phosphoinositide-Binding Ability That Is Correlated with Its Activity." *Biochemical and biophysical research communications* 364.4 (2007): 870-6. Print.

Kagiwada, S., and Zen, R. "Role of the Yeast Vap Homolog, Scs2p, in Ino1 Expression and Phospholipid Metabolism." *Journal of biochemistry* 133.4 (2003): 515-22. Print.

Kagiwada, S., Hosaka, K., Murata, M., Nikawa, J., and Takatsuki, A. "The Saccharomyces Cerevisiae Scs2 Gene Product, a Homolog of a Synaptobrevin-Associated Protein, Is an Integral Membrane Protein of the Endoplasmic Reticulum and Is Required for Inositol Metabolism." *Journal of bacteriology* 180.7 (1998): 1700-8. Print.

Kaiser, S. E., Brickner, J. H., Reilein, A. R., Fenn, T. D., Walter, P., and Brunger, A. T. "Structural Basis of Ffat Motif-Mediated Er Targeting." *Structure* 13.7 (2005): 1035-45. Print.

Kanekura, K., Nishimoto, I., Aiso, S., and Matsuoka, M. "Characterization of Amyotrophic Lateral Sclerosis-Linked P56s Mutation of Vesicle-Associated Membrane Protein-Associated Protein B (Vapb/Als8)." *The Journal of biological chemistry* 281.40 (2006): 30223-33. Print.

Karsten, S. L., Sang, T. K., Gehman, L. T., Chatterjee, S., Liu, J., Lawless, G. M., Sengupta, S., Berry, R. W., Pomakian, J., Oh, H. S., Schulz, C., Hui, K. S., Wiedau-Pazos, M., Vinters, H. V., Binder, L. I., Geschwind, D. H., and Jackson, G. R. "A Genomic Screen for Modifiers of Tauopathy Identifies Puromycin-Sensitive Aminopeptidase as an Inhibitor of Tau-Induced Neurodegeneration." *Neuron* 51.5 (2006): 549-60. Print.

Kato, S., Hayashi, H., Nakashima, K., Nanba, E., Kato, M., Hirano, A., Nakano, I., Asayama, K. and Ohama, E. "Pathological Characterization of Astrocytic Hyaline Inclusions in Familial Amyotrophic Lateral Sclerosis." *The American journal of pathology* 151.2 (1997): 611-20. Print.

Kawano, M., Kumagai, K., Nishijima, M., and Hanada, K. "Efficient Trafficking of Ceramide from the Endoplasmic Reticulum to the Golgi Apparatus Requires a Vamp-Associated Protein-Interacting Ffat Motif of Cert." *The Journal of biological chemistry* 281.40 (2006): 30279-88. Print.

Kim, S., Leal, S. S., Ben Halevy, D., Gomes, C. M. and Lev, S. "Structural Requirements for Vap-B Oligomerization and Their Implication in Amyotrophic Lateral Sclerosis-Associated Vap-B(P56s) Neurotoxicity." *The Journal of biological chemistry* 285.18 (2010): 13839-49. Print.

Kipriyanov, S. M., Little, M., Kropshofer, H., Breitling, F., Gotter, S. and Dubel, S. "Affinity Enhancement of a Recombinant Antibody: Formation of Complexes with Multiple Valency by a Single-Chain Fv Fragment-Core Streptavidin Fusion." *Protein engineering* 9.2 (1996): 203-11. Print.

Kittel, R. J., Wichmann, C., Rasse, T. M., Fouquet, W., Schmidt, M., Schmid, A., Wagh, D. A., Pawlu, C., Kellner, R. R., Willig, K. I., Hell, S. W., Buchner, E., Heckmann, M. and Sigrist, S. J. "Bruchpilot Promotes Active Zone Assembly,

Ca2+ Channel Clustering, and Vesicle Release." *Science* 312.5776 (2006): 1051-4. Print.

Kondylis, V., S. E. Goulding, J. C. Dunne, and C. Rabouille. "Biogenesis of Golgi Stacks in Imaginal Discs of Drosophila Melanogaster." *Molecular biology of the cell* 12.8 (2001): 2308-27. Print.

Konrad, G., T. Schlecker, F. Faulhammer, and P. Mayinger. "Retention of the Yeast Sac1p Phosphatase in the Endoplasmic Reticulum Causes Distinct Changes in Cellular Phosphoinositide Levels and Stimulates Microsomal Atp Transport." *The Journal of biological chemistry* 277.12 (2002): 10547-54. Print.

Krueger, S. R., A. Kolar, and R. M. Fitzsimonds. "The Presynaptic Release Apparatus Is Functional in the Absence of Dendritic Contact and Highly Mobile within Isolated Axons." *Neuron* 40.5 (2003): 945-57. Print.

Kuhlman, P. A., C. A. Hughes, V. Bennett, and V. M. Fowler. "A New Function for Adducin. Calcium/Calmodulin-Regulated Capping of the Barbed Ends of Actin Filaments." *The Journal of biological chemistry* 271.14 (1996): 7986-91. Print.

Kumagai, K., Kawano, M., Shinkai-Ouchi, F., Nishijima, M. and Hanada, K. "Interorganelle Trafficking of Ceramide Is Regulated by Phosphorylation-Dependent Cooperativity between the Ph and Start Domains of Cert." *The Journal of biological chemistry* 282.24 (2007): 17758-66. Print.

Kunst, C. B. "Complex Genetics of Amyotrophic Lateral Sclerosis." *American journal of human genetics* 75.6 (2004): 933-47. Print.

Kwiatkowski, T. J., Jr., D. A. Bosco, A. L. Leclerc, E. Tamrazian, C. R. Vanderburg, C. Russ, A. Davis, J. Gilchrist, E. J. Kasarskis, T. Munsat, P. Valdmanis, G. A. Rouleau, B. A. Hosler, P. Cortelli, P. J. de Jong, Y. Yoshinaga, J. L. Haines, M. A. Pericak-Vance, J. Yan, N. Ticozzi, T. Siddique, D. McKenna-Yasek, P. C. Sapp, H. R. Horvitz, J. E. Landers, and R. H. Brown, Jr. "Mutations in the Fus/Tls Gene on Chromosome 16 Cause Familial Amyotrophic Lateral Sclerosis." *Science* 323.5918 (2009): 1205-8. Print.

Lahey, T., M. Gorczyca, X. X. Jia, and V. Budnik. "The Drosophila Tumor Suppressor Gene Dlg Is Required for Normal Synaptic Bouton Structure." *Neuron* 13.4 (1994): 823-35. Print.

Laurent, F., Labesse, G. and de Wit, P. "Molecular Cloning and Partial Characterization of a Plant Vap33 Homologue with a Major Sperm Protein Domain." *Biochemical and biophysical research communications* 270.1 (2000): 286-92. Print.

Lee, S., S. Kim, M. Nahm, E. Kim, T. I. Kim, and J. H. Yoon. "The Phosphoinositide Phosphatase Sac1 Is Required for Midline Axon Guidance." *Molecules and cells* 32.5 (2011): 477-82. Print.

Lehto, M., S. Laitinen, G. Chinetti, M. Johansson, C. Ehnholm, B. Staels, E. Ikonen, and V. M. Olkkonen. "The Osbp-Related Protein Family in Humans." *Journal of lipid research* 42.8 (2001): 1203-13. Print.

Lehto, M., and V. M. Olkkonen. "The Osbp-Related Proteins: A Novel Protein Family Involved in Vesicle Transport, Cellular Lipid Metabolism, and Cell Signalling." *Biochimica et biophysica acta* 1631.1 (2003): 1-11. Print.

Leigh, P. N., and Garofalo O. "The Molecular Pathology of Motor Neurone Disease." *Motor Neurone Disease* ed. M. Swash and P.N. Leigh.Springer Verlag London (1995): 139-61. Print.

Lemmon, M. A. and Ferguson, K. M. "Signal-Dependent Membrane Targeting by Pleckstrin Homology (Ph) Domains." *The Biochemical journal* 350 Pt 1 (2000): 1-18. Print.

Lev, S., Ben Halevy, D., Peretti, D., and Dahan, N. "The Vap Protein Family: From Cellular Functions to Motor Neuron Disease." *Trends Cell Biol* 18.6 (2008): 282-90. Print.

Levanon, D., Hsieh, C. L., Francke, U., Dawson, P. A., Ridgway, N. D., Brown, M. S. and Goldstein, J. L. "Cdna Cloning of Human Oxysterol-Binding Protein and Localization of the Gene to Human Chromosome 11 and Mouse Chromosome 19." *Genomics* 7.1 (1990): 65-74. Print.

Lin, C. H. and Forscher, P. "Cytoskeletal Remodeling During Growth Cone-Target Interactions." *The Journal of cell biology* 121.6 (1993): 1369-83. Print.

Ling, K., Doughman, R. L., Firestone, A. J., Bunce, M. W., and Anderson, R. A. "Type I Gamma Phosphatidylinositol Phosphate Kinase Targets and Regulates Focal Adhesions." *Nature* 420.6911 (2002): 89-93. Print.

Liu, Y., Boukhelifa, M., Tribble, E., Morin-Kensicki, E., Uetrecht, A., Bear, J. E. and Bankaitis, V. A. "The Sac1 Phosphoinositide Phosphatase Regulates Golgi Membrane Morphology and Mitotic Spindle Organization in Mammals." *Molecular biology of the cell* 19.7 (2008): 3080-96. Print.

Lloyd, T. E., P. Verstreken, E. J. Ostrin, A. Phillippi, O. Lichtarge, and H. J. Bellen. "A Genome-Wide Search for Synaptic Vesicle Cycle Proteins in Drosophila." *Neuron* 26.1 (2000): 45-50. Print.

Loewen, C. J., Gaspar, M. L., Jesch, S. A., Delon, C., Ktistakis, N. T., Henry, S. A., and Levine, T. P. "Phospholipid Metabolism Regulated by a Transcription Factor Sensing Phosphatidic Acid." *Science* 304.5677 (2004): 1644-7. Print.

Loewen, C. J., and T. P. Levine. "A Highly Conserved Binding Site in Vesicle-Associated Membrane Protein-Associated Protein (Vap) for the Ffat Motif of Lipid-Binding Proteins." *The Journal of biological chemistry* 280.14 (2005): 14097-104. Print.

Loewen, C. J., A. Roy, and T. P. Levine. "A Conserved Er Targeting Motif in Three Families of Lipid Binding Proteins and in Opi1p Binds Vap." *The EMBO journal* 22.9 (2003): 2025-35. Print.

Lomen-Hoerth, C. "Characterization of Amyotrophic Lateral Sclerosis and Frontotemporal Dementia." *Dementia and geriatric cognitive disorders* 17.4 (2004): 337-41. Print.

Lowery, L. A., and D. Van Vactor. "The Trip of the Tip: Understanding the Growth Cone Machinery." *Nature reviews. Molecular cell biology* 10.5 (2009): 332-43. Print.

Luty, A. A., J. B. Kwok, C. Dobson-Stone, C. T. Loy, K. G. Coupland, H. Karlstrom, T. Sobow, J. Tchorzewska, A. Maruszak, M. Barcikowska, P. K. Panegyres, C. Zekanowski, W. S. Brooks, K. L. Williams, I. P. Blair, K. A. Mather, P. S. Sachdev, G. M. Halliday, and P. R. Schofield. "Sigma Nonopioid Intracellular Receptor 1 Mutations Cause Frontotemporal Lobar Degeneration-Motor Neuron Disease." *Annals of neurology* 68.5 (2010): 639-49. Print.

Manford, A., T. Xia, A. K. Saxena, C. Stefan, F. Hu, S. D. Emr, and Y. Mao. "Crystal Structure of the Yeast Sac1: Implications for Its Phosphoinositide Phosphatase Function." *The EMBO journal* 29.9 (2010): 1489-98. Print.

Marques, V. D., Barreira, A. A., Davis, M. B., Abou-Sleiman, P. M., Silva, W. A., Jr., Zago, M. A., Sobreira, C., Fazan, V., and Marques, W., Jr. "Expanding the Phenotypes of the Pro56ser Vapb Mutation: Proximal Sma with Dysautonomia." *Muscle & nerve* 34.6 (2006): 731-9. Print.

Marsh, J. L. and Thompson, L. M. "Drosophila in the Study of Neurodegenerative Disease." *Neuron* 52.1 (2006): 169-78. Print.

Maruyama, H., H. Morino, H. Ito, Y. Izumi, H. Kato, Y. Watanabe, Y. Kinoshita, M. Kamada, H. Nodera, H. Suzuki, O. Komure, S. Matsuura, K. Kobatake, N. Morimoto, K. Abe, N. Suzuki, M. Aoki, A. Kawata, T. Hirai, T. Kato, K. Ogasawara, A. Hirano, T. Takumi, H. Kusaka, K. Hagiwara, R. Kaji, and H. Kawakami. "Mutations of Optineurin in Amyotrophic Lateral Sclerosis." *Nature* 465.7295 (2010): 223-6. Print.

Matsuoka, Y., Li, X. and Bennett, V. "Adducin: Structure, Function and Regulation." *Cellular and molecular life sciences : CMLS* 57.6 (2000): 884-95. Print.

Mayer, B. J., Ren, R., Clark, K. L. and Baltimore, D. "A Putative Modular Domain Present in Diverse Signaling Proteins." *Cell* 73.4 (1993): 629-30. Print.

Mayinger, P. "Regulation of Golgi Function Via Phosphoinositide Lipids." *Seminars in cell & developmental biology* 20.7 (2009): 793-800. Print.

Mayinger, P., Bankaitis, V. A., and Meyer, D. I. "Sac1p Mediates the Adenosine Triphosphate Transport into Yeast Endoplasmic Reticulum That Is Required for Protein Translocation." *The Journal of cell biology* 131.6 Pt 1 (1995): 1377-86. Print.

McCrea, H. J., and De Camilli, P. "Mutations in Phosphoinositide Metabolizing Enzymes and Human Disease." *Physiology* 24 (2009): 8-16. Print.

Miech, C., H. U. Pauer, X. He, and T. L. Schwarz. "Presynaptic Local Signaling by a Canonical Wingless Pathway Regulates Development of the Drosophila Neuromuscular Junction." *The Journal of neuroscience : the official journal of the Society for Neuroscience* 28.43 (2008): 10875-84. Print.

Mikitova, V. and Levine, T. P. "Analysis of the Key Elements of Ffat-Like Motifs Identifies New Proteins That Potentially Bind Vap on the Er, Including Two Akaps and Fapp2." *PloS one* 7.1 (2012): e30455. Print.

Miller, M. A., Ruest, P. J., Kosinski, M., Hanks, S. K., and Greenstein, D. "An Eph Receptor Sperm-Sensing Control Mechanism for Oocyte Meiotic Maturation in Caenorhabditis Elegans." *Genes & development* 17.2 (2003): 187-200. Print.

Mulder, D. W., Kurland, L. T., Offord, K. P. and Beard, C. M. "Familial Adult Motor Neuron Disease: Amyotrophic Lateral Sclerosis." *Neurology* 36.4 (1986): 511-7. Print.

Munch, C., R. Sedlmeier, T. Meyer, V. Homberg, A. D. Sperfeld, A. Kurt, J. Prudlo, G. Peraus, C. O. Hanemann, G. Stumm, and A. C. Ludolph. "Point Mutations of the P150 Subunit of Dynactin (Dctn1) Gene in Als." *Neurology* 63.4 (2004): 724-6. Print.

Muresan, V., Stankewich, M. C., Steffen, W., Morrow, J. S., Holzbaur, E. L. and Schnapp, B. J. "Dynactin-Dependent, Dynein-Driven Vesicle Transport in the Absence of Membrane Proteins: A Role for Spectrin and Acidic Phospholipids." *Molecular cell* 7.1 (2001): 173-83. Print.

Mutsuddi, M., Marshall, C. M., Benzow, K. A., Koob, M. D., and Rebay, I. "The Spinocerebellar Ataxia 8 Noncoding Rna Causes Neurodegeneration and Associates with Staufen in Drosophila." *Current biology : CB* 14.4 (2004): 302-8. Print.

Nemoto, Y., B. G. Kearns, M. R. Wenk, H. Chen, K. Mori, J. G. Alb, Jr., P. De Camilli, and V. A. Bankaitis. "Functional Characterization of a Mammalian Sac1 and Mutants Exhibiting Substrate-Specific Defects in Phosphoinositide Phosphatase Activity." *The Journal of biological chemistry* 275.44 (2000): 34293-305. Print.

Ngo, M., and N. D. Ridgway. "Oxysterol Binding Protein-Related Protein 9 (Orp9) Is a Cholesterol Transfer Protein That Regulates Golgi Structure and Function." *Molecular biology of the cell* 20.5 (2009): 1388-99. Print.

Nikawa, J., Murakami, A., Esumi, E., and Hosaka, K. "Cloning and Sequence of the Scs2 Gene, Which Can Suppress the Defect of Ino1 Expression in an Inositol Auxotrophic Mutant of Saccharomyces Cerevisiae." *Journal of biochemistry* 118.1 (1995): 39-45. Print.

Nishimura, A. L., Mitne-Neto, M., Silva, H. C., Richieri-Costa, A., Middleton, S., Cascio, D., Kok, F., Oliveira, J. R., Gillingwater, T., Webb, J., Skehel, P., and

Zatz, M. "A Mutation in the Vesicle-Trafficking Protein Vapb Causes Late-Onset Spinal Muscular Atrophy and Amyotrophic Lateral Sclerosis." *American journal of human genetics* 75.5 (2004): 822-31. Print.

Nishimura, Y., Hayashi, M., Inada, H., and Tanaka, T. "Molecular Cloning and Characterization of Mammalian Homologues of Vesicle-Associated Membrane Protein-Associated (Vamp-Associated) Proteins." *Biochemical and biophysical research communications* 254.1 (1999): 21-6. Print.

Novick, P., B. C. Osmond, and D. Botstein. "Suppressors of Yeast Actin Mutations." *Genetics* 121.4 (1989): 659-74. Print.

Odorizzi, G., M. Babst, and S. D. Emr. "Phosphoinositide Signaling and the Regulation of Membrane Trafficking in Yeast." *Trends in biochemical sciences* 25.5 (2000): 229-35. Print.

Orlacchio, A., C. Babalini, A. Borreca, C. Patrono, R. Massa, S. Basaran, R. P. Munhoz, E. A. Rogaeva, P. H. St George-Hyslop, G. Bernardi, and T. Kawarai. "Spatacsin Mutations Cause Autosomal Recessive Juvenile Amyotrophic Lateral Sclerosis." *Brain : a journal of neurology* 133.Pt 2 (2010): 591-8. Print.

Packard, M., Mathew, D. and Budnik, V. "Fast Remodeling of Synapses in Drosophila." *Current opinion in neurobiology* 13.5 (2003): 527-34. Print.

Parrish, W. R., Stefan, C. J. and Emr, S. D. "Ptdins(3)P Accumulation in Triple Lipid-Phosphatase-Deletion Mutants Triggers Lethal Hyperactivation of the Rho1p/Pkc1p Cell-Integrity Map Kinase Pathway." *Journal of cell science* 118.Pt 23 (2005): 5589-601. Print.

Pennetta, G., Hiesinger, P. R., Fabian-Fine, R., Meinertzhagen, I. A., and Bellen, H. J. "Drosophila Vap-33a Directs Bouton Formation at Neuromuscular Junctions in a Dosage-Dependent Manner." *Neuron* 35.2 (2002): 291-306. Print.

Peretti, D., N. Dahan, E. Shimoni, K. Hirschberg, and S. Lev. "Coordinated Lipid Transfer between the Endoplasmic Reticulum and the Golgi Complex Requires the Vap Proteins and Is Essential for Golgi-Mediated Transport." *Mol Biol Cell* 19.9 (2008): 3871-84. Print.

Petrella, L. N., T. Smith-Leiker, and L. Cooley. "The Ovhts Polyprotein Is Cleaved to Produce Fusome and Ring Canal Proteins Required for Drosophila Oogenesis." *Development* 134.4 (2007): 703-12. Print.

Piao, H., and P. Mayinger. "Growth and Metabolic Control of Lipid Signalling at the Golgi." *Biochemical Society transactions* 40.1 (2012): 205-9. Print.

Piao, Y. S., K. Wakabayashi, A. Kakita, M. Yamada, S. Hayashi, T. Morita, F. Ikuta, K. Oyanagi, and H. Takahashi. "Neuropathology with Clinical Correlations of Sporadic Amyotrophic Lateral Sclerosis: 102 Autopsy Cases Examined between 1962 and 2000." *Brain pathology* 13.1 (2003): 10-22. Print.

Pielage, J., V. Bulat, J. B. Zuchero, R. D. Fetter, and G. W. Davis. "Hts/Adducin Controls Synaptic Elaboration and Elimination." *Neuron* 69.6 (2011): 1114-31. Print.

Pielage, J., Fetter, R. D. and Davis, G. W. "A Postsynaptic Spectrin Scaffold Defines Active Zone Size, Spacing, and Efficacy at the Drosophila Neuromuscular Junction." *The Journal of cell biology* 175.3 (2006): 491-503. Print.

Plowey, E. D. and Chu, C. T. "Synaptic Dysfunction in Genetic Models of Parkinson's Disease: A Role for Autophagy?" *Neurobiology of disease* 43.1 (2011): 60-7. Print.

Ponting, C. P. and Aravind, L. "Start: A Lipid-Binding Domain in Star, Hd-Zip and Signalling Proteins." *Trends in biochemical sciences* 24.4 (1999): 130-2. Print.

Rao, R. P., C. Yuan, J. C. Allegood, S. S. Rawat, M. B. Edwards, X. Wang, A. H. Merrill, Jr., U. Acharya, and J. K. Acharya. "Ceramide Transfer Protein Function Is Essential for Normal Oxidative Stress Response and Lifespan." *Proceedings of the National Academy of Sciences of the United States of America* 104.27 (2007): 11364-9. Print.

Ratnaparkhi, A., G. M. Lawless, F. E. Schweizer, P. Golshani, and G. R. Jackson. "A Drosophila Model of Als: Human Als-Associated Mutation in Vap33a Suggests a Dominant Negative Mechanism." *PloS one* 3.6 (2008): e2334. Print.

Raya, A., F. Revert, S. Navarro, and J. Saus. "Characterization of a Novel Type of Serine/Threonine Kinase That Specifically Phosphorylates the Human Goodpasture Antigen." *The Journal of biological chemistry* 274.18 (1999): 12642-9. Print.

Raya, A., F. Revert-Ros, P. Martinez-Martinez, S. Navarro, E. Rosello, B. Vieites, F. Granero, J. Forteza, and J. Saus. "Goodpasture Antigen-Binding Protein, the Kinase That Phosphorylates the Goodpasture Antigen, Is an Alternatively Spliced Variant Implicated in Autoimmune Pathogenesis." *The Journal of biological chemistry* 275.51 (2000): 40392-9. Print.

Raychaudhuri, S. and Prinz, W. A. "The Diverse Functions of Oxysterol-Binding Proteins." *Annual review of cell and developmental biology* 26 (2010): 157-77. Print.

Reiter, L. T., Potocki, L., Chien, S., Gribskov, M. and Bier, E. "A Systematic Analysis of Human Disease-Associated Gene Sequences in Drosophila Melanogaster." *Genome research* 11.6 (2001): 1114-25. Print.

Ren, J., L. Wen, X. Gao, C. Jin, Y. Xue, and X. Yao. "Dog 1.0: Illustrator of Protein Domain Structures." *Cell research* 19.2 (2009): 271-3. Print.

Renton, A. E. et al. "A Hexanucleotide Repeat Expansion in C9orf72 Is the Cause of Chromosome 9p21-Linked Als-Ftd." *Neuron* 72.2 (2011): 257-68. Print.

Ridgway, N. D., P. A. Dawson, Y. K. Ho, M. S. Brown, and J. L. Goldstein. "Translocation of Oxysterol Binding Protein to Golgi Apparatus Triggered by Ligand Binding." *The Journal of cell biology* 116.2 (1992): 307-19. Print.

Roberts, T. M., and Stewart, M. "Nematode Sperm Locomotion." *Current opinion in cell biology* 7.1 (1995): 13-7. Print.

Robin, G. C., Russell, R. J., Cutler, D. J. and Oakeshott, J. G. "The Evolution of an Alpha-Esterase Pseudogene Inactivated in the Drosophila Melanogaster Lineage." *Molecular biology and evolution* 17.4 (2000): 563-75. Print.

Robinson, D. N., Cant, K. and Cooley, L. "Morphogenesis of Drosophila Ovarian Ring Canals." *Development* 120.7 (1994): 2015-25. Print.

Rocha, N., Kuijl, C., van der Kant, R., Janssen, L., Houben, D., Janssen, H., Zwart, W. and Neefjes, J. "Cholesterol Sensor Orp1l Contacts the Er Protein Vap to Control Rab7-Rilp-P150 Glued and Late Endosome Positioning." *The Journal of cell biology* 185.7 (2009): 1209-25. Print.

Rohde, H. M., Cheong, F. Y., Konrad, G., Paiha, K., Mayinger, P. and Boehmelt, G. "The Human Phosphatidylinositol Phosphatase Sac1 Interacts with the Coatomer I Complex." *The Journal of biological chemistry* 278.52 (2003): 52689-99. Print.

Roos, J., T. Hummel, N. Ng, C. Klambt, and G. W. Davis. "Drosophila Futsch Regulates Synaptic Microtubule Organization and Is Necessary for Synaptic Growth." *Neuron* 26.2 (2000): 371-82. Print.

Rosas, H. D., Salat, D. H., Lee, S. Y., Zaleta, A. K., Pappu, V., Fischl, B., Greve, D., Hevelone, N., and S. M. and Hersch. "Cerebral Cortex and the Clinical Expression of Huntington's Disease: Complexity and Heterogeneity." *Brain : a journal of neurology* 131.Pt 4 (2008): 1057-68. Print.

Rosen, D. R. "Mutations in Cu/Zn Superoxide Dismutase Gene Are Associated with Familial Amyotrophic Lateral Sclerosis." *Nature* 364.6435 (1993): 362. Print.

Ross, C. A., and Poirier, M. A. "Opinion: What Is the Role of Protein Aggregation in Neurodegeneration?" *Nature reviews. Molecular cell biology* 6.11 (2005): 891-8. Print.

Ross, O. A., N. J. Rutherford, M. Baker, A. I. Soto-Ortolaza, M. M. Carrasquillo, M. DeJesus-Hernandez, J. Adamson, M. Li, K. Volkening, E. Finger, W. W. Seeley, K. J. Hatanpaa, C. Lomen-Hoerth, A. Kertesz, E. H. Bigio, C. Lippa, B. K. Woodruff, D. S. Knopman, C. L. White, 3rd, J. A. Van Gerpen, J. F. Meschia, I. R. Mackenzie, K. Boylan, B. F. Boeve, B. L. Miller, M. J. Strong, R. J. Uitti, S. G. Younkin, N. R. Graff-Radford, R. C. Petersen, Z. K. Wszolek, D. W. Dickson, and R. Rademakers. "Ataxin-2 Repeat-Length Variation and Neurodegeneration." *Human molecular genetics* 20.16 (2011): 3207-12. Print.

Ruiz-Canada, C. and Budnik, V. "Introduction on the Use of the Drosophila Embryonic/Larval Neuromuscular Junction as a Model System to Study Synapse Development and Function, and a Brief Summary of Pathfinding and Target Recognition." *International review of neurobiology* 75 (2006): 1-31. Print.

Russ, W. P., and Engelman, D. M. "The Gxxxg Motif: A Framework for Transmembrane Helix-Helix Association." *Journal of molecular biology* 296.3 (2000): 911-9. Print.

Samali, A., Fitzgerald, U., Deegan, S., and Gupta, S. "Methods for Monitoring Endoplasmic Reticulum Stress and the Unfolded Protein Response." *International journal of cell biology* 2010 (2010): 830307. Print.

Sanchez, C., J. Diaz-Nido, and J. Avila. "Phosphorylation of Microtubule-Associated Protein 2 (Map2) and Its Relevance for the Regulation of the Neuronal Cytoskeleton Function." *Progress in neurobiology* 61.2 (2000): 133-68. Print.

Sapp, P. C., B. A. Hosler, D. McKenna-Yasek, W. Chin, A. Gann, H. Genise, J. Gorenstein, M. Huang, W. Sailer, M. Scheffler, M. Valesky, J. L. Haines, M. Pericak-Vance, T. Siddique, H. R. Horvitz, and R. H. Brown, Jr. "Identification of Two Novel Loci for Dominantly Inherited Familial Amyotrophic Lateral Sclerosis." *American journal of human genetics* 73.2 (2003): 397-403. Print.

Saxena, S. and Caroni, P. "Mechanisms of Axon Degeneration: From Development to Disease." *Progress in neurobiology* 83.3 (2007): 174-91. Print.

Schaefer, A. W., Kabir, N. and Forscher, P. "Filopodia and Actin Arcs Guide the Assembly and Transport of Two Populations of Microtubules with Unique Dynamic Parameters in Neuronal Growth Cones." *The Journal of cell biology* 158.1 (2002): 139-52. Print.

Schorr, M., A. Then, S. Tahirovic, N. Hug, and P. Mayinger. "The Phosphoinositide Phosphatase Sac1p Controls Trafficking of the Yeast Chs3p Chitin Synthase." *Current biology : CB* 11.18 (2001): 1421-6. Print.

Schuster, C. M., G. W. Davis, R. D. Fetter, and C. S. Goodman. "Genetic Dissection of Structural and Functional Components of Synaptic Plasticity. I. Fasciclin Ii Controls Synaptic Stabilization and Growth." *Neuron* 17.4 (1996): 641-54. Print.

Shan, X., J. H. Hu, F. S. Cayabyab, and C. Krieger. "Increased Phospho-Adducin Immunoreactivity in a Murine Model of Amyotrophic Lateral Sclerosis." *Neuroscience* 134.3 (2005): 833-46. Print.

Siddique, T., D. Nijhawan, and A. Hentati. "Familial Amyotrophic Lateral Sclerosis." *Journal of neural transmission. Supplementum* 49 (1997): 219-33. Print.

Skehel, P. A., Fabian-Fine, R., and Kandel, E. R. "Mouse Vap33 Is Associated with the Endoplasmic Reticulum and Microtubules." *Proceedings of the National*

Academy of Sciences of the United States of America 97.3 (2000): 1101-6. Print.

Skehel, P. A., Martin, K. C., Kandel, E. R., and Bartsch, D. "A Vamp-Binding Protein from Aplysia Required for Neurotransmitter Release." *Science* 269.5230 (1995): 1580-3. Print.

Sone, M., Suzuki, E., Hoshino, M., Hou, D., Kuromi, H., Fukata, M., Kuroda, S., Kaibuchi, K., Nabeshima, Y., and Hama, C. "Synaptic Development Is Controlled in the Periactive Zones of Drosophila Synapses." *Development* 127.19 (2000): 4157-68. Print.

Soussan, L., Burakov, D., Daniels, M. P., Toister-Achituv, M., Porat, A., Yarden, Y., and Elazar, Z. "Erg30, a Vap-33-Related Protein, Functions in Protein Transport Mediated by Copi Vesicles." *The Journal of cell biology* 146.2 (1999): 301-11. Print.

Spradling, A. "P Element-Mediated Transformation. In Drosophila: A Practical Approach." *D. B. Roberts, ed. (Oxford, IRL Press)* (1986): 175-97. Print.

Spradling, A. C., and G. M. Rubin. "Transposition of Cloned P Elements into Drosophila Germ Line Chromosomes." *Science* 218.4570 (1982): 341-7. Print.

Sreedharan, J., I. P. Blair, V. B. Tripathi, X. Hu, C. Vance, B. Rogelj, S. Ackerley, J. C. Durnall, K. L. Williams, E. Buratti, F. Baralle, J. de Belleroche, J. D. Mitchell, P. N. Leigh, A. Al-Chalabi, C. C. Miller, G. Nicholson, and C. E. Shaw. "Tdp-43 Mutations in Familial and Sporadic Amyotrophic Lateral Sclerosis." *Science* 319.5870 (2008): 1668-72. Print.

St Johnston, D. "The Art and Design of Genetic Screens: Drosophila Melanogaster." *Nature reviews. Genetics* 3.3 (2002): 176-88. Print.

Stathopulos, P. B., J. A. Rumfeldt, G. A. Scholz, R. A. Irani, H. E. Frey, R. A. Hallewell, J. R. Lepock, and E. M. Meiering. "Cu/Zn Superoxide Dismutase Mutants Associated with Amyotrophic Lateral Sclerosis Show Enhanced Formation of Aggregates in Vitro." *Proceedings of the National Academy of Sciences of the United States of America* 100.12 (2003): 7021-6. Print.

Stefan, C. J., Manford, A. G., Baird, D., Yamada-Hanff, J., Mao, Y. and Emr, S. D. "Osh Proteins Regulate Phosphoinositide Metabolism at Er-Plasma Membrane Contact Sites." *Cell* 144.3 (2011): 389-401. Print.

Stewart, B. A., Schuster, C. M., Goodman, C. S. and Atwood, H. L. "Homeostasis of Synaptic Transmission in Drosophila with Genetically Altered Nerve Terminal Morphology." *The Journal of neuroscience : the official journal of the Society for Neuroscience* 16.12 (1996): 3877-86. Print.

Suzuki, H., K. Kanekura, T. P. Levine, K. Kohno, V. M. Olkkonen, S. Aiso, and M. Matsuoka. "Als-Linked P56s-Vapb, an Aggregated Loss-of-Function Mutant of Vapb, Predisposes Motor Neurons to Er Stress-Related Death by Inducing Aggregation of Co-Expressed Wild-Type Vapb." *Journal of neurochemistry* 108.4 (2009): 973-85. Print.

Tahirovic, S., Schorr, M. and Mayinger, P. "Regulation of Intracellular Phosphatidylinositol-4-Phosphate by the Sac1 Lipid Phosphatase." *Traffic* 6.2 (2005): 116-30. Print.

Talbot, K. "Motor Neurone Disease." *Postgraduate medical journal* 78.923 (2002): 513-9. Print.

Tanaka, E., T. Ho, and M. W. Kirschner. "The Role of Microtubule Dynamics in Growth Cone Motility and Axonal Growth." *The Journal of cell biology* 128.1-2 (1995): 139-55. Print.

Tanenbaum, S. B., Gorski, S. M., Rusconi, J. C. and Cagan, R. L. "A Screen for Dominant Modifiers of the Irrec-Rst Cell Death Phenotype in the Developing Drosophila Retina." *Genetics* 156.1 (2000): 205-17. Print.

Tarr, D. E., and Scott, A. L. "Msp Domain Protein-1 from Ascaris Suum and Its Possible Role in the Regulation of Major Sperm Protein-Based Crawling Motility." *Molecular and biochemical parasitology* 143.2 (2005): 165-72. Print.

Taylor, F. R., and A. A. Kandutsch. "Oxysterol Binding Protein." *Chemistry and physics of lipids* 38.1-2 (1985): 187-94. Print.

Terpe, K. "Overview of Tag Protein Fusions: From Molecular and Biochemical Fundamentals to Commercial Systems." *Applied microbiology and biotechnology* 60.5 (2003): 523-33. Print.

Teuling, E., S. Ahmed, E. Haasdijk, J. Demmers, M. O. Steinmetz, A. Akhmanova, D. Jaarsma, and C. C. Hoogenraad. "Motor Neuron Disease-Associated Mutant

Vesicle-Associated Membrane Protein-Associated Protein (Vap) B Recruits Wild-Type Vaps into Endoplasmic Reticulum-Derived Tubular Aggregates." *The Journal of neuroscience : the official journal of the Society for Neuroscience* 27.36 (2007): 9801-15. Print.

Thorpe, H. M., Wilson, S. E. and Smith, M. C. "Control of Directionality in the Site-Specific Recombination System of the Streptomyces Phage Phic31." *Molecular microbiology* 38.2 (2000): 232-41. Print.

Tsuda, H., Han, S. M., Yang, Y., Tong, C., Lin, Y. Q., Mohan, K., Haueter, C., Zoghbi, A., Harati, Y., Kwan, J., Miller, M. A., and Bellen, H. J. "The Amyotrophic Lateral Sclerosis 8 Protein Vapb Is Cleaved, Secreted, and Acts as a Ligand for Eph Receptors." *Cell* 133.6 (2008): 963-77. Print.

van Blitterswijk, M., van Es, M. A., Koppers, M., van Rheenen, W., Medic, J., Schelhaas, H. J., van der Kooi, A. J., de Visser, M., Veldink, J. H. and van den Berg, L. H. "Vapb and C9orf72 Mutations in 1 Familial Amyotrophic Lateral Sclerosis Patient." *Neurobiology of aging* (2012). Print.

Vance, C., B. Rogelj, T. Hortobagyi, K. J. De Vos, A. L. Nishimura, J. Sreedharan, X. Hu, B. Smith, D. Ruddy, P. Wright, J. Ganesalingam, K. L. Williams, V. Tripathi, S. Al-Saraj, A. Al-Chalabi, P. N. Leigh, I. P. Blair, G. Nicholson, J. de Belleroche, J. M. Gallo, C. C. Miller, and C. E. Shaw. "Mutations in Fus, an Rna Processing Protein, Cause Familial Amyotrophic Lateral Sclerosis Type 6." *Science* 323.5918 (2009): 1208-11. Print.

Vance, J. E. and Vance, D. E. "Lipoprotein Assembly and Secretion by Hepatocytes." *Annual review of nutrition* 10 (1990): 337-56. Print.

Venken, K. J. and Bellen, H. J. "Transgenesis Upgrades for Drosophila Melanogaster." *Development* 134.20 (2007): 3571-84. Print.

Voelker, D. R. "Interorganelle Transport of Aminoglycerophospholipids." *Biochimica et biophysica acta* 1486.1 (2000): 97-107. Print.

Voeltz, G. K., Rolls, M. M. and Rapoport, T. A. "Structural Organization of the Endoplasmic Reticulum." *EMBO reports* 3.10 (2002): 944-50. Print.

Volpicelli-Daley, L., and P. De Camilli. "Phosphoinositides' Link to Neurodegeneration." *Nature medicine* 13.7 (2007): 784-6. Print.

Voronov, S. V., S. G. Frere, S. Giovedi, E. A. Pollina, C. Borel, H. Zhang, C. Schmidt, E. C. Akeson, M. R. Wenk, L. Cimasoni, O. Arancio, M. T. Davisson, S. E. Antonarakis, K. Gardiner, P. De Camilli, and G. Di Paolo. "Synaptojanin 1-Linked Phosphoinositide Dyshomeostasis and Cognitive Deficits in Mouse Models of Down's Syndrome." *Proceedings of the National Academy of Sciences of the United States of America* 105.27 (2008): 9415-20. Print.

Wagh, D. A., T. M. Rasse, E. Asan, A. Hofbauer, I. Schwenkert, H. Durrbeck, S. Buchner, M. C. Dabauvalle, M. Schmidt, G. Qin, C. Wichmann, R. Kittel, S. J. Sigrist, and E. Buchner. "Bruchpilot, a Protein with Homology to Elks/Cast, Is Required for Structural Integrity and Function of Synaptic Active Zones in Drosophila." *Neuron* 49.6 (2006): 833-44. Print.

Walch-Solimena, C. and Novick, P. "The Yeast Phosphatidylinositol-4-Oh Kinase Pik1 Regulates Secretion at the Golgi." *Nature cell biology* 1.8 (1999): 523-5. Print.

Wang, L., Sharma, K., Grisotti, G. and Roos, R. P. "The Effect of Mutant Sod1 Dismutase Activity on Non-Cell Autonomous Degeneration in Familial Amyotrophic Lateral Sclerosis." *Neurobiology of disease* 35.2 (2009): 234-40. Print.

Warrick, J. M., H. Y. Chan, G. L. Gray-Board, Y. Chai, H. L. Paulson, and N. M. Bonini. "Suppression of Polyglutamine-Mediated Neurodegeneration in Drosophila by the Molecular Chaperone Hsp70." *Nature genetics* 23.4 (1999): 425-8. Print.

Warrick, J. M., Paulson, H. L., Gray-Board, G. L., Bui, Q. T., Fischbeck, K. H., Pittman, R. N., and Bonini, N. M. "Expanded Polyglutamine Protein Forms Nuclear Inclusions and Causes Neural Degeneration in Drosophila." *Cell* 93.6 (1998): 939-49. Print.

Watanabe, M., M. Dykes-Hoberg, V. C. Culotta, D. L. Price, P. C. Wong, and J. D. Rothstein. "Histological Evidence of Protein Aggregation in Mutant Sod1 Transgenic Mice and in Amyotrophic Lateral Sclerosis Neural Tissues." *Neurobiology of disease* 8.6 (2001): 933-41. Print.

Wei, H. C., J. Sanny, H. Shu, D. L. Baillie, J. A. Brill, J. V. Price, and N. Harden. "The Sac1 Lipid Phosphatase Regulates Cell Shape Change and the Jnk

Cascade During Dorsal Closure in Drosophila." *Current biology : CB* 13.21 (2003): 1882-7. Print.

Weimbs, T., Low, S. H., Chapin, S. J., Mostov, K. E., Bucher, P., and Hofmann, K. "A Conserved Domain Is Present in Different Families of Vesicular Fusion Proteins: A New Superfamily." *Proceedings of the National Academy of Sciences of the United States of America* 94.7 (1997): 3046-51. Print.

Weir, M. L., Klip, A., and Trimble, W. S. "Identification of a Human Homologue of the Vesicle-Associated Membrane Protein (Vamp)-Associated Protein of 33 Kda (Vap-33): A Broadly Expressed Protein That Binds to Vamp." *The Biochemical journal* 333 (Pt 2) (1998): 247-51. Print.

Wenk, M. R. and De Camilli, P. "Protein-Lipid Interactions and Phosphoinositide Metabolism in Membrane Traffic: Insights from Vesicle Recycling in Nerve Terminals." *Proceedings of the National Academy of Sciences of the United States of America* 101.22 (2004): 8262-9. Print.

Weston, C., B. Yee, E. Hod, and J. Prives. "Agrin-Induced Acetylcholine Receptor Clustering Is Mediated by the Small Guanosine Triphosphatases Rac and Cdc42." *The Journal of cell biology* 150.1 (2000): 205-12. Print.

Whitters, E. A., Cleves, A. E., McGee, T. P., Skinner, H. B. and Bankaitis, V. A. "Sac1p Is an Integral Membrane Protein That Influences the Cellular Requirement for Phospholipid Transfer Protein Function and Inositol in Yeast." *The Journal of cell biology* 122.1 (1993): 79-94. Print.

Wiedemann, C., T. Schafer, M. M. Burger, and T. S. Sihra. "An Essential Role for a Small Synaptic Vesicle-Associated Phosphatidylinositol 4-Kinase in Neurotransmitter Release." *The Journal of neuroscience : the official journal of the Society for Neuroscience* 18.15 (1998): 5594-602. Print.

Wirtz, K. W. "Phospholipid Transfer Proteins." *Annual review of biochemistry* 60 (1991): 73-99. Print.

Wolff, T., Guinto, J. B. and Rawls, A. S. "Screen for Genetic Modifiers of Stbm Reveals That Photoreceptor Fate and Rotation Can Be Genetically Uncoupled in the Drosophila Eye." *PloS one* 2.5 (2007): e453. Print.

Wu, C. H., Fallini, C., Ticozzi, N., Keagle, P. J., Sapp, P. C., Piotrowska, K., Lowe, P., Koppers, M., McKenna-Yasek, D., Baron, D. M., Kost, J. E., Gonzalez-Perez, P., Fox, A. D., Adams, J., Taroni, F., Tiloca, C., Leclerc, A. L., Chafe,

S. C., Mangroo, D., Moore, M. J., Zitzewitz, J. A., Xu, Z. S., van den Berg, L. H., Glass, J. D., Siciliano, G., Cirulli, E. T., Goldstein, D. B., Salachas, F., Meininger, V., Rossoll, W., Ratti, A., Gellera, C., Bosco, D. A., Bassell, G. J., Silani, V., Drory, V. E., Brown, R. H., Jr., and Landers, J. E. "Mutations in the Profilin 1 Gene Cause Familial Amyotrophic Lateral Sclerosis." *Nature* 488.7412 (2012): 499-503. Print.

Wyles, J. P., C. R. McMaster, and N. D. Ridgway. "Vesicle-Associated Membrane Protein-Associated Protein-a (Vap-a) Interacts with the Oxysterol-Binding Protein to Modify Export from the Endoplasmic Reticulum." *The Journal of biological chemistry* 277.33 (2002): 29908-18. Print.

Wyles, J. P., and N. D. Ridgway. "Vamp-Associated Protein-a Regulates Partitioning of Oxysterol-Binding Protein-Related Protein-9 between the Endoplasmic Reticulum and Golgi Apparatus." *Experimental cell research* 297.2 (2004): 533-47. Print.

Yamauchi, P. S. and Purich, D. L. "Modulation of Microtubule Assembly and Stability by Phosphatidylinositol Action on Microtubule-Associated Protein-2." *The Journal of biological chemistry* 262.7 (1987): 3369-75. Print.

Yang, Y., A. Hentati, H. X. Deng, O. Dabbagh, T. Sasaki, M. Hirano, W. Y. Hung, K. Ouahchi, J. Yan, A. C. Azim, N. Cole, G. Gascon, A. Yagmour, M. Ben-Hamida, M. Pericak-Vance, F. Hentati, and T. Siddique. "The Gene Encoding Alsin, a Protein with Three Guanine-Nucleotide Exchange Factor Domains, Is Mutated in a Form of Recessive Amyotrophic Lateral Sclerosis." *Nature genetics* 29.2 (2001): 160-5. Print.

Yao, K. M., and K. White. "Neural Specificity of Elav Expression: Defining a Drosophila Promoter for Directing Expression to the Nervous System." *Journal of neurochemistry* 63.1 (1994): 41-51. Print.

Yavari, A., Nagaraj, R., Owusu-Ansah, E., Folick, A., Ngo, K., Hillman, T., Call, G., Rohatgi, R., Scott, M. P. and Banerjee, U. "Role of Lipid Metabolism in Smoothened Derepression in Hedgehog Signaling." *Developmental cell* 19.1 (2010): 54-65. Print.

Yin, H. L. and Janmey, P. A. "Phosphoinositide Regulation of the Actin Cytoskeleton." *Annual review of physiology* 65 (2003): 761-89. Print.

Yoshida, S., Y. Ohya, M. Goebl, A. Nakano, and Y. Anraku. "A Novel Gene, Stt4, Encodes a Phosphatidylinositol 4-Kinase in the Pkc1 Protein Kinase Pathway of Saccharomyces Cerevisiae." *The Journal of biological chemistry* 269.2 (1994): 1166-72. Print.

Yoshida, S., Y. Ohya, A. Nakano, and Y. Anraku. "Genetic Interactions among Genes Involved in the Stt4-Pkc1 Pathway of Saccharomyces Cerevisiae." *Molecular & general genetics : MGG* 242.6 (1994): 631-40. Print.

Yuan, Y., Gao, X., Guo, N., Zhang, H., Xie, Z., Jin, M., Li, B., Yu, L., and Jing, N. "Rsac3, a Novel Sac Domain Phosphoinositide Phosphatase, Promotes Neurite Outgrowth in Pc12 Cells." *Cell research* 17.11 (2007): 919-32. Print.

Zago, S., Poletti, B., Morelli, C., Doretti, A., and Silani, V. "Amyotrophic Lateral Sclerosis and Frontotemporal Dementia (Als-Ftd)." *Archives italiennes de biologie* 149.1 (2011): 39-56. Print.

Zarow, C.. Vinters, H. V., Ellis, W. G., Weiner, M. W., Mungas, D., White, L. and Chui, H. C. "Correlates of Hippocampal Neuron Number in Alzheimer's Disease and Ischemic Vascular Dementia." *Annals of neurology* 57.6 (2005): 896-903. Print.

Zhang, P., S. Talluri, H. Deng, D. Branton, and G. Wagner. "Solution Structure of the Pleckstrin Homology Domain of Drosophila Beta-Spectrin." *Structure* 3.11 (1995): 1185-95. Print.

Zinsmaier, K. E., Eberle, K. K., Buchner, E., Walter, N. and Benzer, S. "Paralysis and Early Death in Cysteine String Protein Mutants of Drosophila." *Science* 263.5149 (1994): 977-80. Print.